OLLSCOIL NA GAILLIMHE
UNIVERSITY OF GALWAY

# Application of Flow Cytometry and Membrane Inlet Mass Spectrometry as Tools to Assess Dimethyl Sulfide Produced in Emiliania huxleyi (CHC108) Cultures


Submitted By: Adelaide Lavenant Wink

Supervisor:

Professor Peter Croot

College of Science and Engineering,

School of Natural Sciences, Earth and Ocean Sciences

University of Galway


A Dissertation Submitted in Partial Fulfilment of the Master of Science (M.Sc.) in Ocean, Atmosphere and Climate

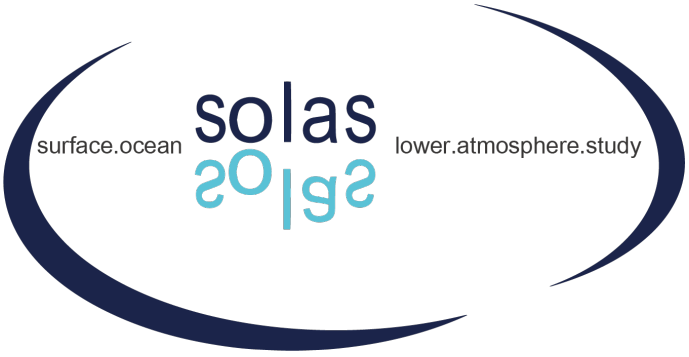

# Table of Contents

# Declaration

All work provided in this study is my own unless an in-text acknowledgement has been provided. This work has not been submitted anywhere else for consideration of an alternative degree, or publishing.

# Acknowledgements

I would like to thank my research supervisor Dr. Peter Croot for his hard work and continued support in this new master's program throughout the planning and research parts. I would like to thank Dr. Jessica Gier for her hard work in starting up the new SOLAS masters in ocean, atmosphere, and climate change. I would like to thank Dr. Jurgita Ovadnevaite and Dr. Dagmar Stengel for all of their hard work in navigating the new masters and making it a success. I would like to thank everyone in the SOLAS community who agreed to give a oneon-one lecture during one of the modules. This opened my eyes to all of the possibilities and gaps in our knowledge of atmospheric-oceanic interactions that still exist. I would like to thank SOLAS as a community for inspiring communication between atmospheric and oceanic scientists. I would like to thank the people in the Croot lab for their kindness and light-hearted attitudes that made the lab experience what it was. It would not have been the same without it. I would like to thank Callum Hagan for his continued support and advice in unsure times. Finally, I would like to thank David Wink and Amelie Lavenant-Wink for advice, continued support throughout my studies.

# Abstract

Dimethyl sulphide (DMS) is a key component in the global sulphur cycle with emphasized significance in areas away from anthropogenic sources. Phytoplankton produce DMS when under stress as a defence mechanism from abiotic and biotic influences such as high wind stress and grazing. *E. huxleyi* was used as the phytoplankton of choice because of the cosmopolitan nature of the species along with the more robust nature of the coccolith. DMS has a high diffusion rate in the atmosphere so immediately monitoring the levels in the water column has proven difficult especially when looking at continuous input flux. In this study, membrane inlet mass spectrometry was used to monitor DMS flux over varying periods of time along with a possible variation of DMS under Mass 47 which excludes one of the methyl groups under different stressors. This continuous observation allowed for the observation in minute changes over longer periods of time rather than using the snapshot method which looks at chemical concentrations at singular points in time. This novel technique can give insights to the response times of the phytoplankton to the changing environment in real time. The added stressors to the water column did result in an increase of DMS but the lag time to the addition and the visible increase in DMS did not follow the expected trend. Of the parameters tested here, the most likely to initiate DMS production is heavy metal loading and water column acidification.

# Introduction

## Phytoplankton, ocean biogeochemistry and impact on the atmosphere

The relationship between the ocean and the atmosphere is a complex machine with many moving parts of which not all interactions are completely understood. SOLAS (surface ocean lower atmosphere studies) define the interactions via five different components i) greenhouse gasses and the ocean, ii) air-sea interface and fluxes of masses and energy, iii) atmospheric deposition and ocean biogeochemistry, iv) interconnections between the marine ecosystems, aerosols, and clouds, and v) ocean biogeochemical control on atmospheric chemistry. Along with these core themes, there are intersectional themes such as the polar oceans, climate intervention, and science and society. The focus in this study is looking at theme v and subsequently the climate implications. One of the main mechanisms of controlling sulphur and nitrogen cycle fluxes into the ocean and atmosphere are phytoplankton. Marine phytoplankton contribute roughly 50% of global productivity and drive the carbon cycle as an integral part of the oceanic carbon pump (*Dedman et al.,* 2023). These organisms are integral parts of several biogeochemical cycles in the marine ecosystem including the sulphur cycle. Phytoplankton productivity alone is comparable to terrestrial plants (*Hader and Gao, 2015*). Carbon and nitrogen fixation leads to several important by-products that are eventually released into the water column. Once by-products of these biological processes enter the water column, further breakdown occurs or diffusion into the atmosphere. Gas exchange occurs in the surface level of the ocean and the marine boundary layer, with the physical and biogeochemical properties impacting this flux (*Altieri et al., 2021*) by altering the size distribution of aerosols, both primary and secondary in the atmosphere. Aerosols are particles that can be directly or indirectly from the surface of the ocean. The aerosol uptake can even reach the stratosphere with partial or whole diatoms, a type of phytoplankton, have been found as a base for ice nucleation. These particles scatter light and UV radiation in the atmosphere but can also act as cloud condensation nuclei (CCN). CCN seed clouds and depending on the type of CCN will influence the brightness of the cloud. Sulphur based CCN will brighten clouds.

Climate change has altered atmospheric chemistry with one of the most famous examples being the ozone holes from the use of chlorofluorocarbons (CFCs). One of the secondary consequences of the holes in the ozone would be the increase in solar radiation (*Falkowski, 1994*) into the water column. This increase in the surface water temperature will kick start higher wind speeds, potentially leading to an uptick in upwelling rates. The upwelling forces nutrients that have been sequestered at the bottom of the ocean to the surface. Any limiting nutrients may be replenished, and cause a phytoplankton explosion (*Falkowski, 1994*). This

explosion would also lead to increased rates of both carbon and nitrogen fixation. As the nutrients sink through the water column and nutrient level no longer supports the bloom, the phytoplankton would undergo stress at the environmental change. This would result in a reduced phytoplankton number in the bloom. Higher sea surface temperatures, temperature thresholds vary by species and sometimes strain, correlate with a decreased productivity of phytoplankton (*Fernandes, 2012*). Increased surface temperatures will lead to more extensive stratification and a subsequent decrease in the mixed layer depth (*Hader and Gao, 2015*). Higher surface temperatures will decrease oxygen concentrations in these more stratified zones, especially in coastal regions. Without the influx of nutrients and lower-level mixing, large decreases in phytoplankton bloom numbers and rate of productivity. Other potential sources for nutrients come from atmospheric deposition e.g., through dust deposition. Dust particles can have high iron concentrations, though the form of iron deposited in the water column may not be bioavailable. Atmospheric deposition could also introduce toxic substances to the water column further impeding phytoplankton productivity (*Altieri et al., 2021*). Modelling the effects of atmospheric deposition on the productivity of phytoplankton has many nuanced influences and interactions that on the surface may not seem relevant make the models difficult to make entirely accurate, especially when looking at a mixed species bloom. Other drawbacks of models that have multiple inputs require high levels of computer power which often would be impractical in a day-to-day setting.

## DMS production and diffusion into the atmosphere

Some scientists suggest that an amplification of the sulphur cycle will stabilize the climate (*Kloster et al., 2007*). These suggestions mostly came in the form of the CLAW hypothesis (Fig. 1) which posits that the feedback loop is established by phytoplankton and some bacteria. This loop can work in smaller scale studies as there was an increase in cloud cover in areas where there was a higher DMS concentration. The issue arises when applying the concept to a global scale as there are many other factors to consider and cannot be a one-to-one input output model. The CLAW

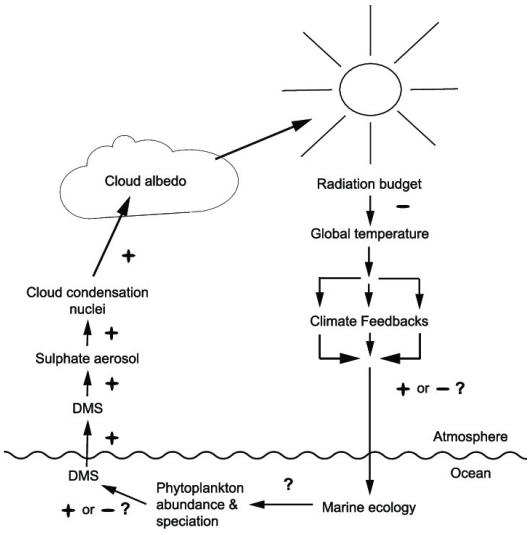


*Figure 1 Depiction of the CLAW hypothesis and how DMS positively and negatively impacts climate (Vogt and Liss, 2013)*

hypothesis was first put forward by Charlson, Lovelock, Andrae, and Warren in 1987 (*Ayers & Cainey, 2007*). This has been seen in the proposition in the use of manmade particles similar to volcanic emissions to rapidly cool the atmosphere. Dimethyl sulphide (DMS) potentially contributes to around 23% of global sulphur entering the atmosphere (*Fung et al., 2022, Thierstein et al.,* 2004). Around 93% of the world's oceans emit DMS into the atmosphere (*Hulswar et al.,* 2022) with some hotspots in coastal zones. DMS is derived from the cellular product dimethylsulfoniopriponate (DMSP) and is a biogenic trace gas which is volatile (*Thierstein et al., 2004, Yu et al., 2021*). DMSP can be produced to aid in changing stressors in the environment through abiotic factors such as lower pH, UV and light fluctuations, ocean acidification and biotic factors such as grazing. The compound can also aid in other functions such as osmoregulation and cryoprotection (*Chiu and Shinzato, 2022*). Each species has different tolerances and survival strategies, so accurately predicting and modelling global DMS production has been difficult to achieve. Some marine bacteria have the ability to produce DMSP and DMS as well (Figure 2), along with some being able to convert DSMP to DMS. Bacteria can also play a crucial role in the DMS sink by oxidizing DMS to dimethyl sulfoxide (DMSO) (*Teng et al. 2021*). This symbiotic relationship with phytoplankton must not ignored as when separated in a lab setting, the phytoplankton population declined rapidly because of the key role that the bacteria play within the ecosystem. The symbiotic bacteria will uptake the waste products from primary production (*Bratbak and Thingstad, 1985*) and convert the products back to a usable inorganic form for the phytoplankton to continue to grow and flourish (*Behringer et al., 2018*) which may mediate nutrient consumption and provide a buffer from nutrient competition between the phytoplankton and bacteria. This has been proven both in the field and in the lab as a fundamental relationship for survival. DMS oxidation can take up to two days once in the atmosphere with common products being DMSO, $H_2SO_4$ (*Fung et al., 2022*). The largest loss of DMS, around 80%, is through chemical loss, with around 40% through hydroxyl radical (OH) oxidation and up to 23% through nitrate oxidation (*Fung et al., 2022*). Nitrate oxidation of DMS is especially prevalent in the northern hemisphere. The product of the oxidation of both OH (*Vogt and Liss, 2013*) and nitrate are sulphur dioxide and sulphates ($SO_4^{2-}$).

The breakdown to $SO_2$ and $SO_4^{2-}$ are important components in the atmosphere. Both primary and secondary aerosols have potential to scatter light and UV radiation themselves

(*Altieri et al., 2021, Chiu and Shinzato, 2022*), but can also form the basis for cloud condensation nuclei (CCN) (Fig. 2). Sulphates acting as CCN make clouds whiter thus increasing the cloud's albedo (*Hulswar et al., 2021*). High albedo areas are highly reflective places such as the north and south poles. Low albedo areas absorb all the incoming heat like the ocean. Having a small highly reflective area above the ocean dampens the amount of radiation absorbed and could potentially have a cooling effect. The drawback to this process is that smaller amounts of light reaching the ocean surface would impede phytoplankton community growth, and consequently hinder DMS production. The lessening input of DMS would lower the whiteness of the clouds, so the long-lasting effects of the cooling via this method may not be sustainable.

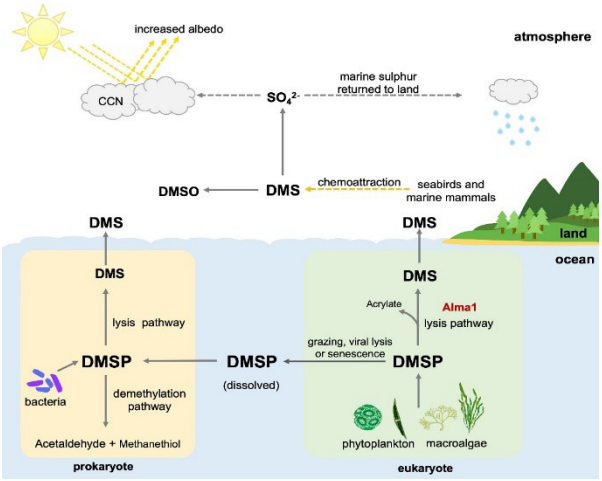


*Figure 2 DMS cycle and interactions in the atmosphere and the ocean (Chiu and Shinzato, 2022).*

Observations have been made of decreased production in sulphur-based compound production in phytoplankton e.g., DMS and DMSP when nitrogen is a limiting factor (*Hader and Gao, 2015*). In the future, projections predict increases in the main oxidants of DMS (*Kluster et al. 2007*). These projections are under the assumption that the overall atmospheric DMS burden of 22% will remain constant. Other models predict that the global DMS burden will decrease in the warmer climate. Is this due to an oxidation problem or a source problem?

## Why use *E. huxleyi*?

Coccolithophores are abundant in all oceans and account for up to 10% of the phytoplankton biomass globally (*Menschel et al., 2016*). Even in the Arctic Ocean and high latitude Southern Ocean, there are traces of *E. huxleyi* (*Tyrrell and Merico, 2004*). *E. huxleyi* in its various strains can be found in all oceans; with large populations existing in the mid-high latitudes in both the Northern and Southern Hemisphere (*Menschel et al., 2016*). Coccolithophore blooms can be heavily dominated by the E. huxleyi, reaching as high as 90% of the bloom (*Menschel et al., 2016*). Coccolithophore blooms thrive especially when met with the following conditions: high light, low silicate concentrations, higher phosphate, and low concentrations of dissolved $CO_2$ (*Tyrrell and Merico, 2004*). The dissolved $CO_2$ concentration interferes with the calcification process, $Ca^{2+} + 2HCO_3^- \longrightarrow CaCO3 + H_2O + CO_2$ Eq. 1(*Tyrrell and Gao, 2004*). These blooms are also associated with low chlorophyll concentration so can be difficult to quantify

using satellite imaging (*Tyrrell and Gao,* 2004). This species can be used as a good indicator for DMSP and DMS production (*Yu et al., 2021*), with alterations to the production having negative implications for the global sulphur biogeochemical cycle. Unlike other phytoplankton, *E. huxleyi* does not react to the increase in $CO_2$, and instead encourages photosynthesis, growth, and calcification (*Hader and Gao, 2015*). In most species, decreases were observed rather than the positive relationship observed in *E. huxleyi*. The other side is that as more $CO_2$ is added to the water column, the more acidity is introduced and will break down the $CaCO_3$ shell. The growth promotion is a short-term effect and will not adequately predict the future of the species in the next 100 years.

E. huxleyi, in some regions, make up 60-80% of carbonate fluxes below 1000m. *E. huxleyi* is the primary calcite producer (*Mordecai et al., 2017*) on the planet as the species overproduces the calcium carbonate shells(*Tyrrell and Merico, 2004*) and the high carbonate fluxes are most likely due to the shedding of that $CaCO_3$ shell (*Menchel et al., 2016*) These coccolithophores play a major role in the biological carbon pump to transport carbon from the surface waters to marine sediment (*Tsuji et al., 2009, Mordecai et al., 2017*). This is in part due to the unique primary carbon metabolism in coccolithophores when compared to other phytoplankton. In the water, the coccoliths will change the optical properties of the surface water. The blooms alone will increase the albedo of the surrounding water (*Tyrrell and Merico, 2004*). In turbid waters, where these blooms tend to occur, traps light and heat (*Tyrrell and Merico, 2004*). This prevents the heat from further penetrating the water column.

The aim of this study is to look at what combination of factors achieve the highest DMS output along with predicting the timescale that max concentration will occur. Prominent factors included in the baseline were temperature of the samples, nutrient supply, and light cycles prior to gas sampling. This was done to ensure that the DMS produced was in response to the controlled stressors. One of the stressors that featured in this study was light. The samples were covered as a method to induce a sort of “jet lag” as the normal 12 hour day night cycles that the cultures were grown in were interrupted. The prolonged darkness will induce a stress response as the phytoplankton could no longer photosynthesize.. Along with the added stress of not being able to photosynthesize, heavy metals and aggressive compounds were added into the water column. The combination of stressors should initiate the start of DMS production. Some of the questions that this study wanted to focus on were i) on what time frame will the phytoplankton react to the added stressors ii) how much DMS will be emitted, and iii) at what time point in the culture’s cycle will yield the most DMS?

Flow cytometry of *E. huxleyi*

Flow cytometry would be a suitable method for monitoring the growth of the culture by using three methods: ras, DNA staining and cellular membrane staining to monitpr the culturegrowth as a whole including the symbiotic bacteria populations.. Flow cytometry works by exposing the fluid from the culture to fluorescent light. The software can then determine the size of the cells by the amount of light that did not respond back to the sensor. The size and position of the cell is then placed on graphs that can look at time, cell size, chlorophyll size, and scatter level. *E. huxleyi* displaces more light than the surrounding bacteria, making it an easier population to sort out from the bacteria living in the culture. There are several sub methods that can be implemented to assess different areas of growth and change within the cultures. The raw count is the fluorescence level without any other staining methods. The reagent sybr green is a DNA dye that is used to stain cells previously fixed with glutaraldehyde. The reagent 5-chloromethylfluorescein (CMFDA) is applied to live cells and the dye is taken in by the cell into the cell membrane (*Marie et al., 2014*). CMFDA reacts with thiol, an organic sulphur compound in the cell, to lose the acetyl groups that quench fluorescence through thiol-aided-hydrolysis (*MacIntyre et al., 2016*). This dye can be used to monitor movement of the cells.

Application of MIMS to Algal Cultures

Membrane Inlet Mass Spectrometry (MIMS) is used to determine the gas concentrations in a water sample by sorting gases by mass. Common examples include water vapour, carbon dioxide ($CO_2$), oxygen $O_2$, argon (Ar), methane ($CH_4$) and DMS. MIMS can be used to look at the gas concentration changes simultaneously throughout the run time. This method also allows for stressors to be added over a period of time, noting all changes rather than the more common snapshot method. This will be valuable being able to quantify stress response and recovery times. As the membrane only allows for gas to pass through the membrane there would not be a way for the coccoliths to clog the membrane as this could interfere with the readings. While it is possible to convert DMSP to DMS via alkaline hydrolysis and then measure the resulting DMS using the MIMS, this was not attempted as other researchers had found that the strongly alkaline solutions used to rapidly convert DMSP to DMS could damage the PMDS membrane of the MIMS. We did however perform some small experiments using Labco exetainers to convert the DMSP to DMS using base and then acidify back to neutral pH, however as the exetainers are gas tight, there was a considerable build-up of pressure in the vial making it difficult to carry out the injection reproducibility and safely.

MIMs have been used in the field to monitor DMS, but did not address E. huxleyi blooms specifically ( *Herr et al., 2019*, *Jarníková et al., 2018*) and with the aim to further calculate the air-sea flux of DMS. While these studies are very useful in mapping out the DMS produced in

the ocean, *E. huxleyi* blooms respond differently to stressors due to the robust coccolith when compared to other phytoplankton species. Other lab based experiments which utilize MIMS and *E. huxleyi* focus on the biological stressors such as grazing or viral infection and the resulting DMS from those stressors (*Evans et al., 2007*). While these are also useful studies, the changes in chemical and physical stressors will impact the behaviour of the biological stressors. A few studies did look at the response of E. huxleyi to increasing pCO2 and temperature (*Feng et al., 2009*) but did not specifically investigate the DMS production or *E. huxleyi*, but rather how a specific bloom in the North Atlantic responded to these increased parameters, both in community structure and chemical cycling. One of the studies did look at the DMSP, the precursor to DMS, production from E. huxleyi, but used a snapshot method (*McParland et al., 2020*) and while useful does not fully explore the full response nor any potential recovery as the use if MIMS would allow. With an ever changing ocean, exploring the full range of phytoplankton responses to a variety of inputs is crucial in understanding how the ecosystem will shift in the future.

Objectives of this study- hypothesis to be tested:

The aim of this study was to quantify DMS production of E. huxleyi cultures over prolonged periods of time, weeks to months, in response to varied abiotic stressors as well as looking at any recovery is one stressor is removed. Stressors to be included are lack of light/prevention of photosynthesis and heavy metal loading.

The following questions were to be addressed:

- Does the DMS in the culture change as the culture ages?
- Are the symbiotic bacteria linked in any way to DMS production?
- If and how does the thiol content, measured through CMFDA, vary within a culture as it ages?
- What percentage of cells are active versus inactive?
- Do the coccoliths, the calcium carbonate part of the cell, alter the fluorescent light field and if so, how easily can the coccoliths be removed?

Sub-sections of these questions include looking into the relationship between the multi-day experiments and the individual experiments. The individual bacterial populations can be determined through flow cytometry including as the average cell grows and shrinks.

# Methods

The *E. huxleyi* strain that was used, CHC108, was collected off the coast of Chile at the Tongoy station. The strain was then isolated from other phytoplankton species in the sample prior to this experiment.

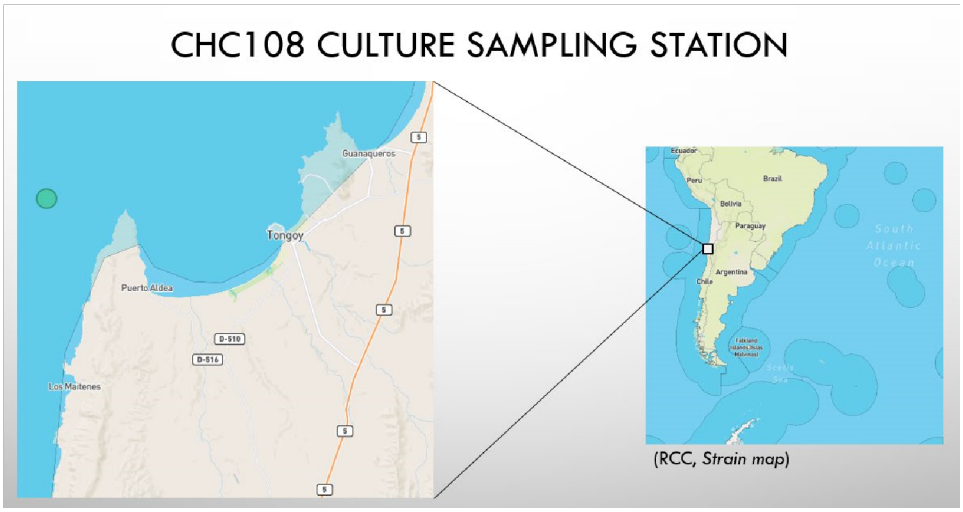


*Figure 3 Map depicting where E. huxleyi strain CHC108 was sampled at the Tongoy station in the Southern Ocean (Strain map (no date) Strain map | Roscoff Culture Collection.).*

## Culture Number Measurements:

Culture numbers were counted using flow cytometry. The first batch was followed over a period of 17 days. The two 500mL Erlenmeyer flasks filled with red sea medium and CHC108 strain were started on 13-04-23. The culture room has air conditioning and is kept at 20 ºC, the incubator for the cultures was kept at 15ºC. The CHC108 strain was collected at the Tongoy station (30.15 º S, 71.42 ºW) off the coast of Chile. Batches 2, 3, and 4 were monitored daily over a period of 9-12 days, after establishing when peak growth concentration occurred. Cultures in the stationary phase were kept in the incubator for up to 3 months.

Materials:

- Flow Cytometer
- Computer with C flow + program
- 7Eppendorf tubes ( 2mL)
- Black Permanent Marker
- 2 Erlenmeyer Flasks (500mL)
- Red Sea Medium
- CHC108 coccolithophore strain
- MQ Water
- Squeeze bottle
- 3 pipette and pipette tips (200µL)

- 40µL Glutaraldehyde
- 40µL SYBR Green Dye
- 100µL 5-chloromethylfluorescein diacetate (CMFDA) Dye

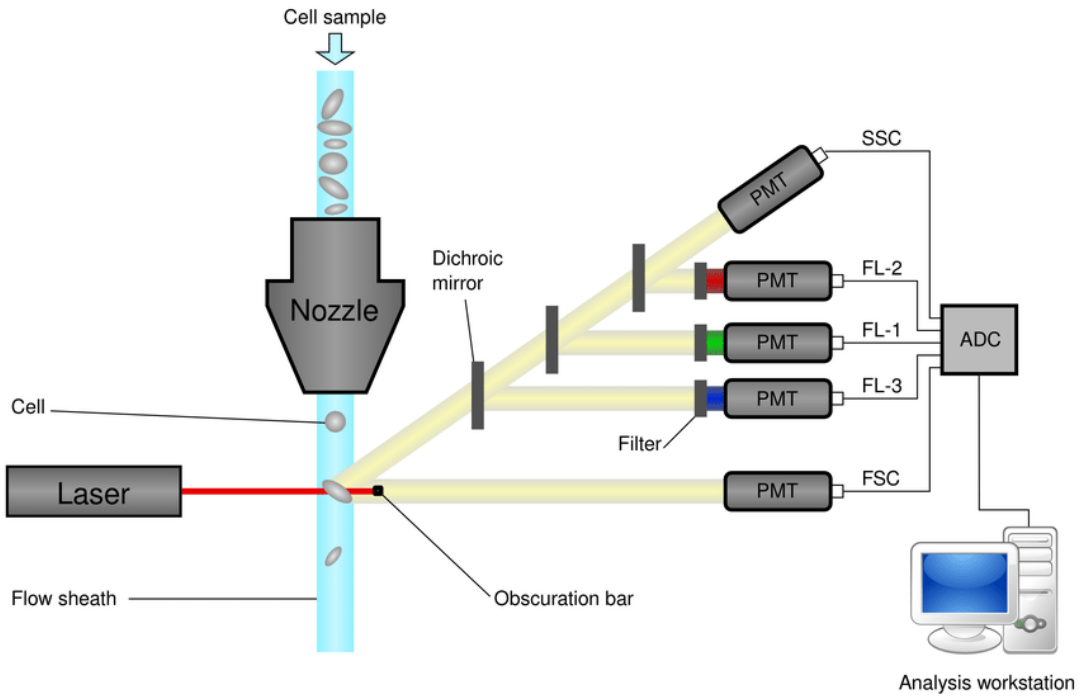


*Figure 4 Diagram depicting how a flow cytometer works. (O'Neill et al., 2013).*

A flow cytometer works by inputting cell samples, along with some sheath liquid to prevent the system from getting overwhelmed with cell counts, and exposing the sample cells to an excitation laser. The light then can be picked up by five different detectors based on the wavelength. The forward scatter (FSC) that measures the height and width of the cells by roughly calculating the diameter, side scatter (SSC) which measures the surface structures of the cells. FL1, 2, and 3 measure the fluorescence with FL-2 looking at red wavelengths, Fl-1 looking at green wavelengths and FL-3 looking at blue wave lengths (Fig. 4). In this experiment set up, chlorophyll fluorescence was the main goal with these detectors so FL-1 and FL-3 were the main ones used though FL-2 was used for the sybr green runs. FL-4 is an optional detector that can be added onto the system and measures the wavelengths between Fl-2 and FL-1. The florescence is quantified by the area pulse. The area pulse comes from compiling the height values per time slice which would be set around 10MHz. The fluorescence measurements was determined via relative fluorescence. All parameters were put into log scale except for time. -A and -H refer to area and height respectively.

Variation to the procedure occurred as the batches progressed. Deviations and timeframe when the deviation occurred from the procedure were outlined as sub bullet points.

Procedure:

1. The flow cytometer was turned on along with the adjoining computer program
2. Batch CHC108 A and CHC108 B, each in a 500mL Erlenmeyer flask, were retrieved from the 15ºC fridge which has a 12-hour day night cycle.
3. CMFDA was taken out of the freezer and placed into the fridge to thaw
4. 2 2mL Eppendorf tubes were labelled CHC108 A and CHC108 B respectively with the black permanent marker
5. Both batches were shaken prior to sampling to ensure that the coccolithophores were not concentrated at the bottom of the conical flasks. This should be done prior to every sampling type
6. Approximately 2mL of CHC108 A and 2mL of CHC108 B was poured into the respectively labelled Eppendorf tubes
7. Q water from a squeeze bottle was poured into another 2mL Eppendorf tube
8. The MQ Eppendorf was placed on the flow cytometer
9. The following parameters were set on the computer program:
    a. Graph one: Time vs. FSC-H (log)
    b. Graph two: FSC-H (log) vs FL3-H (log)
    c. Graph three: FL3-H (log) vs. FL2-H (log)
    d. Graph four: SSC-H (log) vs. FL4-H (log)
    e. Thresholds: FSC-H: 800, FL3-H: 800
10. Speed was set to fast with a limit of 10,000 event counts and 2-minute timer
11. H1 was labelled MQ and then start was pressed
12. After the run was finished, the MQ Eppendorf vial was replaced with the one labelled CHC108 A
13. Speed was set to slow and the limit for events was lifted
14. The run was started in A1
15. After the run was over, the same was done for CHC108 B in A2
16. After the raw samples were done, 2 2mL Eppendorf were labelled CHC108 A and CHC1008 B respectively
17. Conical flasks were shaken prior to sampling
18. Approximately 2mL of CHC108 A and 2mL of CHC108 B was poured into the respectively labelled Eppendorf tubes
19. 20 µL glutaraldehyde was added to each Eppendorf vial
20. Inverted and left to sit for 15 minutes
21. 20 µL of SYBR Green Dye was added to each Eppendorf vial

22. Inverted and left to sit for 10 minutes
    a. In later cultures, the samples were left for 30 minutes and 60 minutes as it was discovered that the samples were not being completely stained.
    b. The cultures were also placed in an orbital shaker set at first to 30ºC then at 37ºC. After coming out of the orbital shaker, the Eppendorf vials were inverted 2-3 times before loading into the flow cytometer.
23. The following parameters were added to the computer software:
    a. Graph five: FL1-H (log) vs. FL3-H (log)
    b. Graph six: FL4-H (log) vs. SSC-A (log)
24. Both vials were then run individually in B1 and B2 respectively
25. Final run MQ run was carried out in H2
26. The system was shut off while waiting for the CMFDA to thaw
27. Once the CMFDA was completely thawed out, the flow cytometer and computer were turned on
    a. In batch 2, Day 6 the CMFDA became no longer viable so was not used for the rest of batch 2, batch 3, and the first two days of batch 4
28. Previous .c6 file was opened to add dame day results after the incubation period
29. 2 2mL Eppendorf were labelled CHC108 A and CHC1008 B respectively
30. Conical flasks were shaken prior to sampling
31. Approximately 2mL of CHC108 A and 2mL of CHC108 B was poured into the respectively labelled Eppendorf tubes
32. 50 µL of CMFDA was added to each Eppendorf vials
33. CMFDA was put back in the freezer
34. The two conical flasks were placed back in the 12-hour cycle 15ºC fridge
35. CHC108 A was run in C1 and CHC108 B was run in C2
36. MQ was run again, and the system was shut down
37. Steps 1-36 were repeated each day of sampling Culture growth rates were determined

    using: $\mu = (1/t) * \ln(N_t/N_0)$ Eq. 1

Cell doubling time equation: $t = (1/\mu)$ Eq. 2 using average growth rates

Calibration beads (6 peak and 8 peak from Spherotech) were used as daily/weekly QA/QC checks for the 6 flow cytometer channels. During the period of this research there was no significant shift, or drift, in the relative performance of the detectors. FSC-H is the amount of forward light scattering upon impact with the cultures and measures the cell size. FL3-H is a

fluorescence channel that detect the auto-fluorescence of the chlorophyll in the sample (*Mondal and Singh, 2022*).

DMS, pCO2, DIC, and DOC Measurements:

Dissolved gases in the cultures were measured using a Hiden HPR40 DSA membrane inlet mass spectrometry (MIMS). MIMS has two sensor detective types, faraday, and secondary electron multiplier (SEM). The faraday detector was used to monitor more abundant molecules such as $H_2O$ (m/z 18) $N_2$ (m/z 28), $O_2$ (m/z 32), and Ar (m/z 40). Less abundant masses were detected using the secondary electron multiplier (SEM), this includes DMS (m/z 62 and 47), methane thiol (m/z 47), along with $CO_2$ (m/z 44, 45, and 46), $O_2$ isotopes (m/z 33, 34, 36). Argon (m/z 40) was also measured on the SEM to act as an internal standard and calibration gas. In the case of DMS, an m/z of 62 was used as the main peak, the breakdown peak at m/z 47 (loss of methyl group) can also be used but needs to be corrected for the possible contribution of methane thiol (m/z 47).

Membrane Inlet Mass Spectrometer (MIMS) – Materials:

- Water bath and thermometer
- Excel sheet
- Cuvette cell with magnetic stirrer
- Membrane Inlet Mass Spectrometer (MIMS)
- Massoft 7 computer software
- Massoft 10 computer program
- MQ water

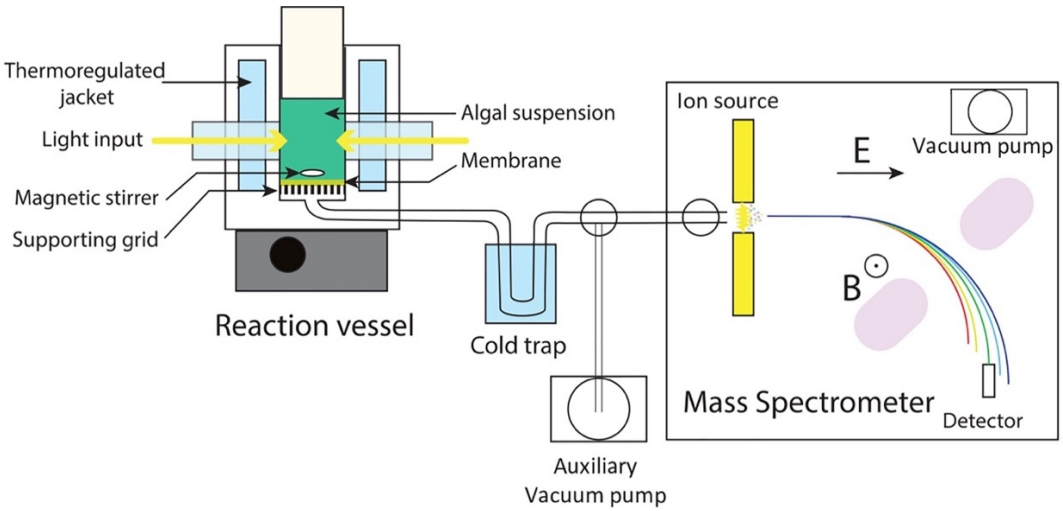


*Figure 5 A schematic similar to the setup of the MIMS unit run in this study including the cuvette cell or reaction vessel with a magnetic stirrer and some type of thermal regulation (Burlacot et al., 2020). The two detectors that were available in the MIMS were faraday and SEM.*

The main difference in the setup in Fig. 5 and the one used in this study was the use of the cold trap. Two water baths were used to regulate the cuvette, rather than a thermoregulated jacket,

and no cold trap was used as the gas was pumped through to the mass spectrometer. Two thermometers were set in each water bath to monitor the controlled temperature as often times the surrounding room was warmer than the water baths. There was no additional light input other than the natural light in the room unless specifically outlined in that experiment timeline. A cover was used to obstruct light from getting in which completely encapsulated the cuvette. The cuvette had five available speeds. The speed of the magnetic stirrer of the cuvette pushes the gas trapped in the water towards the membrane that was located at the bottom of the cuvette. This part was crucial in preventing the gases exchanging in the small headspace at the top of the cuvette. Every time the cuvette was filled with a new sample, the technique tried to prevent a headspace from forming but was not always successful. The cuvette was rinsed out with MQ water three times to prevent culture contamination from previous cultures or from chemical used as stressors.

Procedure:

1. The cuvette attachment was added onto the MIMS
2. The magnetic stirrer was set to speed 3
3. A recirculating flow from the water bath was attached to the cuvette. The water bath was set to 15ºC to keep the culture at the same temperature as the incubator.
    a. Other temperature settings can be 20ºC. This was mostly done for the first couple DMS readings, but was then changed to 15ºC
4. MQ water was passed through the cuvette to wash out any particulates left from previous experiments
5. CHC108 culture was poured into the cuvette and allowed to overflow from the top so there was no headspace left at the top of the cuvette.
6. MIMS vacuum pump was turned on
7. Turn on sample injection valve (button was pressed)
8. Massoft 7 was opened and synced with the MIMS
9. The green valve was slightly opened
10. Wait for pressure to return to the area around $4.0e^{-6}$
    a. Time will cause the pressure to dip below $4.0e^{-6}$
11. The RC interface was turned on
12. On the Massoft 7 software* the green record button was pressed.
    a. *The Massoft 10 software was added and updated in June/July. The overall functions of the software are the same. Similar settings to the ones in Massoft 7 were implemented

13. The baseline was followed for 30 minutes to measure the control
14. Time, temperature, pressure, cuvette speeds were initially recorded. Temperature, pressure, and time were subsequently recorded to ensure that conditions were the same. Deliberate changes made to the environment were recorded, along with time of change, pressure and both temperature readings.
15. Each change was monitored for a minimum of 30 minutes. Each MIMS session was over the course of 6 hours per day. Monitoring of the culture and DMS concentrations could span over 2-3 days.

There were several types of experiments that were run. A cover was put over the cuvette to block out all light to induce stress. Blocking out the light will interfere with the diurnal cycle that occurs naturally and a diurnal cycle was established in the incubator in which the cultures were stored. Other added stressors include $H_2O_2$ and added Cu to induce oxidative stress. Heavy metal loading can occur in the world oceans especially where there is evidence of strong anthropogenic influence. These tests were run over several days. There were five days of MIMS records but some of the tests had several days without records.

# Results

## Culture graphs and growth rates

Counts for the CHC108 cells in unstained samples were gated by cell size (FSC-H) and chlorophyll fluorescence (FL3-H). The gates were set so they did not include any bacteria in the sample. The coccolithophore strain was isolated from other phytoplankton species at the time of field sampling. Symbiotic bacteria were left in as in previous experiments, the coccolithophore strain died without the bacterial products in the environment. The CHC108 strain was significantly larger than the competing bacteria due to the $CaCO_3$ coccolith and were easily isolated in the flow cytometer graph parameters. The peak day determined when the next batch should be started, and the average growth rate was used to determine whether the culture has been altered or contaminated.

The average growth rates for all batches in raw, DNA stain (sybr green), and CMFDA for cultures A and B. The purpose of tracking the growth rates was to ensure that the cultures were not contaminated by external bacteria and to ensure that the coccolithophores were the same for both cell size and that the production of coccoliths. The cell size and the chlorophyll concentrations were taken into consideration because after the initial exponential growth, the cell numbers may not increase but there will be changes to cell size, including the coccolith shell, and the chlorophyll size due to nutrients. Another thing for consideration would be looking at when the coccolithophores would be put under stress. If the stressors were added too early, then the culture would not be fully formed. If the stressors were added too late, then the cells may already be in the stages of dying and would not yield a notable change to the DMS concentrations. This would apply mostly to the raw growth rates and potentially to the CMFDA growth rates as it would measure the cell drawing the dye into the cell membrane. The disconnect with the DNA stain steamed from the glutaraldehyde which aided in fixing the cells and the change in cell number would not be reflective of cell multiplication.

Batch 1

Batch 1 was started on 13-04-23. The culture used was taken from an old culture which was renewed about every 3 weeks. The culture was 16 days old at the time of the MIMS run.

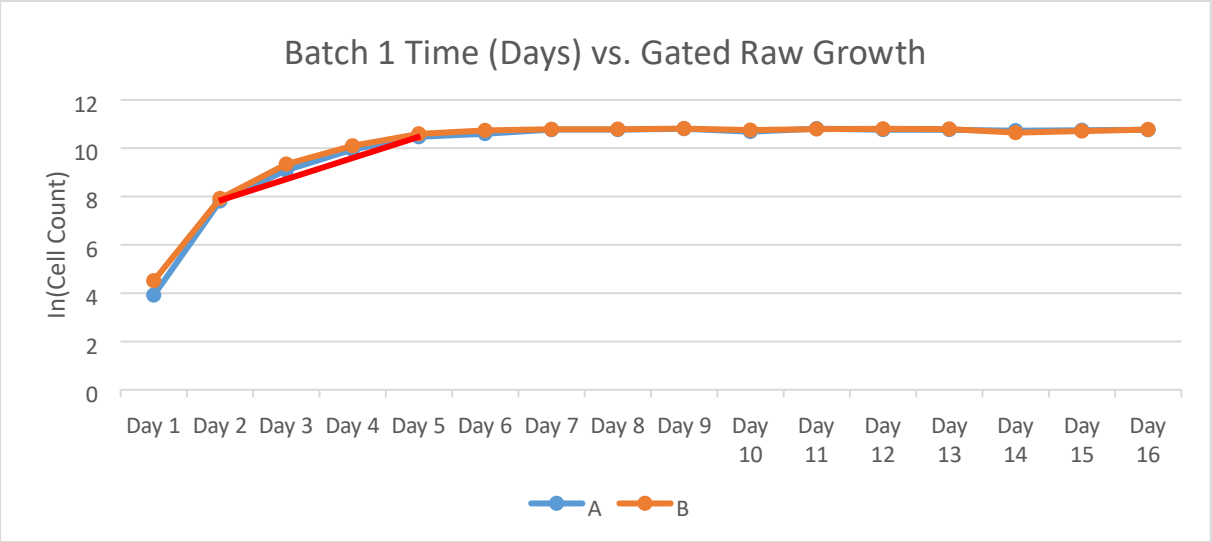


*Figure 6 Batch 1 Gated Raw ln(Cell Counts) vs. Time (days). Batch was grown over the course of 16 days. The gated counts were obtained from a polygon in the raw counts in the FSC-H x FLH-3. Any gaps in the data (Days 6, 7, 8, 13 and 14) were filled in using the =FORECAST function, then the natural log was taken of all the data. Red line represents the exponential growth phase.*

| | Average Growth Rate | Standard Deviation | Doubling time | Peak growth day |
|---|---|---|---|---|
| A | 0.997 $day^{-1}$ | 0.088 | 1.445 doublings $day^{-1}$ | Day 9-11 |
| B | 0.91 $day^{-1}$ | 0.07 | 1.319 doublings $day^{-1}$ | Day 9 |

*Table 1 Batch 1 Gated Counts Average growth rates, with doubling time and peak growth day.*

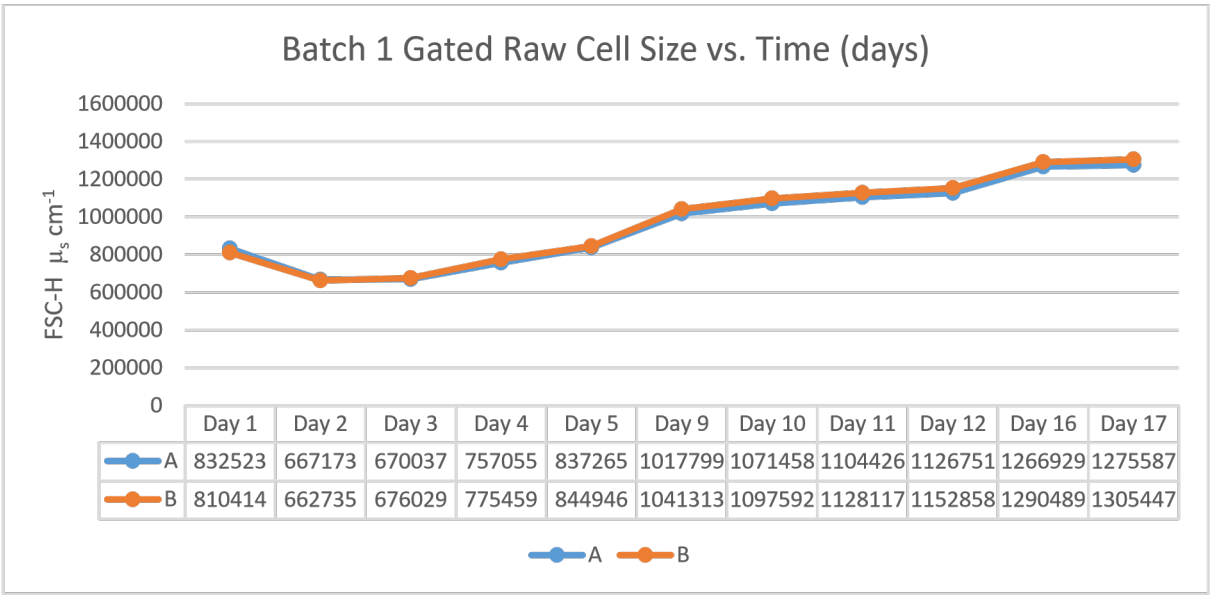


*Figure 7 Gated Raw Cell Size vs. Time (days).*

| | Average Cell Size | Minimum Cell Size | Peak Cell Size | Peak Day |
|---|---|---|---|---|
| A | $9.661x10^5$ | $6.672x10^5$ | $1.276x10^6$ | Day 17 |
| B | $9.805x10^5$ | $6.627x10^5$ | $1.305x10^6$ | Day 17 |

*Table 2 Description of the average, min, and max cell size of cultures A and B. Peak Cell size was also included.*

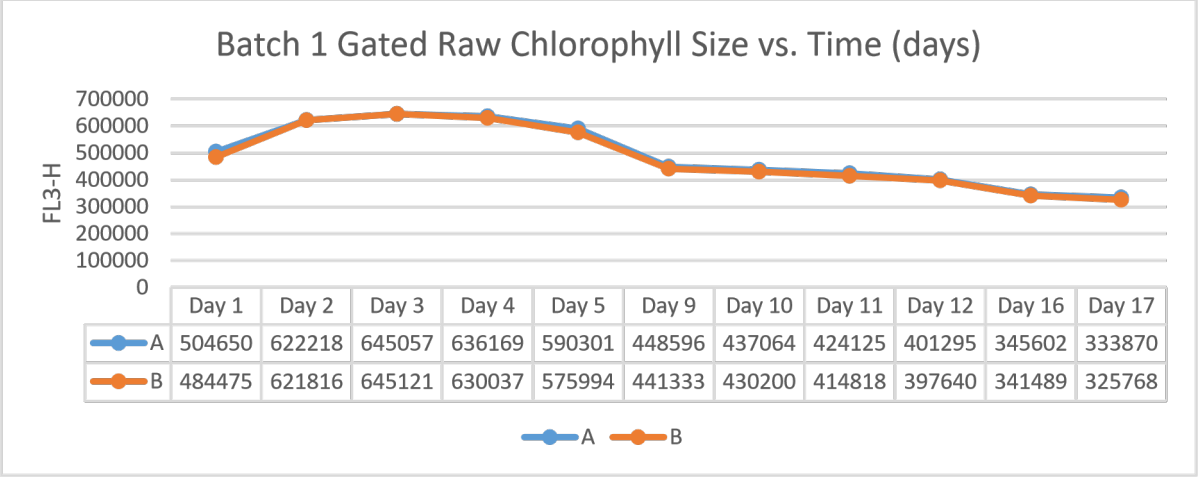


*Figure 8 Batch 1 Gated Raw Chlorophyll Size vs. Time (Days).*

| | Average Chlorophyll Size | Minimum Chlorophyll Size | Maximum Chlorophyll Size | Peak Day |
|---|---|---|---|---|
| A | $4.899x10^5$ | $3.339x10^5$ | $6.451x10^5$ | Day 3 |
| B | $4.826x10^5$ | $3.258x10^5$ | $6.451x10^5$ | Day 3 |

*Table 3 Batch 1 chlorophyll size (average, min, and max) as the culture matures. Looking at the chlorophyll size indicated around what point the cultures start to struggle or decline.*

The average growth rate and standard deviations were taken from the exponential growth phase. The doubling times was determined from the average growth rates. The peak day determined the end of the growth period. The gated average growth rates of A and B have a difference of 0.087 $day^{-1}$ (Table 1). The doubling time of culture A was slightly faster than culture B with a difference of 0.067 doublings $day^{-1}$. The peak growth days were about the same, day 9 (Fig. 6), indicating that culture did not experience any deviations or negative influences. The average cell size between A and B were similar which was to be expected with a difference of $1.44x10^4$ (Table 2). As the culture count increased, as did the cell size with a peak size of $1.276x10^6$ (A) and $1.305x10^6$ (B) on Day 17 (Fig. 5). The chlorophyll size (per cell) peaked on day 3 (Fig. 6) with a max chlorophyll (per cell) size of $6.451x10^5$ (A) and $6.451x10^5$ (B). Both cultures have similar chlorophyll sizes with the difference being $7.296x10^3$ (Table 3). There was a sharp decline in chlorophyll size between Day 5 and Day 9 with a continued decline through to Day 17 (Fig. 8).

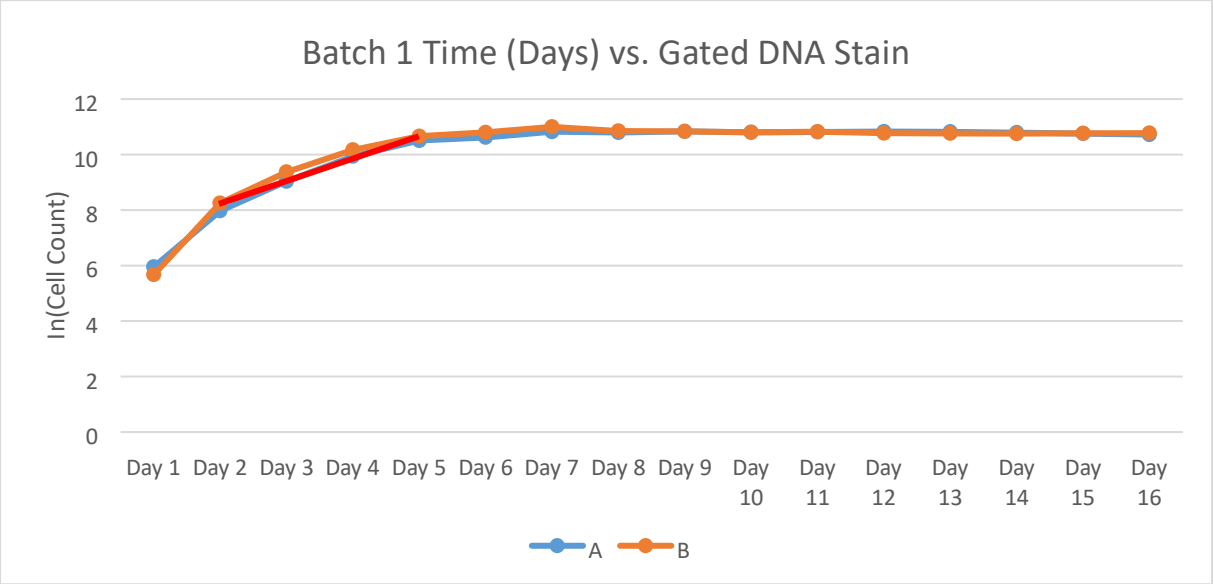


*Figure 9 Batch 1 Gated DNA Stain ln(Cell Counts) vs. Time (days). Days without data (Day 6, 7, 8, 13, and 14) were filled using =FORECAST. Batch 1 was grown over the course of 16 days. Red line represents the exponential growth phase.*

| | Average Growth Rate | Standard Deviation | Doubling Time | Peak Growth Day |
|---|---|---|---|---|
| A | 0.897 $day^{-1}$ | 0.031 | 1.3 doublings $day^{-1}$ | Day 9 |
| B | 1.043 $day^{-1}$ | 0.068 | 1.512 doublings $day^{-1}$ | Day 9 |

*Table 4 Batch 1 Gated Stain Average Growth Rate, Doubling time, and peak growth day*

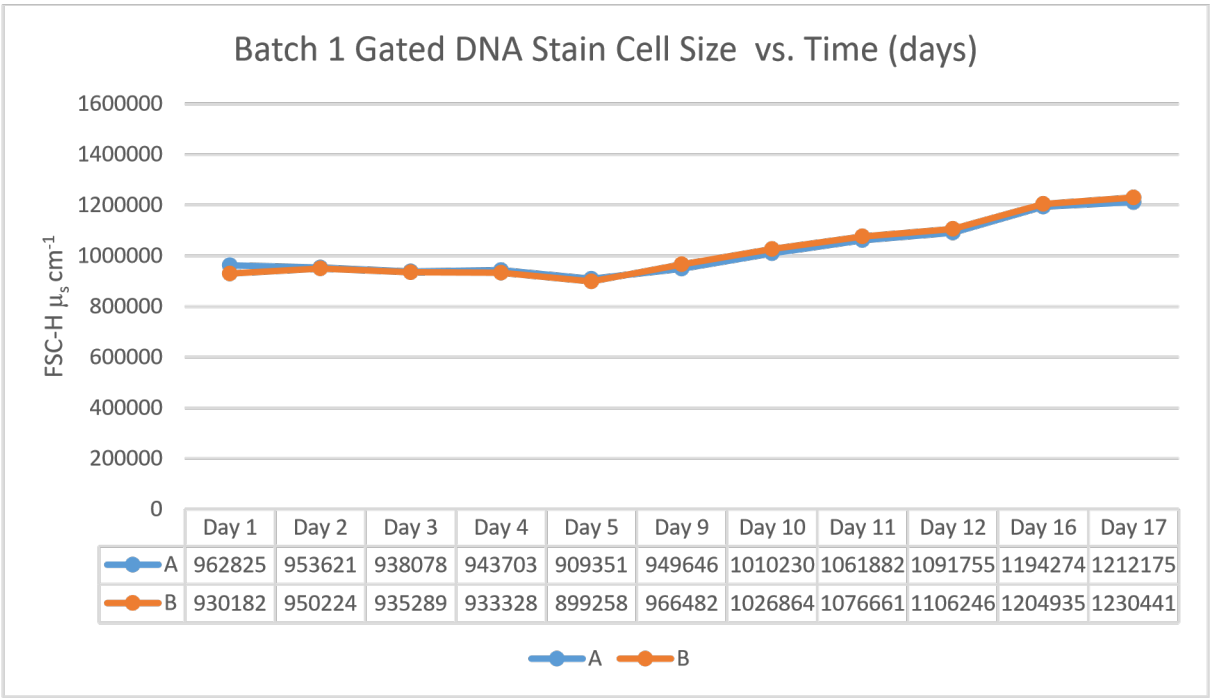


*Figure 8 Batch 1 Gated DNA Stain Cell Size vs. Time (days).*

| | Average Cell Size | Minimum Cell Size | Maximum Cell Size | Peak Day |
|---|---|---|---|---|
| A | $1.021x10^6$ | $9.094x10^5$ | $1.212x10^6$ | Day 17 |
| B | $1.024x10^6$ | $8.993x10^5$ | $1.23x10^6$ | Day 17 |

*Table 5 Looked at cell size (average, min, max) for cultures A and B for the DNA-stained cells.*

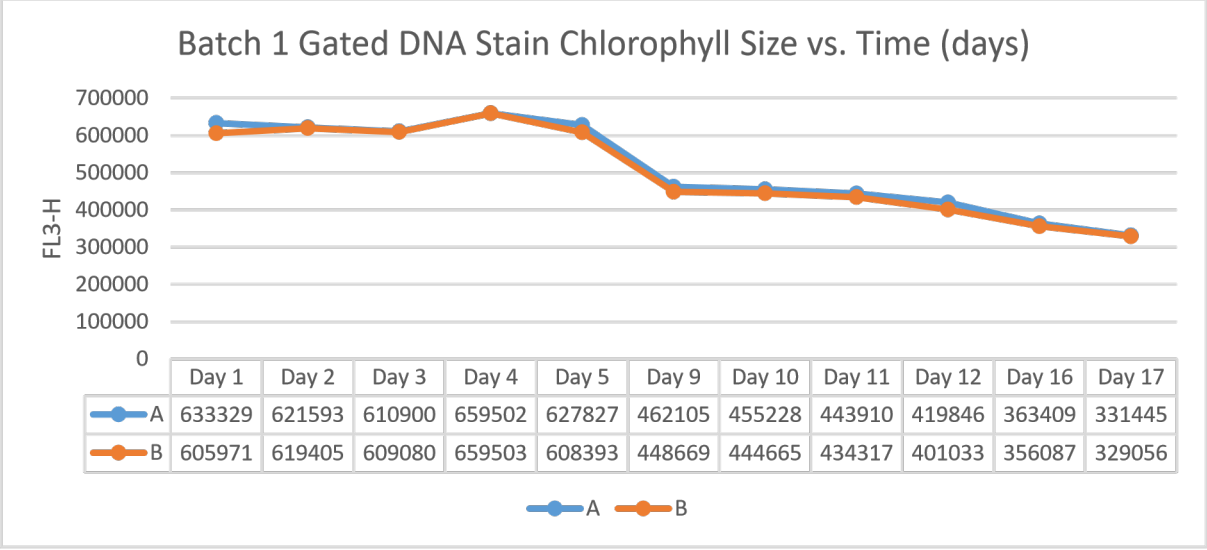


*Figure 11 Batch 1 Gated DNA Stain Chlorophyll Size vs. Time (Days). The FL3-H channel measures auto-fluorescence of chlorophyll.*

| | Average Chlorophyll Size | Minimum Chlorophyll Size | Maximum Chlorophyll Size | Peak Day |
|---|---|---|---|---|
| A | $5.117x10^5$ | $3.314x10^5$ | $6.595x10^5$ | Day 4 |
| B | $5.015x10^5$ | $3.291x10^5$ | $6.595x10^5$ | Day 4 |

*Table 6 Batch 1 Chlorophyll size (average, min, and max) for DNA-stained cells.*

The gated DNA Stain average growth rate between A and B have a difference of 0.146 $day^{-1}$ (Table 4). The doubling time of culture B is faster than Culture A but the peak growth rate than culture A and B is day 9 (Fig. 9). The difference in doubling time between A and B was 0.212 doublings per day. The peak day of both cultures was Day 9. There were no major differences in the CMFDA after Day 9. The average cell size between A and B were similar with a difference of 2942 which was to be expected (Table 5). The cell size increased as the culture matured with a peak cell size on Day 17 (Fig. 8) with a cell size of 1212175 (A) and $1.23x10^6$ (B). The average chlorophyll size between A and B were the same with a difference of $1.027x10^4$ (Table 6). The peak chlorophyll occurred on Day 4 (Fig. 11) with a max of $6.595x10^5$ (A) and $6.595x10^5$ (B). There was a large decline of chlorophyll size between Day 5 and Day 9 with a continued decrease through to Day 17.

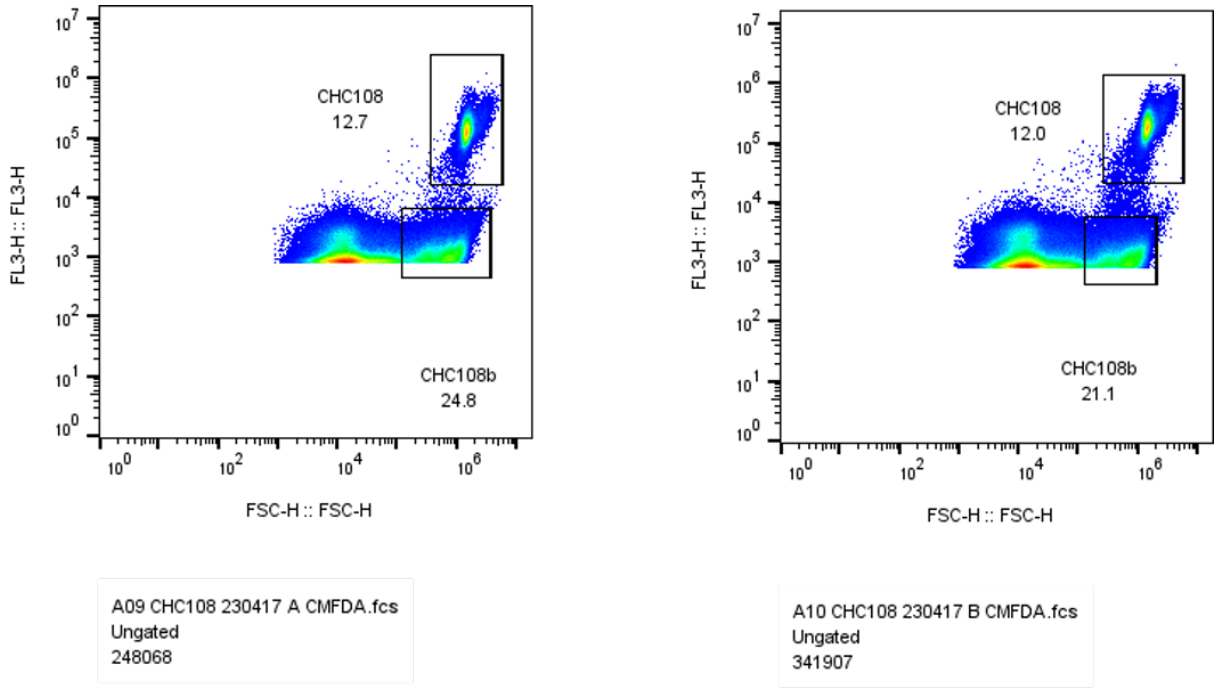


*Figure 12 Batch 1 FSC-H vs. FL3H for A (left) and B (right) stained with CMFDA. The CHC108 gated areas were the determined coccolithophores. The CHC108b were either free coccoliths or coccoliths that have been compromised. Graphs were made using Flow-Jo.*

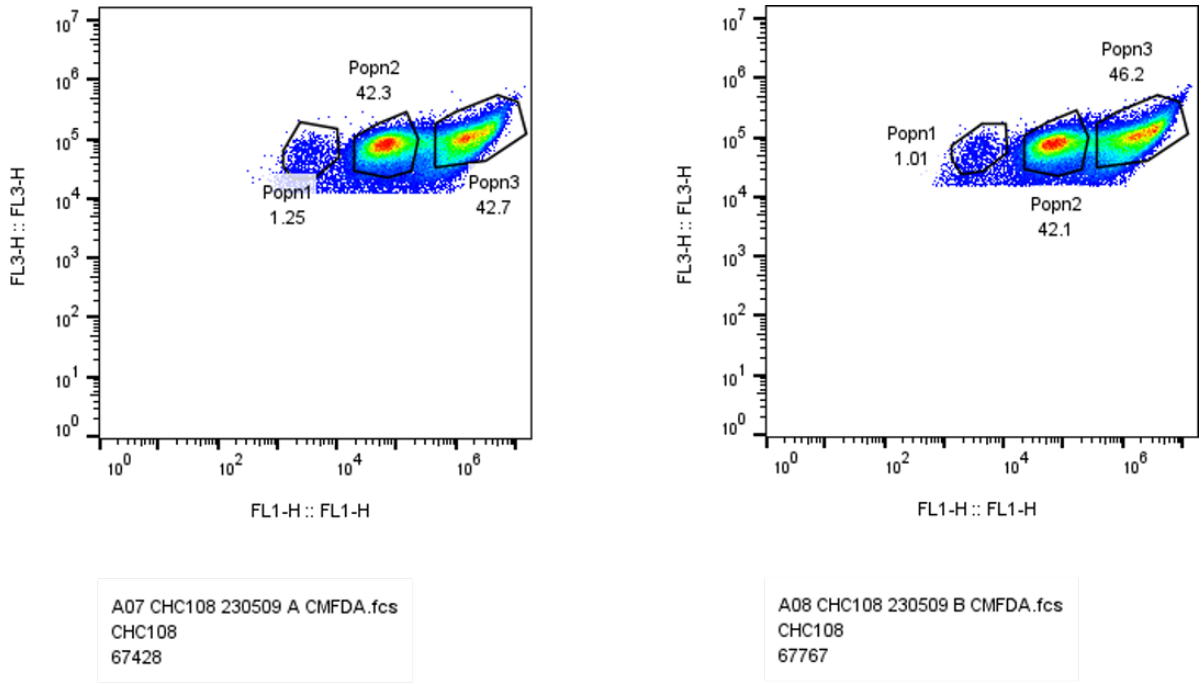


*Figure 13 Batch 1FL1-H vs. FL3-H for A (left) and B (right) with three distinctive coccolithophore populations.*

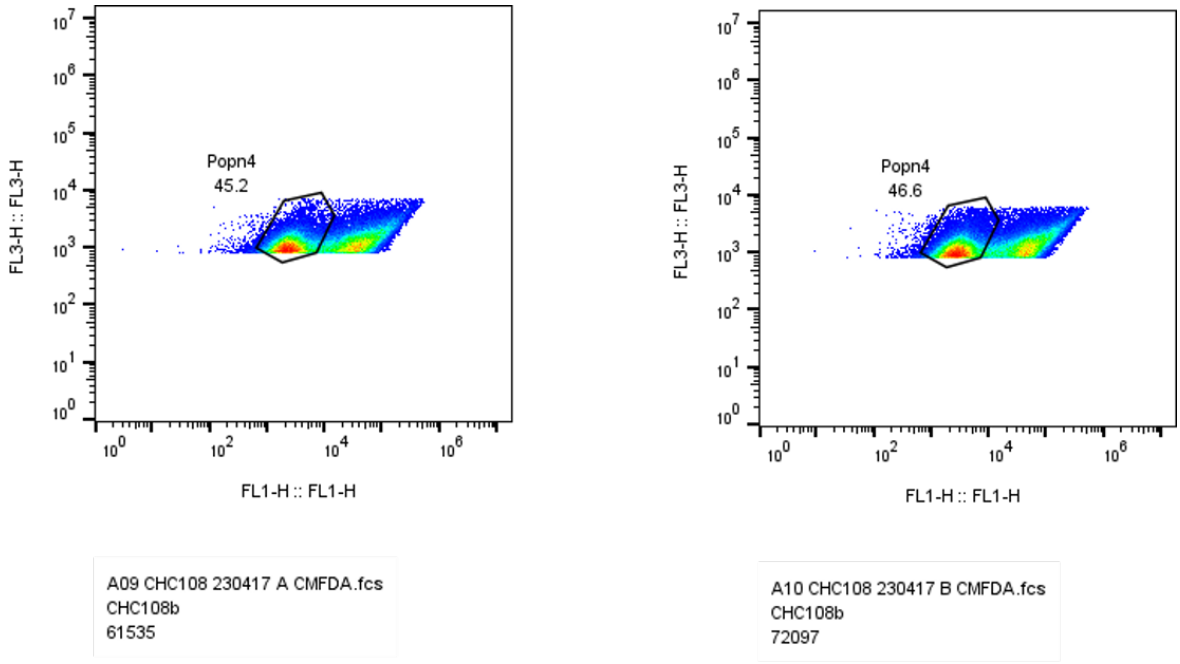


*Figure 14 Batch 1 FL1-H vs. FL3H for A (left) and B (right). Further gating section for the coccolithophore populations in Fig. 48*

Three coccolithophore populations were observed within the lower portion of Fig. 10. The left most one was the smallest and least stained with the CMFDA (Fig. 13). The other coccolithophore populations, denoted as popn2 and popn3 had significantly more thiol content. Upon further inspection of the coccolithophore population in Fig. 12, another population that had been overlapped was unveiled denoted as popn4 (Fig. 14). Overlaps in population due to the bacteria having similar sizing can cause populations to be overlooked.

Batch 2

Batch 2 was started on 09-05-23.

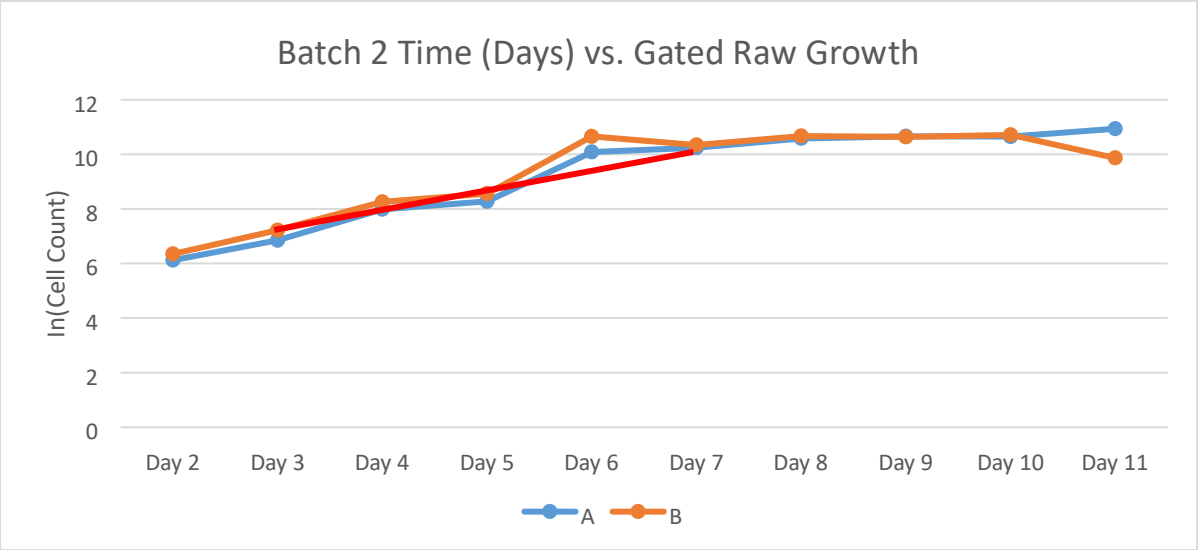


*Figure 15 Batch 2 gated raw ln(Cell Counts) vs time (days). Days without data (Day 5 and 6) were filled using =FORECAST. Batch 2 was grown over the course of 11 days. The gated counts were taken from a polygon in the upper right corner of the FSC-H x FLH-3. Red line represents the exponential growth phase.*

| | Average growth rate | Standard deviation | Doubling time | Peak growth Day |
|---|---|---|---|---|
| A | 0.529 $day^{-1}$ | 0.01 | 0.767 doublings $day^{-1}$ | Day 9 |
| B | 0.516 $day^{-1}$ | 0.01 | 0.749 doublings $day^{-1}$ | Day 10 |

*Table 7 Batch 2 Raw Gated average growth rates, doubling times, and peak growth day*

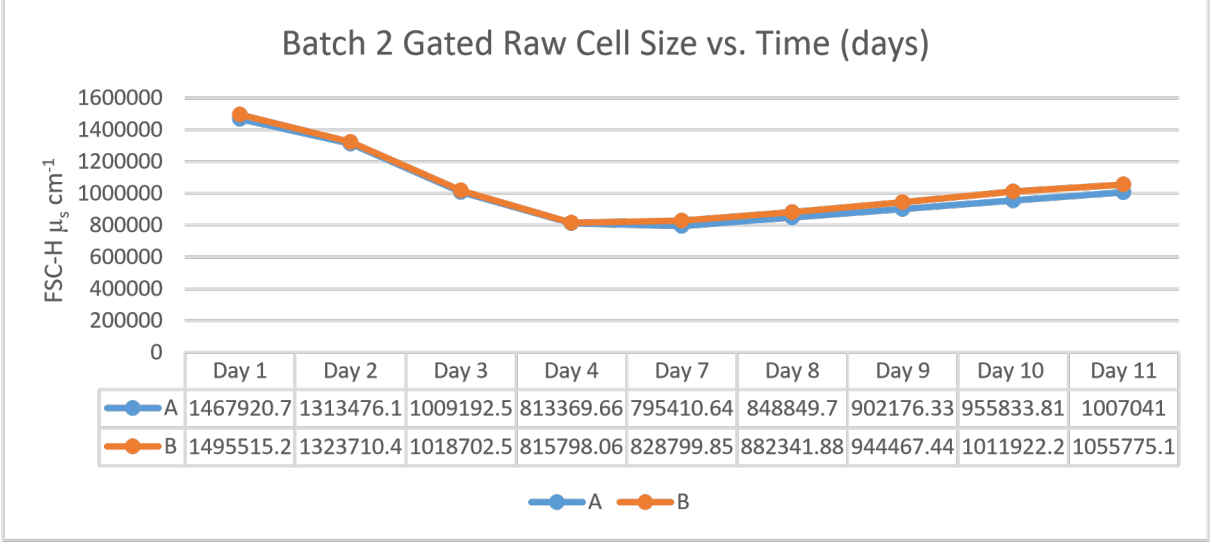


*Figure 14 Batch 1 Gated Raw Cell Size vs. Time (days).*

| | Average Cell Size | Minimum Cell Size | Maximum Cell Size | Peak Day |
|---|---|---|---|---|
| A | $1.013x10^6$ | $7.954x10^5$ | $1.468x10^6$ | Day 1 |
| B | $1.042x10^6$ | $8.158x10^5$ | $1.496x10^6$ | Day 1 |

*Table 8 Batch 2 cell size (average, min, and max) for raw A and B cultures*

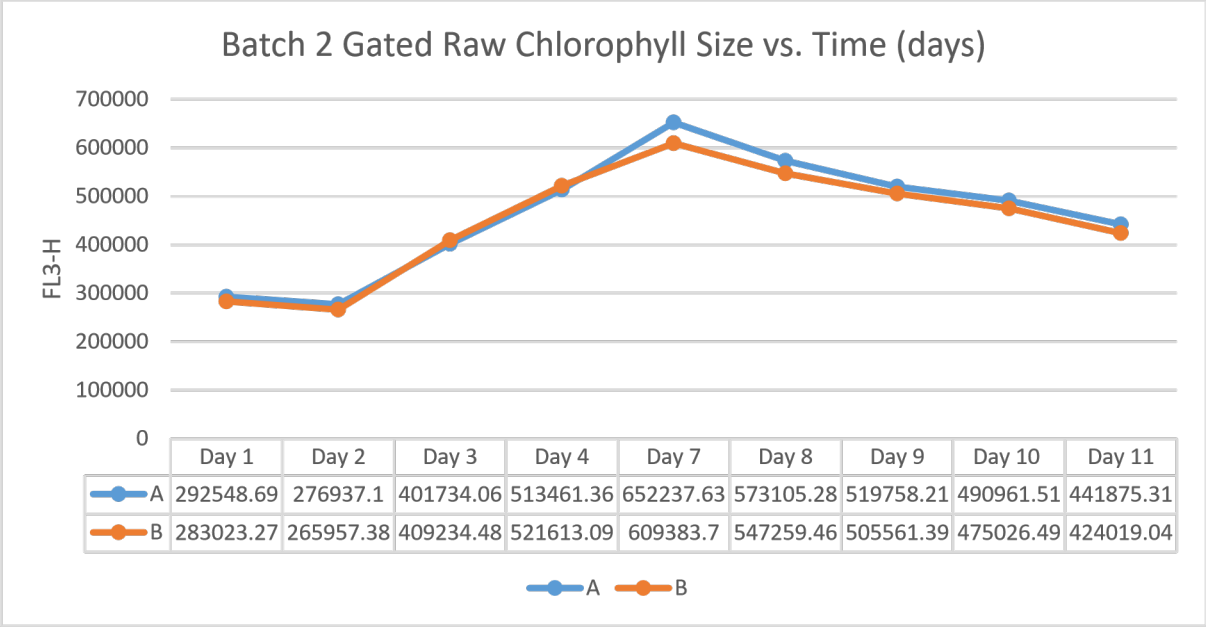


*Figure 17 Batch 2 Gated Raw Chlorophyll Size vs. Time (days).*

| | Average Chlorophyll Size | Minimum Chlorophyll Size | Maximum Chlorophyll Size | Peak Day |
|---|---|---|---|---|
| A | $4.625x10^5$ | $2.769x10^5$ | $6.522x10^5$ | Day 7 |
| B | $4.49x10^5$ | $2.66x10^5$ | $6.094x10^5$ | Day 7 |

*Table 9 Batch 2 raw chlorophyll size (average, min, and max).*

The average gated growth rate between A and B were the same with a difference of 0.013 $day^{-1}$ (Table 7). Culture A had a slightly faster doubling time than culture B with a difference of 0.018 doublings $day^{-1}$. The peak growth days were reflective of the doubling time with peak growth A at day 9 and the peak growth of B on day 10 (Fig.15). Cultures A and B had similar average cell size with a difference of $2.931x10^4$ (Table 8). Day one was the peak for both A and B (Fig. 16) with a sharp decline in cell size till Day 4. The deviation between A and B started on Day 7 and continued to expand till Day 11 with the largest difference of $4.872x10^4$. The average chlorophyll sizes were similar overall with a difference between the two being $1.35x10^4$ (Table 9), with deviations starting on Day 7 and continued through Day 11 (Fig. 17). Both chlorophyll sizes peaked on Day 7 with the largest difference in size which occurred at $4.285x10^5$.

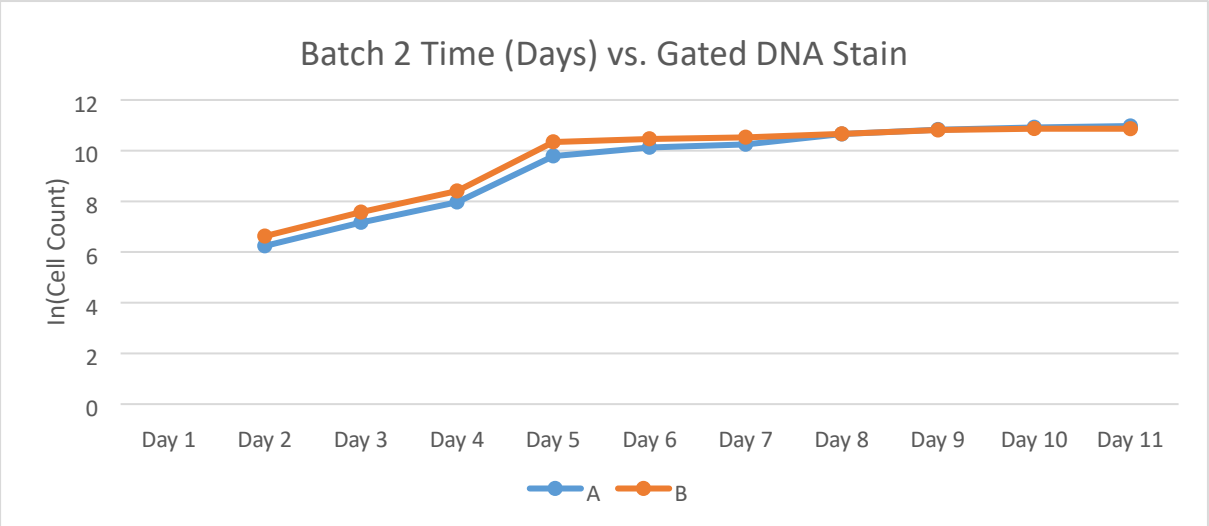


*Figure 18 Gated DNA Stain ln(Cell Counts) vs. time (days). Days without data (Days 5 and 6) were filled using =FORECAST. Batch 2 was grown over the course of 11 days. The gated stain was taken from SSC-A x FLH-4.*

| | Average growth rate | Standard deviation | Doubling time | Peak growth day |
|---|---|---|---|---|
| A | 0.519 $day^{-1}$ | 0.01 | 0.752 doublings $day^{-1}$ | Day 11 |
| B | 0.502 $day^{-1}$ | 0.008 | 0.728 doublings $day^{-1}$ | Day 10 |

*Table 10 Gated DNA Stain average growth rates, doubling times, and peak growth days.*

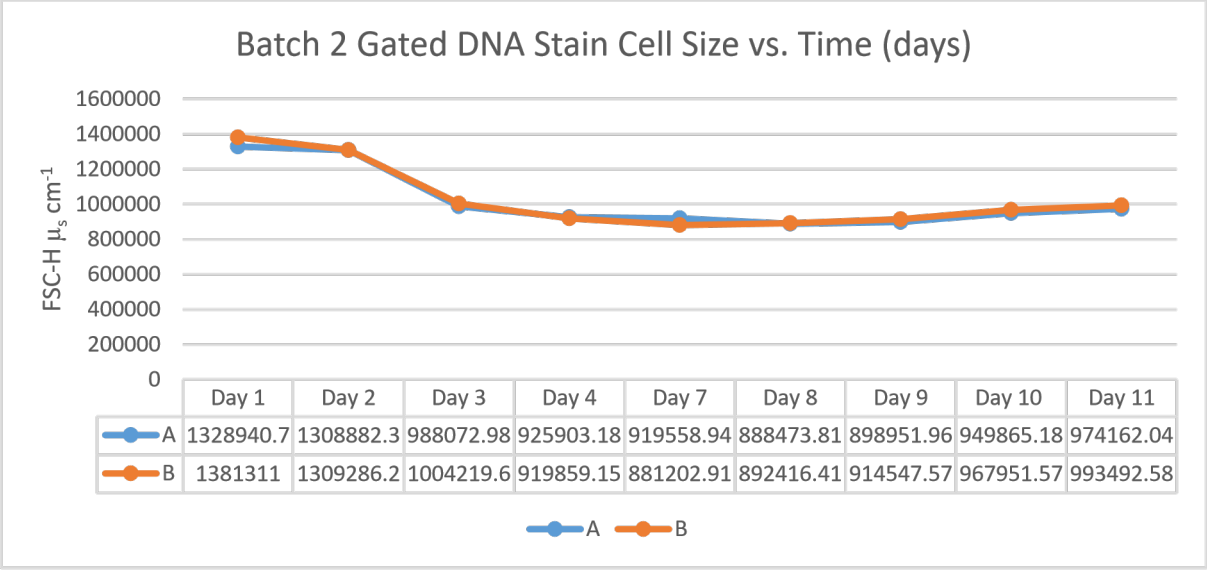


*Figure 17 Batch 2 Gated DNA Stain Cell Size vs. Time (days).*

| | Average Cell Size | Minimum Cell Size | Maximum Cell Size | Peak Day |
|---|---|---|---|---|
| A | $1.02x10^6$ | $8.885x10^5$ | $1.329x10^6$ | Day 1 |

| | | | | |
|---|---|---|---|---|
| B | $1.029x10^6$ | $8.812x10^5$ | $1.38x10^6$ | Day 1 |

*Table 11 Batch 2 cell size (average, min and max) for cells with DNA stain.*

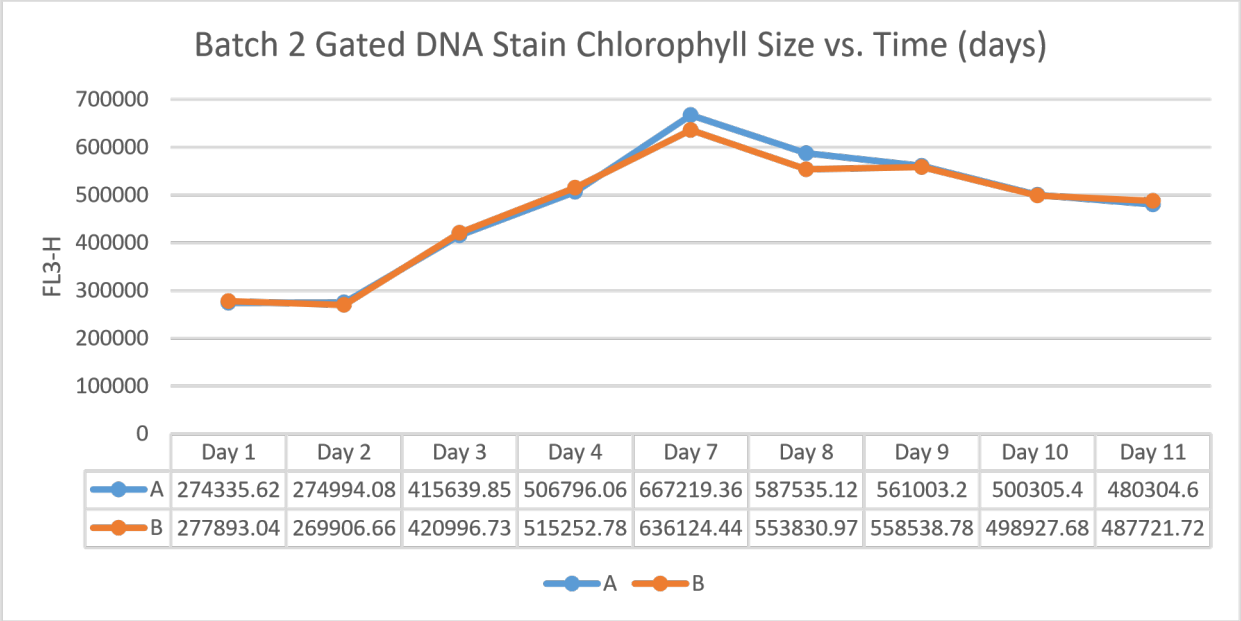


*Figure 20 Batch 2 Gated DNA Stain Chlorophyll Size vs. Time (days).*

| | Average Chlorophyll Size | Minimum Chlorophyll Size | Maximum Chlorophyll Size | Peak Day |
|---|---|---|---|---|
| A | $4.742x10^5$ | $2.743x10^5$ | $6.672x10^5$ | Day 7 |
| B | $4.688x10^5$ | $2.699x10^5$ | $6.361x10^5$ | Day 7 |

*Table 12 Batch 2 DNA Stain cultures A and B chlorophyll sizes (average, min, and max).*

The average growth rates of gated DNA stain of cultures A and B were the same with a difference of 0.017 $day^{-1}$ (Table 10). The doubling times of cultures A and B were the same as well with a difference of 0.024 doublings $day^{-1}$. Culture A had a slightly faster doubling time when compared to culture B but had a later peak growth day at day 11 (Fig. 18), while culture B had a peak growth on day 10. The average cell size between A and B were similar with a slight difference of 9053 (Table 11). There were slight deviations in cell size on Day 1 and Day 7 (Fig. 19). There were no large fluctuations throughout the culture. The average chlorophyll size between A and B were similar with a difference between the two being $5.438x10^3$ with big deviations occurring on Day 7 and Day 8 (Fig. 20). The difference in max chlorophyll sizes was $3.109x10^4$ (Table 12).

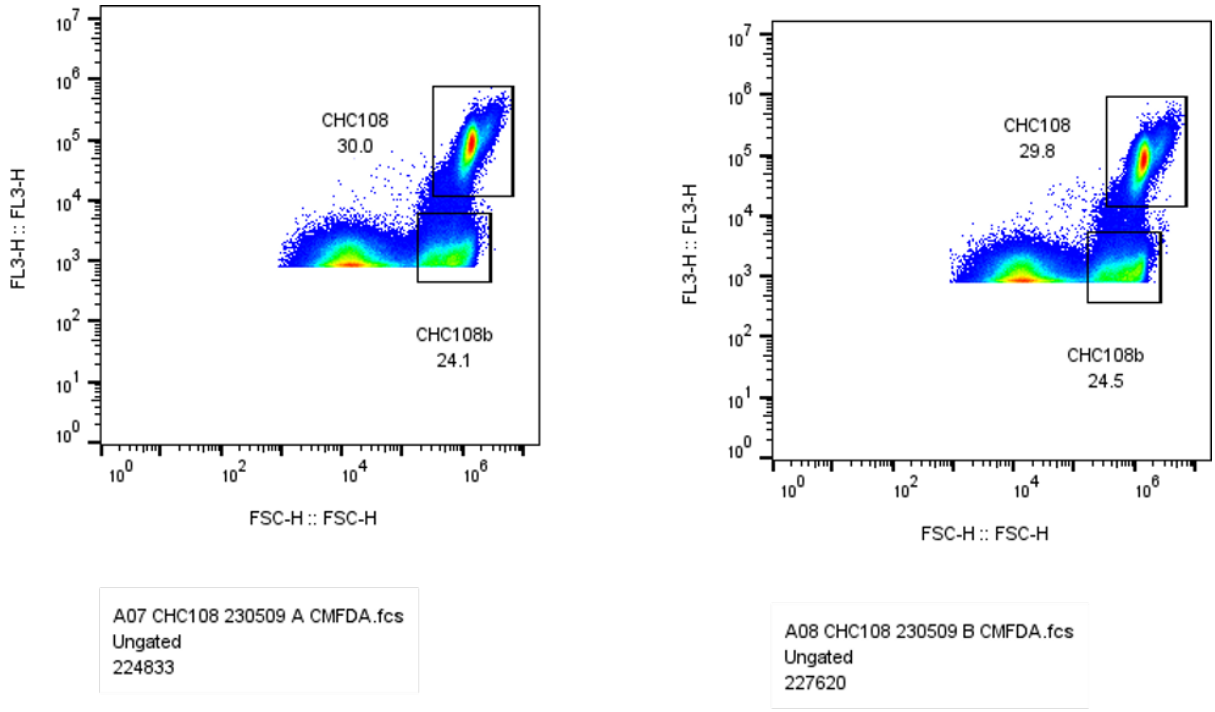


*Figure 21 Batch 2 FSC-H vs. FL3-H for A (left) and B (right). Gated area, CHC108, was determined to be the coccolithophores. The other areas were bacterial cultures and coccoliths that had been precipitated out.*

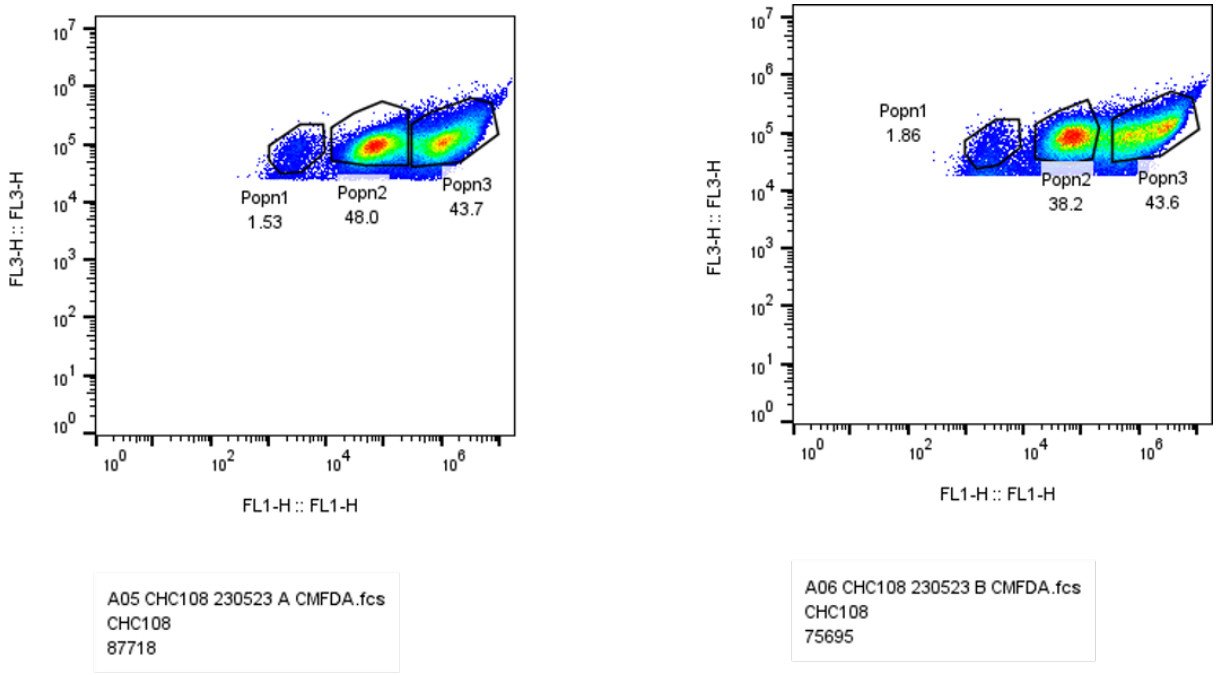


*Figure 22 Batch 2 FL1-H vs. FL3-H for A (left) and B (right) stained with CMFDA. The three gates are different coccolithophore populations within the cultures.*

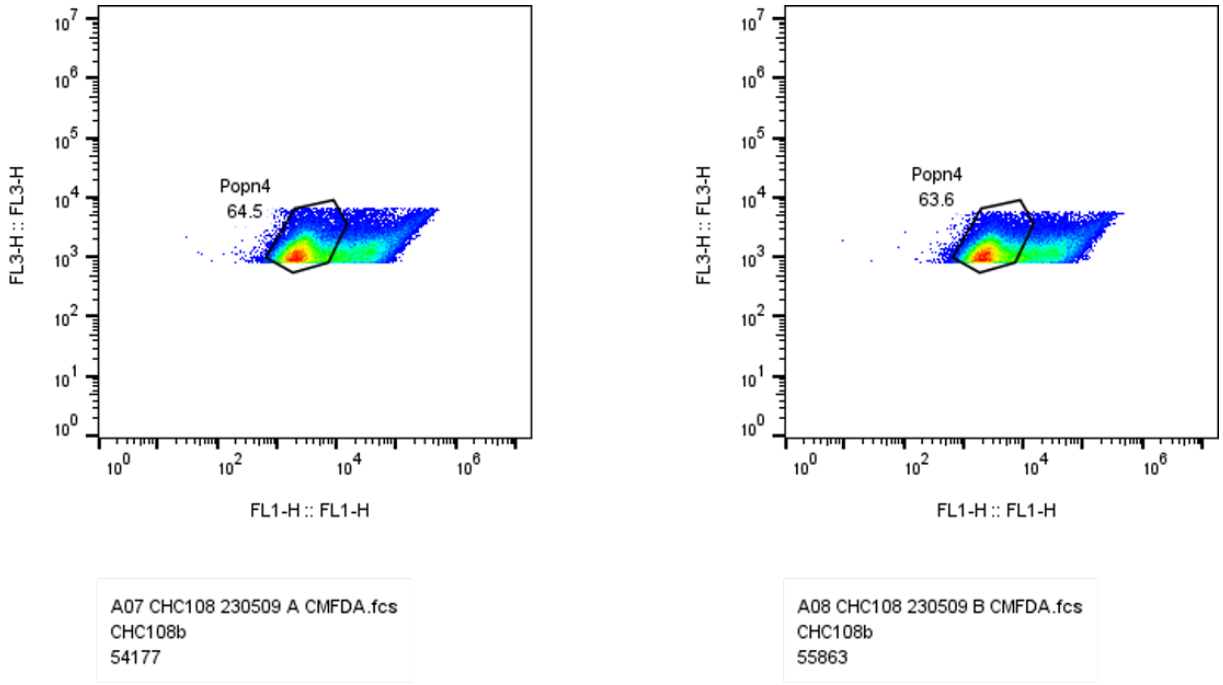


*Figure 23 Batch 2 FL1-H vs. FL3-H for A (left) and B (right) stained CMFDA. Further separating the different coccolithophore populations.*

There were three coccolithophore populations that were identified with the CMFDA stain. The population that was denoted with popn1 had very little thiol in the cells and were not easily stained. The other two populations had high concentrations of thiol in the cells. In culture B, there appeared to be another population in popn3 located on the right side of the gate (Fig. 22). Expanding the area around popn2 and popn3, there was another population within the same size range as popn2, which was denoted by popn4 (Fig. 23). This fourth population also had a high thiol concentration.

Batch 3

Batch 3 was started on 23-05-23. Data on day 3 was skewed for both cultures due to mechanical errors with the flow cytometer that were repaired the following day for testing. For culture A there was an unusual spike in cell count. Culture B did not register that there were any cells in the sample. This was due to a technical error and was resolved the next day of sampling.

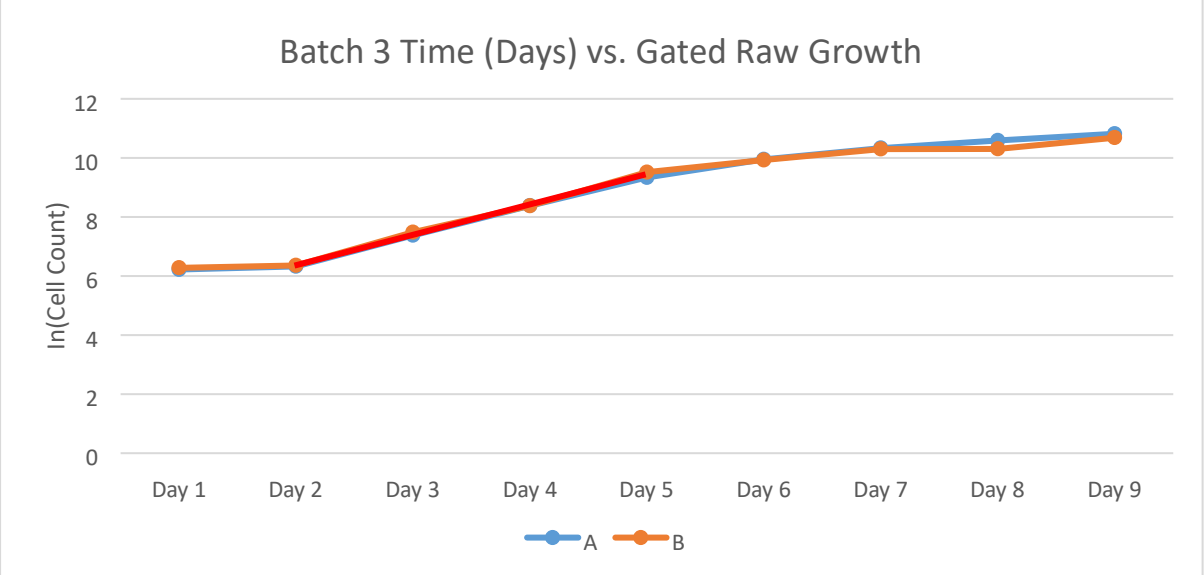


*Figure 24 Batch 3 gated raw ln(Cell Count) vs. time (days). Days without data (Day 5 and 6) were filled using =FORECAST. Batch 3 was grown over the course of 9 days. The gated counts come from a polygon drawn on the FSC-H x FLH-3. Red line represents the exponential growth.*

| | Average growth rate | Standard deviation | Doubling time | Peak growth day |
|---|---|---|---|---|
| A | 0.514 $day^{-1}$ | 0.007 | 0.745 doublings $day^{-1}$ | Day 9 |
| B | 0.499 $day^{-1}$ | 0.006 | 0.723 doublings $day^{-1}$ | Day 9 |

*Table 13 Batch 3 Gated Raw average growth rates, doubling times, and peak growth day*

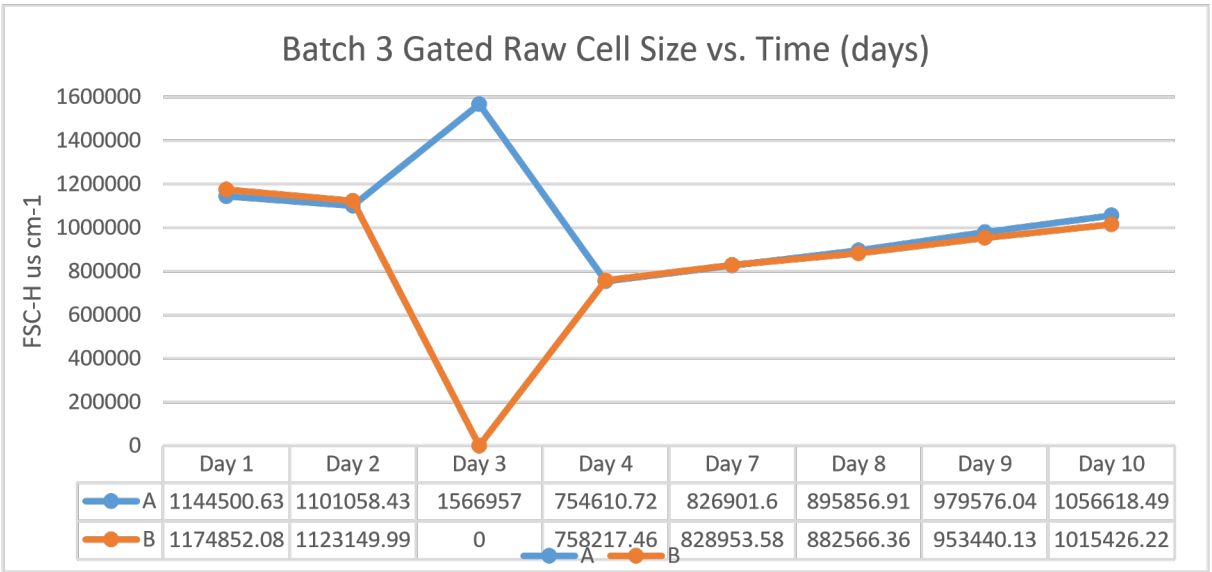


*Figure 25 Batch 3 Gated Raw Cell Size vs. Time (days). Day 3 had some data that was skewed.*

| | Average Cell Size | Minimum Cell Size | Maximum Cell Size | Peak Day |
|---|---|---|---|---|
| A | $1.041x10^6$ | $7.546x10^5$ | $1.567x10^6$ | Day 3 |
| B | $8.421x10^5$ | 0 | $1.015x10^6$ | Day 1 |

*Table 14 Batch 3 raw cell size (average, min, and max) of cultures A and B.*

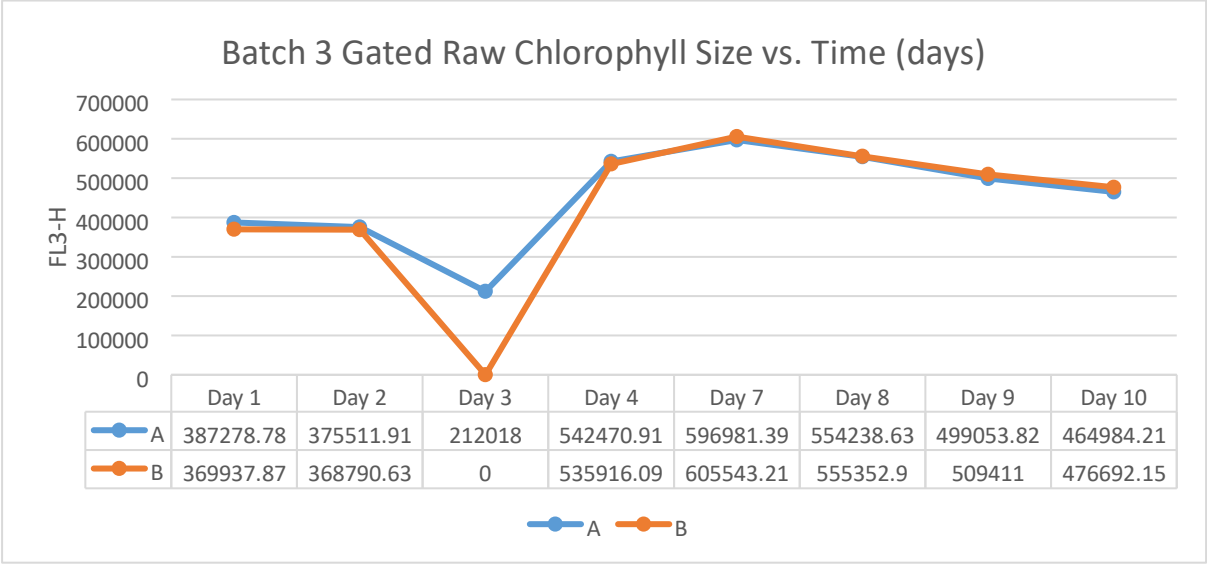


*Figure 26 Batch 3 Gated Raw Chlorophyll Size vs. Time (days). Day 3 had some data that was skewed.*

| | Average Chlorophyll Size | Minimum Chlorophyll Size | Maximum Chlorophyll Size | Peak Day |
|---|---|---|---|---|
| A | $4.541x10^5$ | $2.12x10^5$ | $5.97x10^5$ | Day 7 |
| B | $4.277x10^5$ | 0 | $6.055x10^5$ | Day 7 |

*Table 15 Batch 3 Raw chlorophyll sizes (average, min, and max).*

Average gated raw growth rate of both A and B were remarkably similar with a difference of 0.015 $day^{-1}$ (Table 13). The doubling times of both A and B were close with a difference of 0.022 doublings $day^{-1}$. Both cultures had peaked growth that occurred on day 9 (Fig. 24) which were reflective of the doubling times. Day 3 culture B data was skewed. The average cell size without Day 3 data was $9.624x10^5$ for culture B and $9.656x10^5$. The difference in average cell size was $1.987x10^5$ including the Day 3 data and $3.217x10^3$ excluding the Day 3 data. The peak day for culture A was Day 3, but not including the Day 3 data, the peak was Day 1 (Table 14). The peak day for culture B was Day 1. As with the cell size data, Day 3 skewed the averages of the chlorophyll size. The average chlorophyll size A without the Day 3 data was $4.886x10^5$ and the average chlorophyll size without the Day 3 data for culture B was $4.888x10^5$ (Fig. 26). The difference in average sizes between A and B, with Day 3 data was $2.636x10^4$ and excluding the day 3 data was 160.6 (Table 15). The peak growth for both A and B occurred on Day 7.

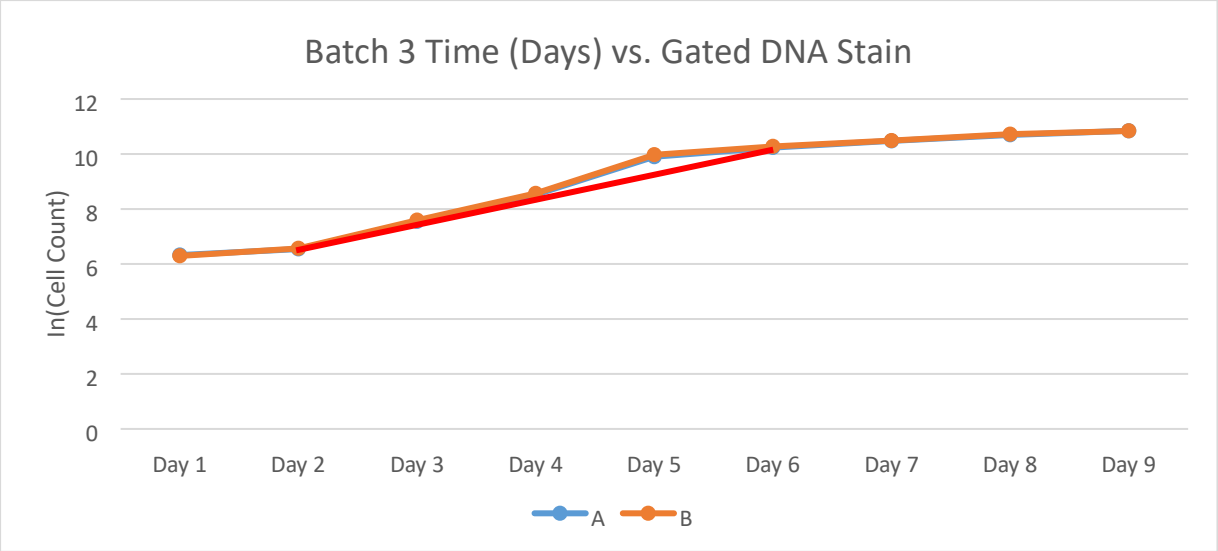


*Figure 27 Gated DNA Stain ln(Cell Counts) vs. time (days). Days without data (Day 5 and 6) were filled using =FORECAST. Batch 3 was grown over the course of 9 days. The gated count comes from a polygon grown on the SCC-A x FLH-4 graph. Red line represents the exponential growth phase.*

| | Average growth rate | Standard deviation | Doubling time | Peak growth day |
|---|---|---|---|---|
| A | 0.52 $day^{-1}$ | 0.007 | 0.753 doublings $day^{-1}$ | Day 9 |
| B | 0.532 $day^{-1}$ | 0.007 | 0.771 doublings $day^{-1}$ | Day 9 |

*Table 16 Batch 3 Gated DNA Stain average growth rates, doubling times, and peak growth day.*

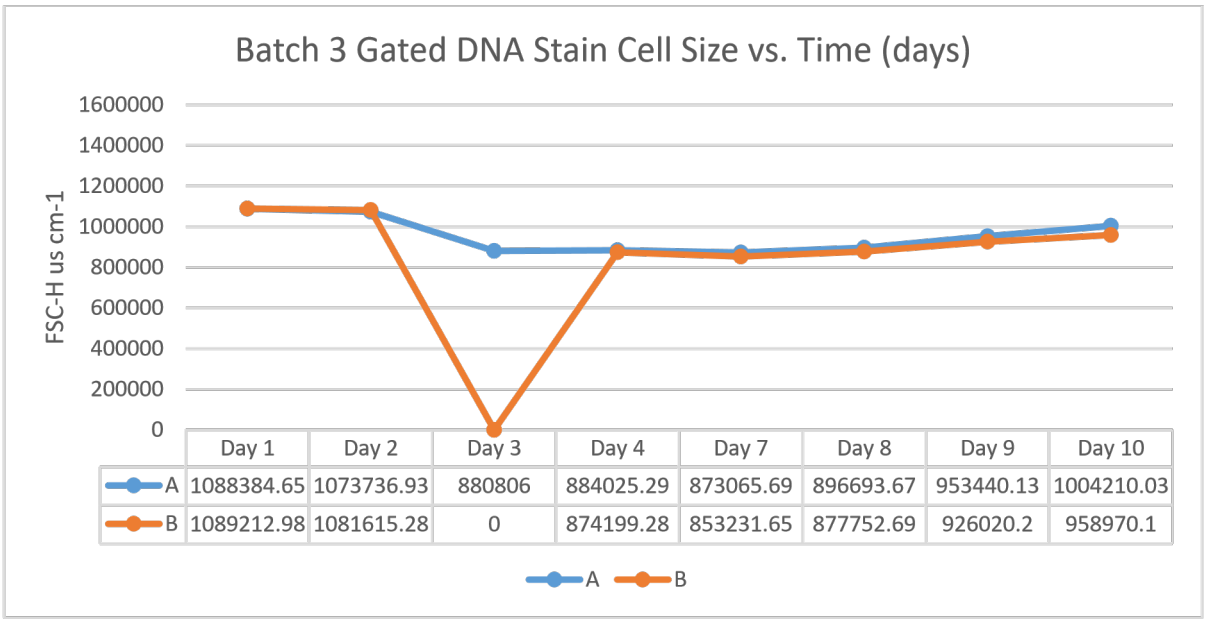


*Figure 28 Batch 3 Gated DNA Stain Cell Size vs. Time (days). Day 3 had some data that was skewed.*

| | Average Cell Size | Minimum Cell Size | Maximum Cell Size | Peak Day |
|---|---|---|---|---|
| A | $9.568x10^5$ | $8.731x10^5$ | $1.088x10^6$ | Day 1 |
| B | $8.326x10^5$ | 0 | $1.089x10^6$ | Day 1 |

*Table 17 Batch 3 DNA Stain cell size (average, min, and max).*

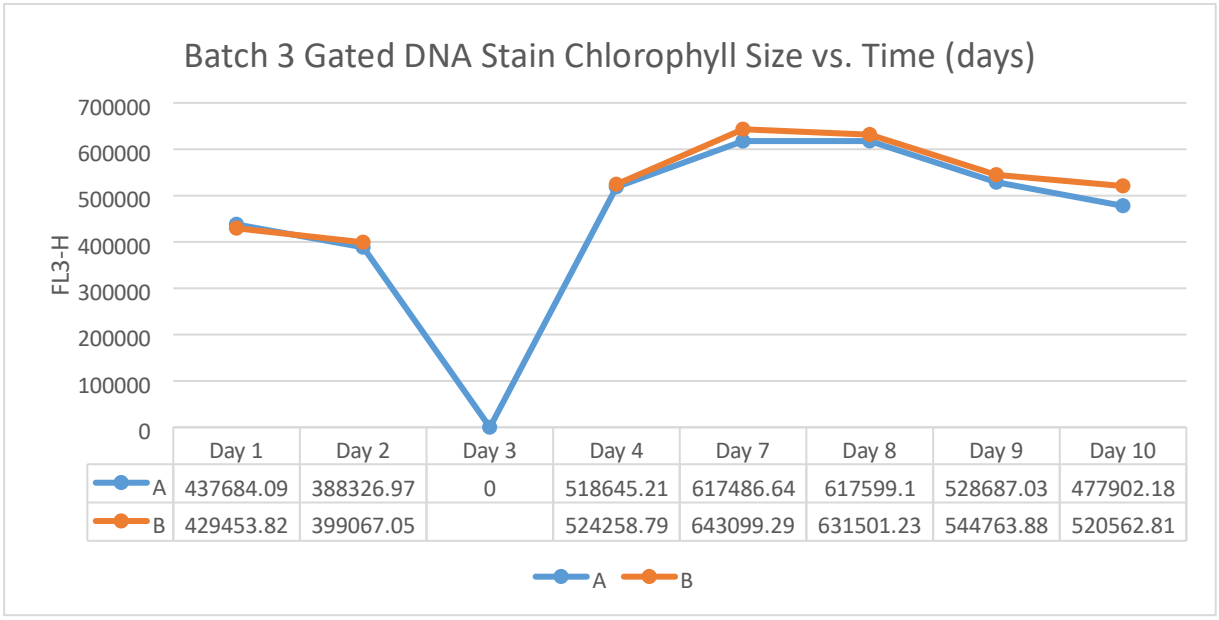


*Figure 29 Batch 3 Gated DNA Stain Chlorophyll Size vs. Time (days). Day 3 had some data that was skewed.*

| | Average Chlorophyll Size | Minimum Chlorophyll Size | Maximum Chlorophyll Size | Peak Day |
|---|---|---|---|---|
| A | $4.78x10^5$ | $2.382x10^5$ | $6.176x10^5$ | Day 8 |
| B | $4.616x10^5$ | 0 | $6.431x10^5$ | Day 7 |

*Table 18 Batch 3 DNA Stain Chlorophyll Size (average, min and max).*

The average gated DNA stain growth rates of A and B were remarkably similar with a difference of 0.012 $day^{-1}$ (Table 16). The doubling time of cultures A and B had a negligible difference of 0.018 doublings $day^{-1}$. Both cultures had growth peak that occurred on the same day, Day 9 (Fig. 27). Similar to the raw data, Day 3 data skewed the averages. The average cell size A without Day 3 data was $9.677x10^5$ and the average cell size for culture B without the Day 3 data was $9.516x10^57$. The difference in average cell size between A and B including the Day 3 data was $1.242x10^5$ and without was $1.608x10^4$ (Table 17). Both cultures had peak cell size on Day 1 with a difference between the two of them was 828.33. Day 3 data skewed the average chlorophyll size for A and B. The averages excluding day 3 data for culture A was $5.123x10^5$ and for culture B was $5.275x10^5$ (Table 18). The difference between A and B including Day 3 data was $1.645x10^4$ and excluding the Day 3 data was $1.52x10^4$. Culture A and B had different peak day; culture A peaked on Day 8 and culture B peaked on Day 7 (Fig.29).

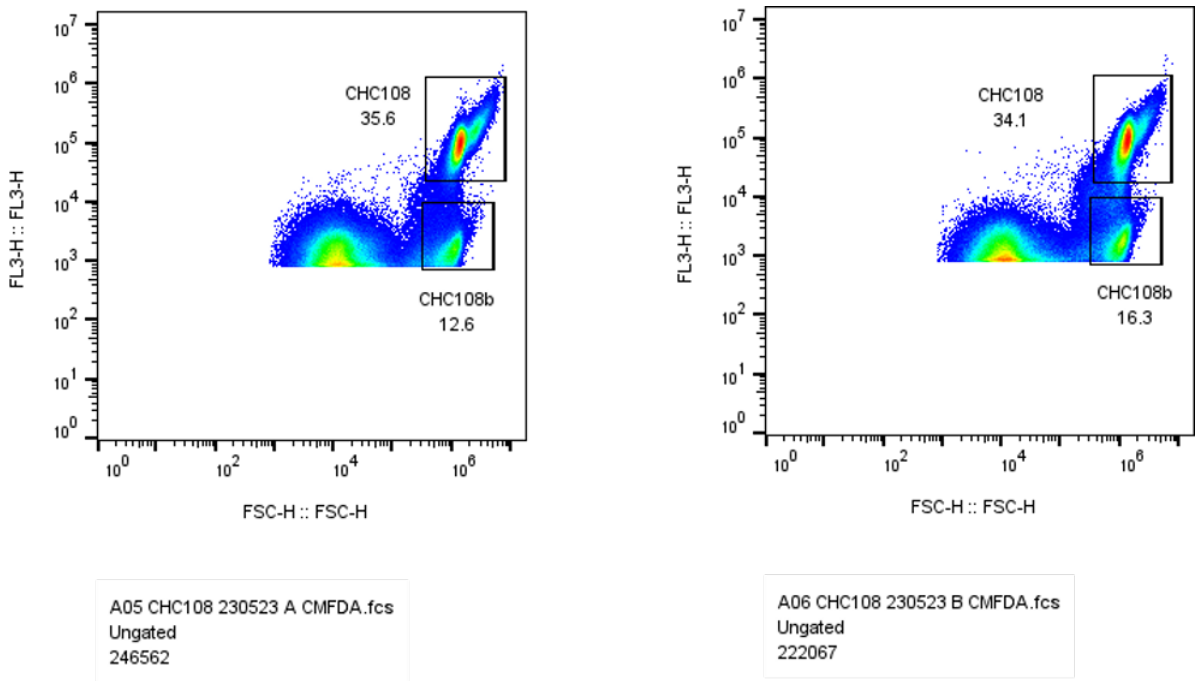


*Figure 30 Batch 3 FSC-H vs. FL3-H A (left) and B (right) stained with CMFDA. Gated area, CHC108, were determined to be coccoliths. The other gated areas, CHC108b, were most likely coccoliths that have precipitated out.*

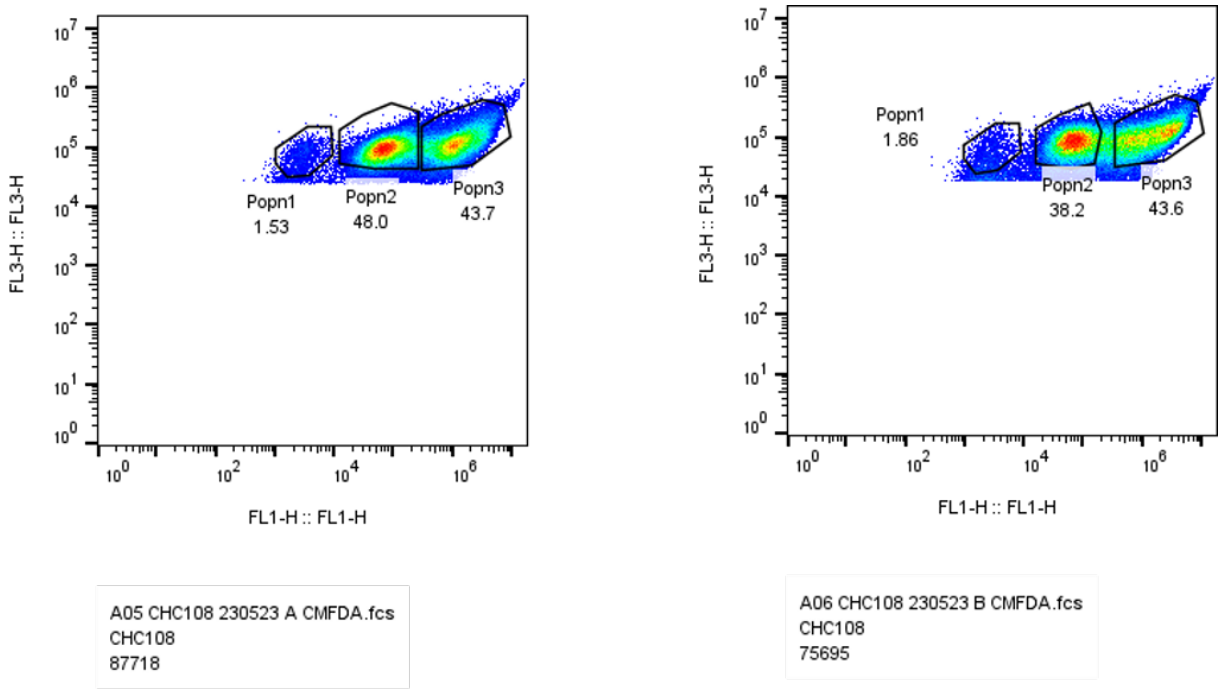


*Figure 31 Batch 3 FL1-H vs. FL3-H for A (left) and B (right). The gated areas were distinct coccolithophore populations within the cultures*

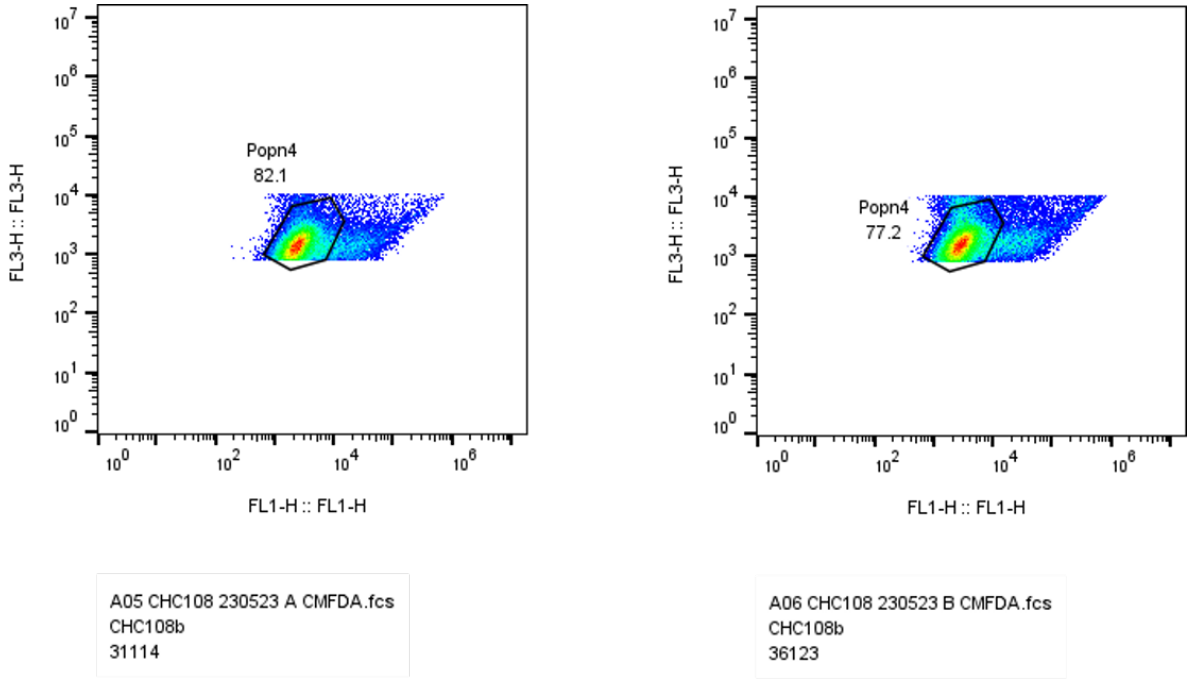


*Figure 32 Batch 3 FL1-H vs. FL3-H for A (left) and B (right). The gated areas were further distinguished coccolithophore populations.*

There were three distinct coccolithophore population identified in batch 3. The left most was the smallest and had the least amount of thiol compared to the other two populations (Fig. 32). Culture A was comparable to the previous batch in terms of distribution and intensity of staining. Culture B had a wider staining with slightly less intensity in popn2. In popn3, the staining was more intense than in that of the previous staining with larger cells

in the same population. Expanding the area around popn2 and popn3, uncovered the same population in batches 1 and 2, though in culture B there was a larger distribution of the CMFDA staining (Fig. 33).

Batch 4

Batch 4 was started using batch 2 as opposed to Batch 3 and started on 06-07-23.

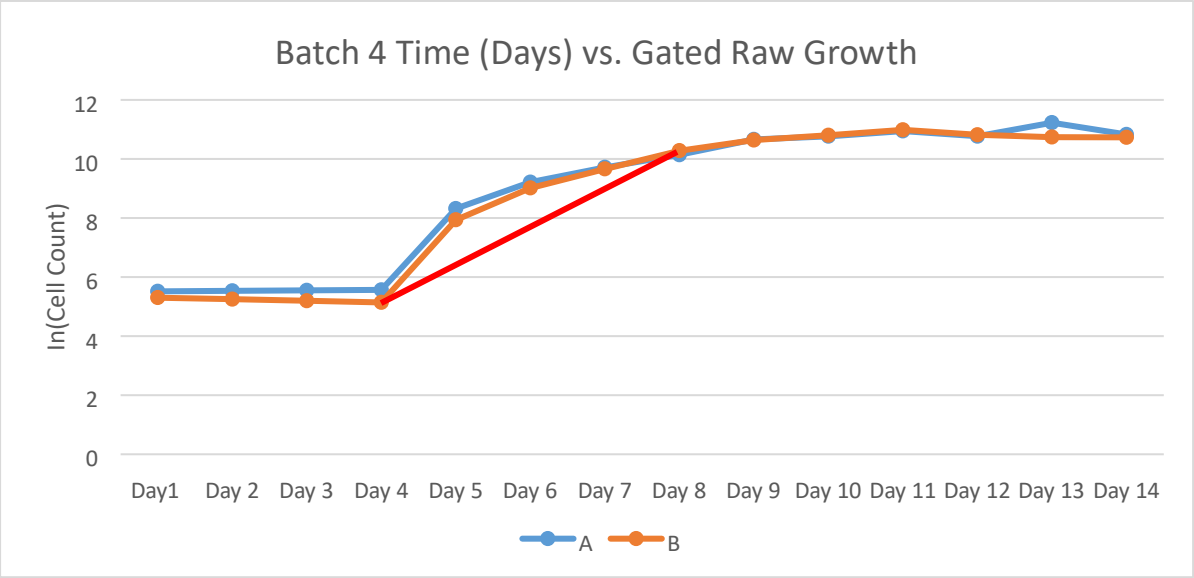


*Figure 33 Batch 4 Gated Raw ln(Cell Count) vs time (days). Days without data (Day 3, 4, 10, 11, 13) were filled using =FORECAST. Batch 4 was grown over the course of 14 days. The gated portion was obtained from a polygon in the upper part of the FCH-1 x FLH-3 graph. Red line represents the exponential growth phase.*

| | Average Growth Rate | Standard Deviation | Doubling Time | Peak Growth Day |
|---|---|---|---|---|
| A | 0.56 $day^{-1}$ | 0.011 | 0.812 doublings $day^{-1}$ | Day 14 |

| | | | | |
|---|---|---|---|---|
| B | 0.574 day$^{-1}$ | 0.01 | 0.832 doublings day$^{-1}$ | Day 12 |

*Table 19 Batch 4 Gated Raw average growth rates, doubling times, and peak growth rates.*

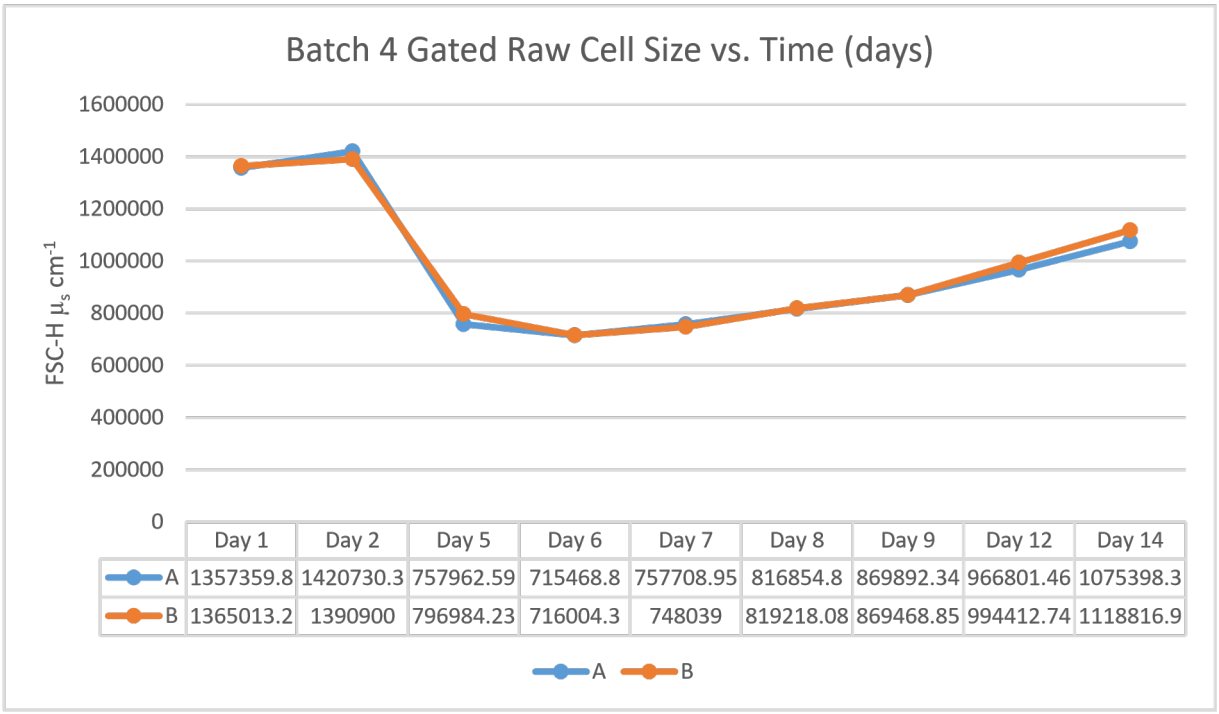


*Figure 10 Batch 4 Gated Raw Cell Size vs. Time (Days).*

| | Average Cell Size | Minimum Cell Size | Maximum Cell Size | Peak Day |
|---|---|---|---|---|
| A | 2.628x10$^5$ | 7.155x10$^5$ | 1.421x10$^6$ | Day 2 |
| B | 2.578x10$^5$ | 7.16x10$^5$ | 1.391x10$^6$ | Day 2 |

*Table 20 Batch 4 Raw Cell Size (average, min, and max).*

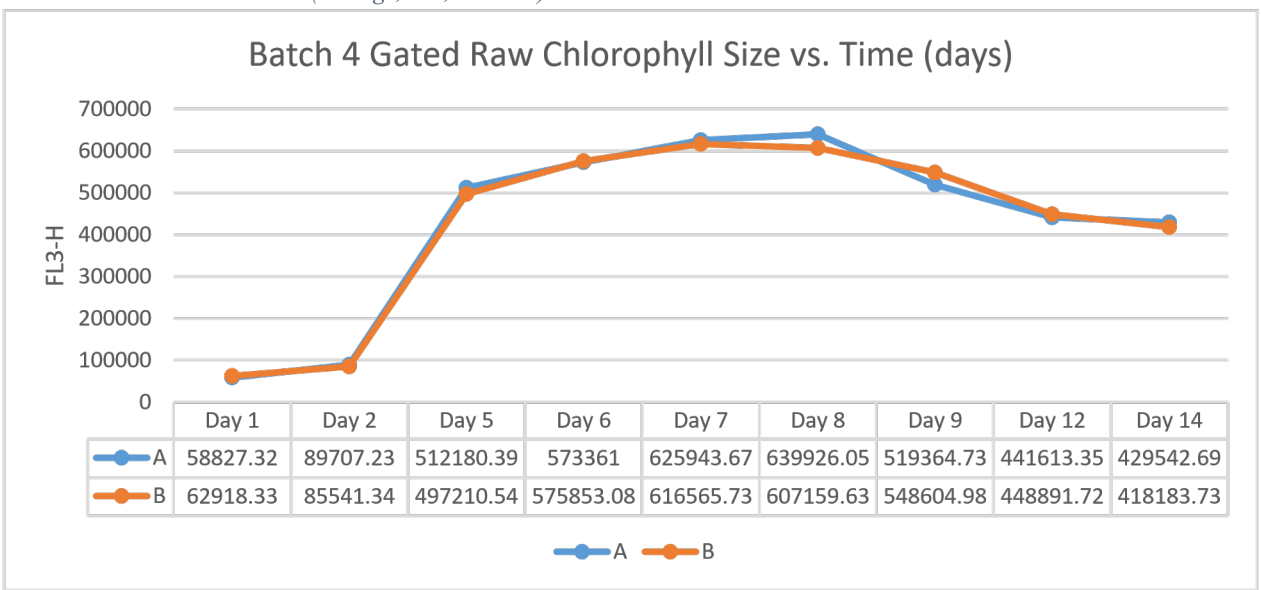


*Figure 35 Batch 4 Gated Raw Chlorophyll Size vs. Time (days)*

| | Average Chlorophyll Size | Minimum Chlorophyll Size | Maximum Chlorophyll Size | Peak Day |
|---|---|---|---|---|
| A | $4.323x10^5$ | $5.883x10^4$ | $6.399x10^5$ | Day 8 |
| B | $4.29x10^5$ | $6.292x10^4$ | $6.166x10^5$ | Day 7 |

*Table 21 Chlorophyll Size for batch 4 (average, min, max)*

The average gated growth rates of both A and B were similar with a negligible difference of 0.008 $day^{-1}$ (Table 19). The doubling time of both A and B were also similar with a difference of 0.2 doublings $day^{-1}$. Culture B had a faster doubling time than culture A. This was reflected in the peak growth day of culture B, day 12, occurred before the peak growth day of culture A, Day 14 (Fig. 34). The average cell size between A and B were similar with very few deviations occurring on Day 2, 5, 12, and 14 (Fig. 35). The difference between the average cell size of A and B was $5.04x10^3$ (Table 20). Peak day for both A and B occurred on Day 2 with a drastic drop from Day 2 to Day 5. An interesting point to note was A was larger on day 2 but the cell size dropped farther than culture B. Cell size steadily increased for both cultures with culture B having a larger cell size than A. The average difference between A and B was $4.934x10^3$ (Table 21), and culture A and B grew together with a deviation that occurred at Day 7 to Day 12 (Fig. 35). The peak growth day for both cultures occurred on Day 8. The difference of the peak chlorophyll size between the two cultures was $2.6x10^4$.

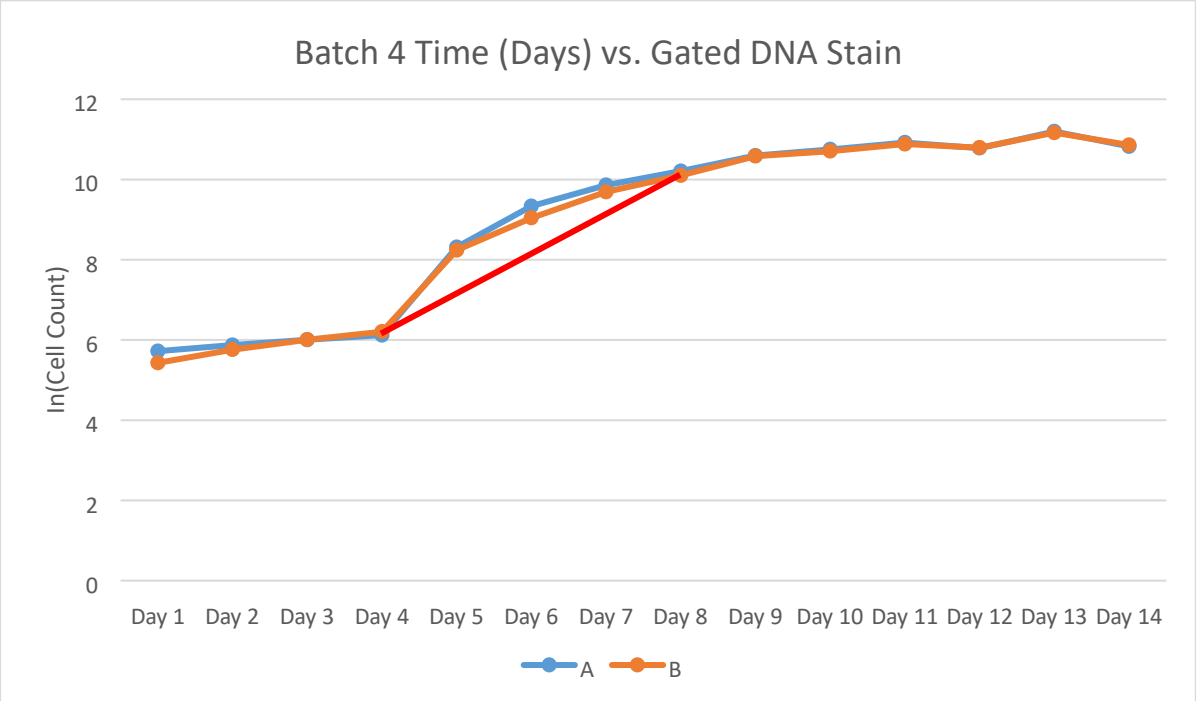

*Figure 36 Batch 4 Gated DNA Stain ln(Cell Counts) vs. time (days). Days without data (Days 3, 4, 10, 11, and 13) were filled using =FORECAST. Batch 4 was grown over the course of 14 days. The gated counts were taken from a rectangle drawn on FLH-1 x FLH-3. Red line represents the exponential growth phase.*

| | Average Growth Rate | Standard Deviation | Doubling Time | Peak Growth Day |
|---|---|---|---|---|
| A | 0.514 $day^{-1}$ | 0.013 | 0.745 doublings $day^{-1}$ | Day 14 |
| B | 0.538 $day^{-1}$ | 0.014 | 0.78 doublings $day^{-1}$ | Day 14 |

*Table 22 Batch 4 Gated DNA Stain average growth rates, doubling times, and peak growth days.*

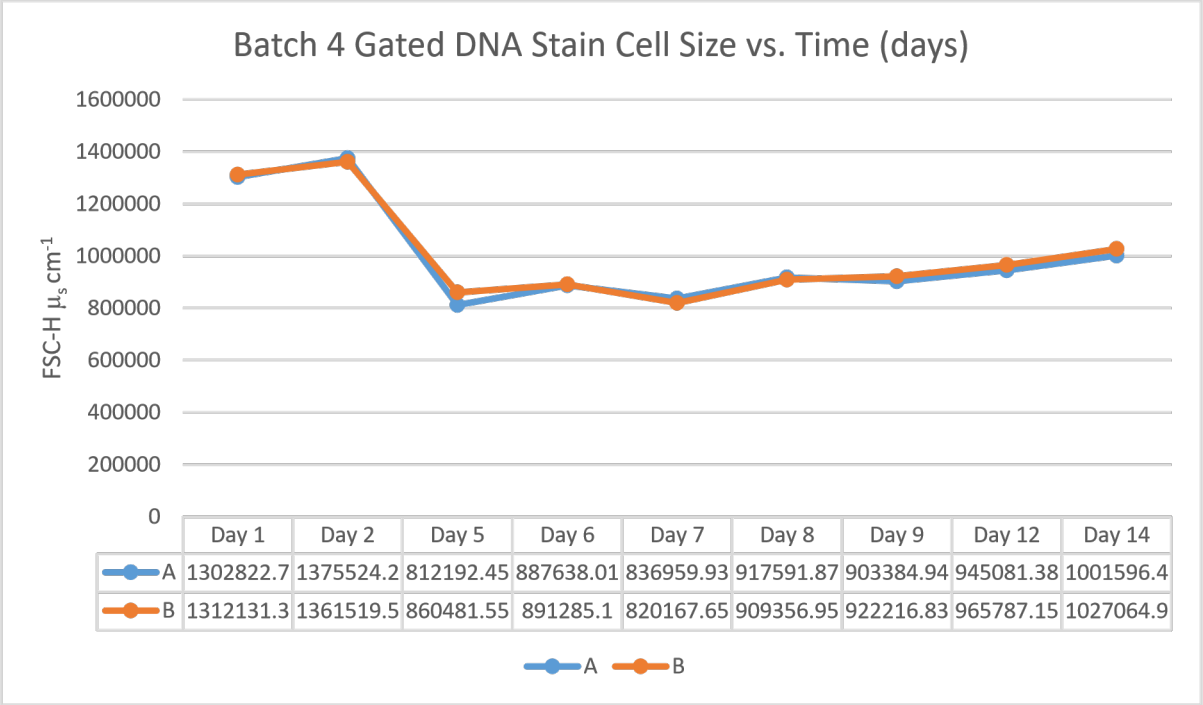


*Figure 37 Batch 4 Gated DNA Stain Cell Size vs. Time (days)*

| | Average Cell Size | Minimum Cell Size | Maximum Cell Size | Peak Day |
|---|---|---|---|---|
| A | $9.981x10^5$ | $8.122x10^5$ | $1.376x10^6$ | Day 2 |
| B | $1.008x10^6$ | $8.605x10^5$ | $1.362x10^6$ | Day 2 |

*Table 23 Batch 4 Gated DNA Stain Cell Size (Average, min, and max) along with peak day growth.*

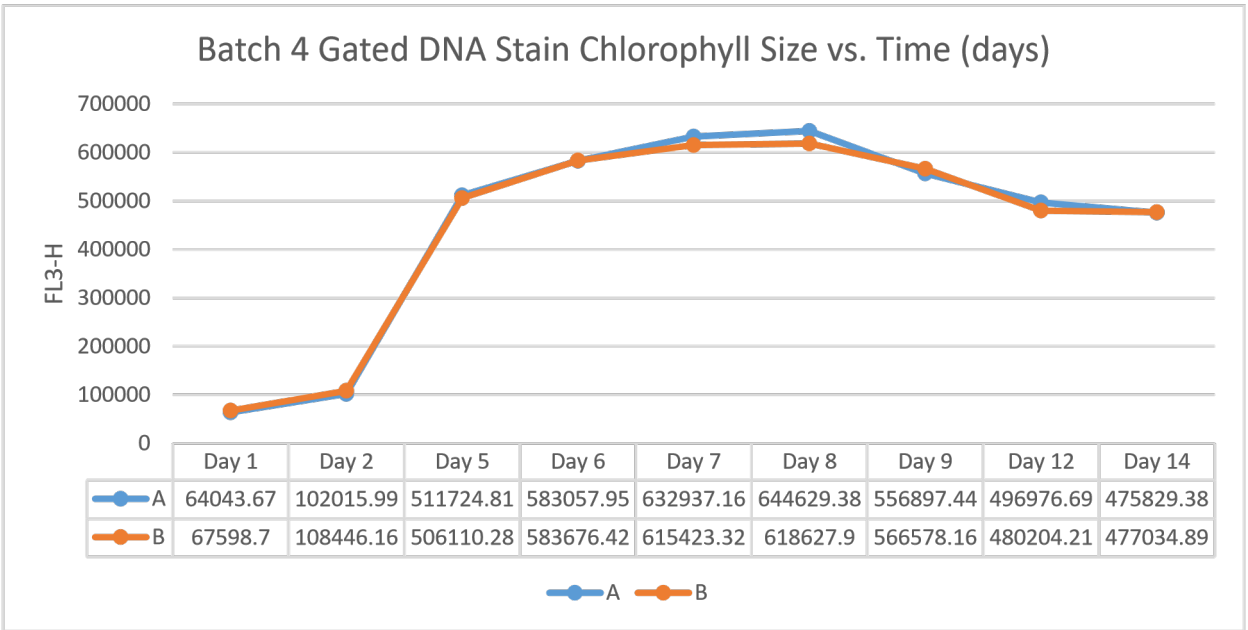


*Figure 38 Batch 4 Gated DNA Stain Chlorophyll Size vs. Time (days).*

| | Average Chlorophyll Size | Minimum Chlorophyll Size | Maximum Chlorophyll Size | Peak Day |
|---|---|---|---|---|
| A | $4.52x10^5$ | $6.404x10^4$ | $6.446x10^5$ | Day 8 |
| B | $4.471x10^5$ | $6.76x10^4$ | $6.186x10^5$ | Day 8 |

*Table 24 Batch 4 DNA Stain chlorophyll size (average, min, and max).*

The gated DNA stain growth rate of culture B was slightly higher than culture A with a difference of 0.024 $day^{-1}$ (Table 22). The doubling time of culture B was faster than that of culture A with a difference of 0.035 doublings $day^{-1}$. Both culture A and culture B had peak growth on Day 14 which would be in line with the close doubling time and growth rate. The average cell size between A and B were similar with small deviations that occurred on Day 2, Day 5, and Day 14 (Fig. 38). The difference between the average cell size of A and B was $9.691x10^3$. Peak cell size occurred for both A and B on Day 2. Culture A had a more significant drop from Day 2 to Day 5. Then gradual increases throughout the remaining days though there were some small dips on Day 7 and Day 9. The average chlorophyll size difference between A and B was $4.934x10^3$ (Table 24), and culture A and B grew together with a deviation that occurred at Day 7 to Day 12 (Fig. 39). The peak growth day for both cultures occurred on Day 8. The difference of the peak chlorophyll size between the two cultures was $2.6x10^4$.

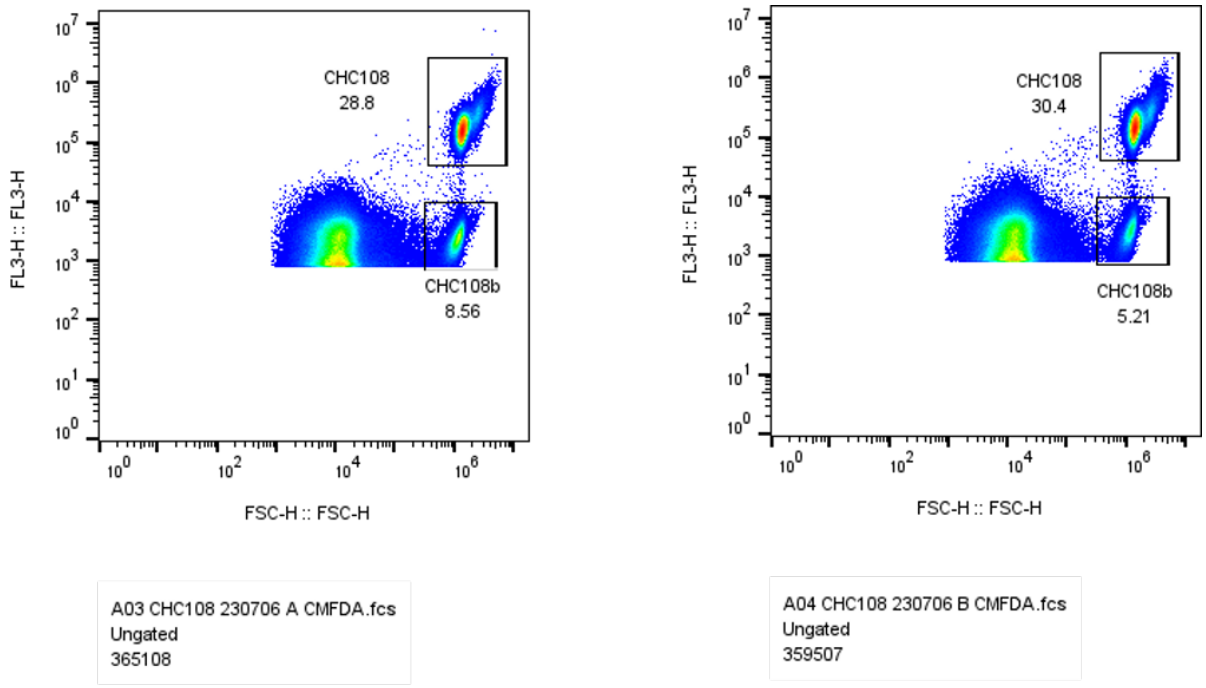


*Figure 39 Batch 4 FSC-H vs. FL3-H for A (left) and B (right) stained with CMFDA. Gated area CHC108 were determined to be coccolithophores. The other, CHC108b, areas were either free coccoliths or coccoliths that have been compromised*

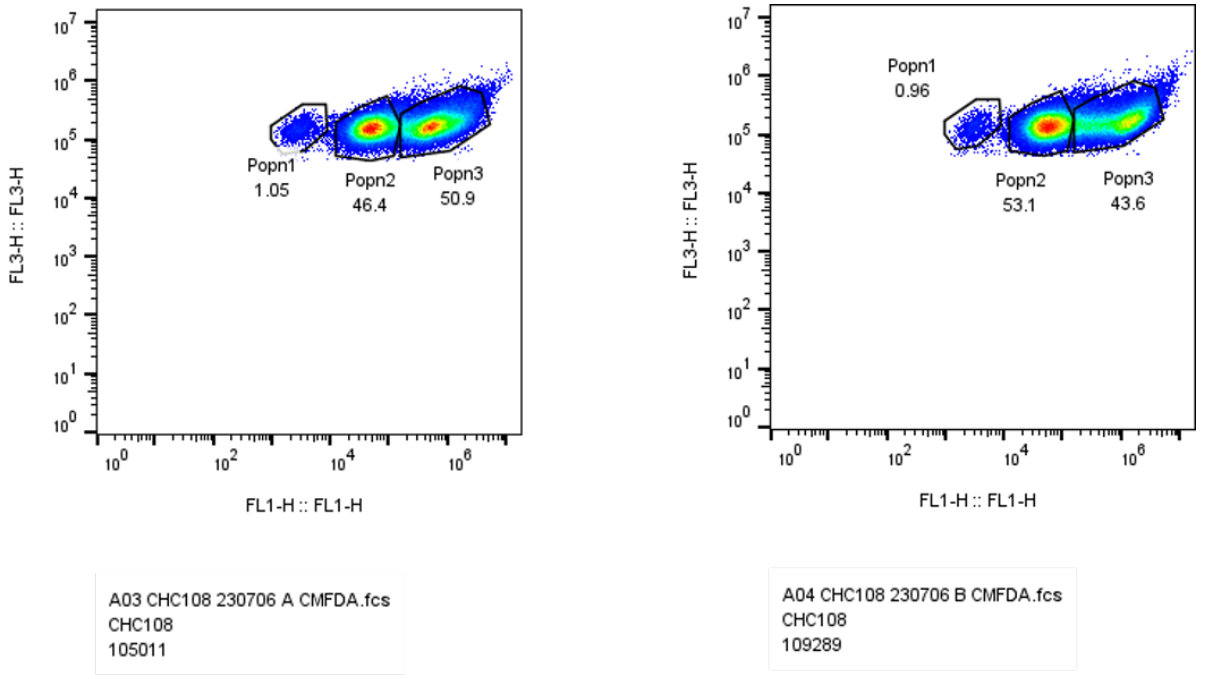


*Figure 40 Batch FL1-H vs. FL3-H for A (left) and B (right). The gated areas are distinctive coccolithophore populations*

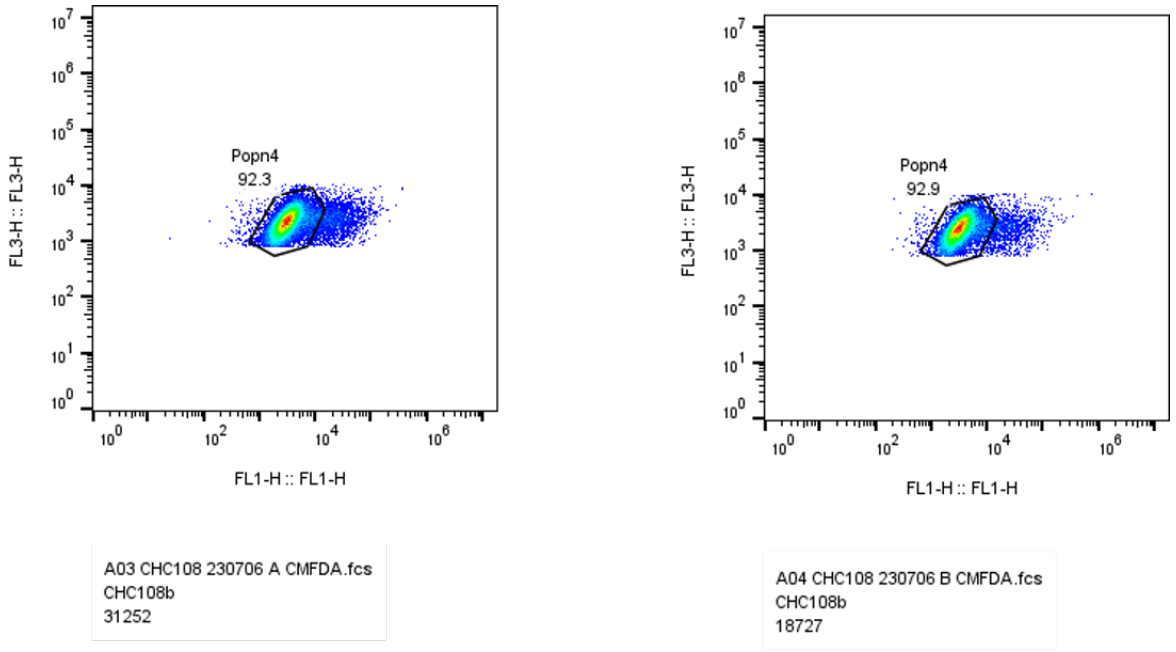


*Figure 41 Batch 4 FL1-H vs. FL3-H for A (left) and B (right). The gated areas were further distinguished coccolithophore groups.*

There were three distinct coccolithophore populations as seen in the previous batches. The population with the least amount of thiol was smaller than in batches 2 and 3. For popn2, Culture A was similar to that of Culture B (Fig. 40). Popn3 the size distributions were similar for both A and B, though B had lower thiol content than in A. Another thing to note is that the population of B was no longer split as it had been in batches 2 and 3. Expanding population 2 and 3, Culture A had more cells that were larger but the staining pattern were almost identical (Fig. 41).

| | Average Gated Raw Growth Rate | Average Total Raw Growth Rate | Average Gated DNA Stain Growth Rate | Average Total DNA Stain Growth Rate |
|---|---|---|---|---|
| A | 0.649 $day^{-1}$ | 0.517 $day^{-1}$ | 0.613 $day^{-1}$ | 0.278 $day^{-1}$ |
| B | 0.625 $day^{-1}$ | 0.523 $day^{-1}$ | 0.654 $day^{-1}$ | 0.178 $day^{-1}$ |

*Table 25 Average growth rates for all batches.*

The average raw growth rate of both A and B (Table 25) were similar with A having a higher growth rate (0.029 $day^{-1}$) than B when it came to the gated coccolithophores. The overall growth rates for all species within the culture were the same with a slight increase in culture B (0.002 $day^{-1}$). The DNA stain (sybr green) did not fully stain all cells within the culture. As a result, the DNA that was stained in all batches was far less than other species that underwent the same process. The working theory was as follows; the coccolith that *E. huxleyi* produced prevented the DNA stain from fully penetrating the inner cell, in part to do with the coccolith that other species do not have surrounding the cells. The empty

coccoliths that stayed in the culture may have contributed to the light limitation present. The property of the Erlenmeyer flask may have initially let in more light than the usual transfer flask but as the culture became saturated, light limitations were introduced. There were two ways that this could be remedied, although time did not permit in this study. First would be to look at other strains of *E. huxleyi* that stopped producing coccoliths. The second would be to use an acid to break down the coccolith as the DNA stain did not rely on live cells to synthesize the dye. This second step was tried on CHC108 but did not seem to improve the staining process. The coccoliths may have become thicker due to the container that the culture was stored in. CMFDA was injected into the sample while the sample was still alive because the dye is reliant on the individual cells to take it up into the cell membrane (*MacIntyre & Cullen, 2016*).

| | Average Raw Gated Doubling Time | Average Total Raw Doubling Time | Average Gated DNA Stain Doubling Time | Average Total DNA Stain Doubling Time |
|---|---|---|---|---|
| A | 0.942 doublings $day^{-1}$ | 0.777 doublings $day^{-1}$ | 0.886 doublings $day^{-1}$ | 0.418 doublings $day^{-1}$ |
| B | 0.906 doublings $day^{-1}$ | 0.933 doublings $day^{-1}$ | 0.948 doublings $day^{-1}$ | 0.415 doublings $day^{-1}$ |

*Table 26 Average doubling times for all batches.*

The doubling times for all gated rates were around 2 days (Table 26). The doubling time is the average time it would take for the starting culture number to double. The doubling time of the DNA concentrations would also be affected by the lack of staining underneath the coccolith leading to the large disparity between the other tested doubling times.

| | Average Raw Gated Peak Growth Day | Average Total Raw Peak Growth Day | Average Gated DNA Stain Peak Growth Day | Average Total DNA Stain Peak Growth Day | Average Gated CMFDA Peak Growth Day | Average Total CMFDA Peak Growth Day |
|---|---|---|---|---|---|---|
| A | Day 10.5 | Day 10.75 | Day 10.75 | Day 11.5 | Day 9.5 | Day 9 |
| B | Day 10 | Day 9.75 | Day 10.5 | Day 8.75 | Day 9 | Day 9 |

*Table 27 Average Peak growth days over all batches except for the CMFDA with only considered batches 1 and 2*

The average raw peak growth day, both gated and total, were the same with the difference being around plus or minus 6 hours (Table 27). DNA stain peak growth was higher for both gated and total (A and B). The difference between the gated and total A: 18 hours and difference

between gated and total B: 42 hours. The CMFDA had the same peak growth day of day 9 except for the addition of 12 hours for the gated A batch.

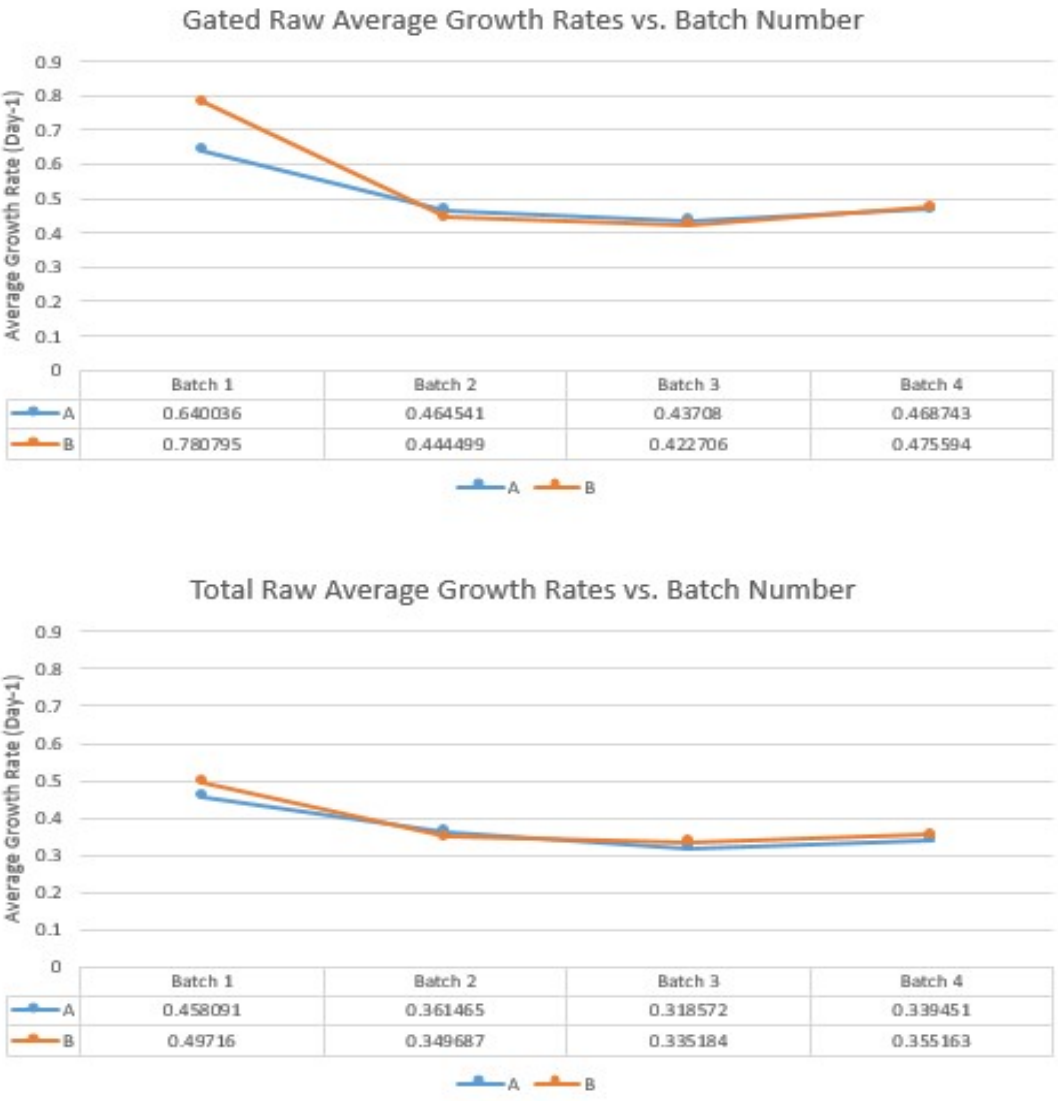


*Figure 43 The average raw growth rates of both gated and total of all batches (1-4). The purpose was to see if and how fluctuations in growth rate occurred and when through the experiment time period.*

Batch 1 had the highest average raw growth rate for both the gated and total culture (Fig. 43). Between batch 2 and 3 both gated and total there was a slight or negligible decrease in growth rate for both gated and total growth rates. This was applicable to cultures A and B. Between batches 3 and 4 there was a slight increase in growth rate. The increase in growth in batch 4 was intriguing as these cultures were started with samples from batch 2 rather than batch 3, which would typically slow down the growth rather than increase it. The difference in the growth rates comes from the total having varied species of bacteria in conjunction with *E. huxleyi*.

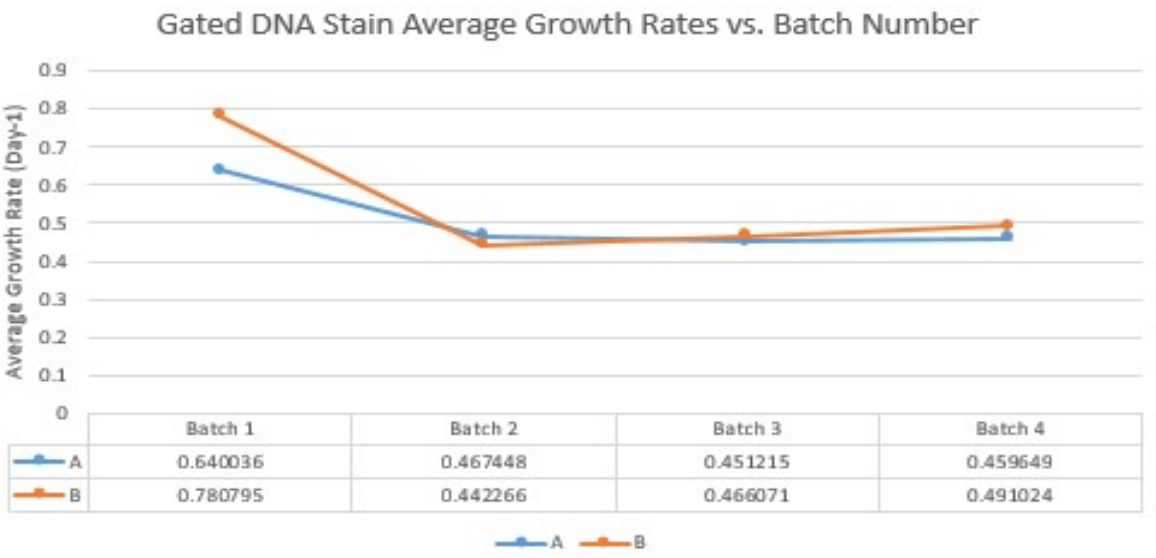


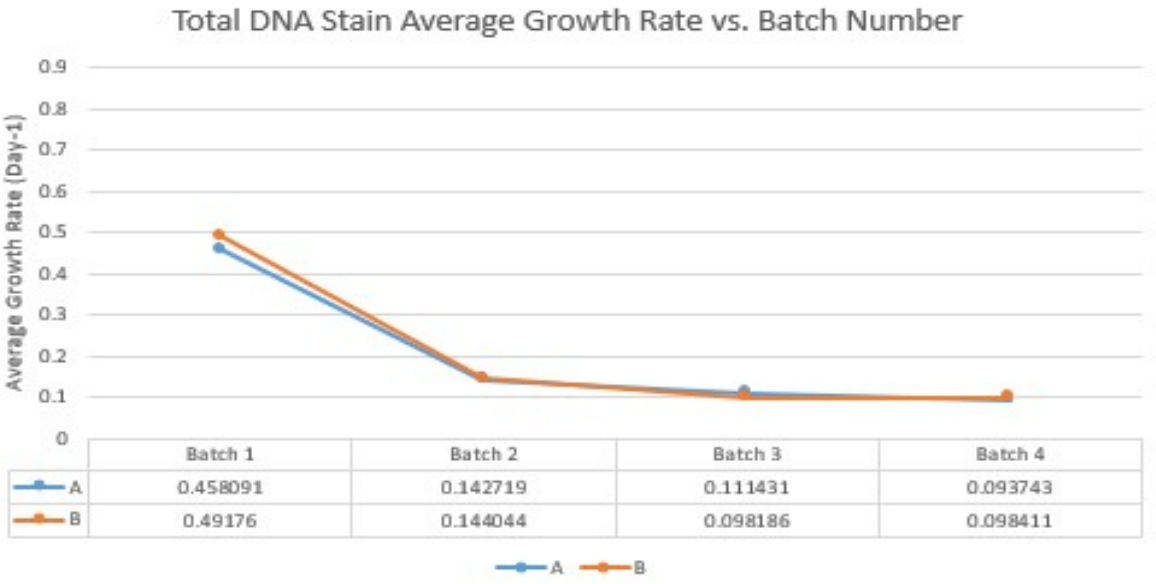


*Figure 44 The average DNA Stain growth rate both gated and total over all batches (1-4).*

Cultures A and B typically follow the same growth rate progression with a significantly higher average growth rate in batch 1 with a decrease to an average that is similar over batches 2, 3, and 4 (Fig. 44). The biggest difference between the total and the gated average growth rates comes at batch 4 where there was a slight increase in the gated growth rates and a slight decrease in culture A total growth rate. Total culture B increased a miniscule amount ($2.25 \times 10^{-5}$).

DMS MIMS readings

Day 1

Batch 2 Sample A was added at 13:22. The culture was 16 days old at the time of the MIMS run. $H_2{}^{18}O$ water was added 1 hour 18 minutes. Direct blue light (80 µmol photons/$m^2$/s) was added at 1 hour, 52 minutes.

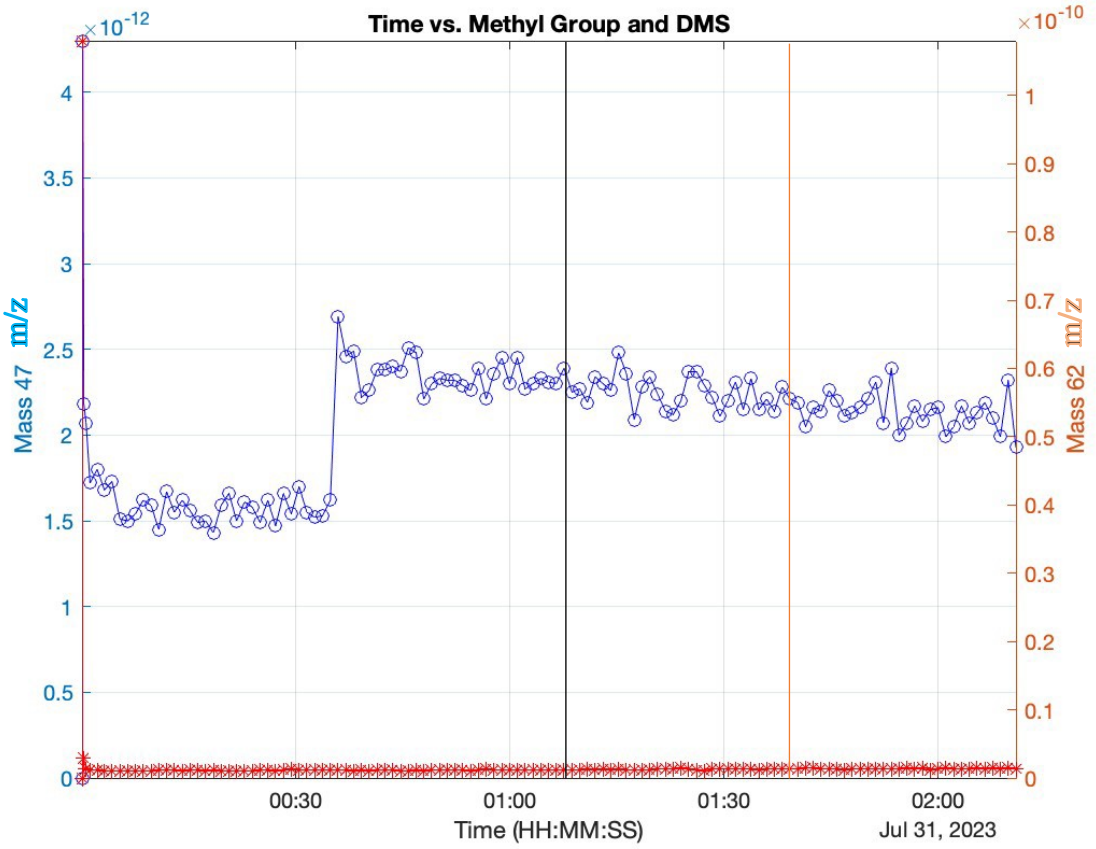


*Figure 45 Time in hours vs. Mass 47m/z and Mass 62 m/z concentration. Max time is 2 hours and 11 minutes. (Day 1). The black line represents the $H_2{}^{18}O$ water being added to the water column and the orange line represents the addition of the direct blue light. Note that the Mass 47 axis started at $0e^{-12}$ and Mass 62 axis started at $0e^{-10}$.*

| | Standard Deviation | Max Value | Min Value | Average Value | Max Time Value |
|---|---|---|---|---|---|
| Mass 47 | $4.154e^{-13}$ | $4.30e^{-12}$ | 0 | $2.07e^{-12}$ | 02:12:01 |
| Mass 62 | $9.552e^{-12}$ | $1.08e^{-10}$ | 0 | $2.09e^{-12}$ | 02:12:01 |

*Table 28 Average, min, and max concentrations of Mass 47 and Mass 62 on 25-05-23*

The jump in concentration around 37 minutes was not explainable. The methyl groups that were detected in the mass 47 band were not specifically DMS because the profile of mass 62 does not match the profile of mass 47. DMS production was not expected to be high, and

the concentration that was detected was negligible. The differences in the two data sets were not significant which was to be expected as there was not a true added stressor (Table 28).

P-value below 0.05 is statistically significant. T-stat of 2 or higher is statistically significant. The t-stat describes the variability within a sample. Higher degrees of freedom will allow more power to reject the null hypothesis.

| | H value | p-value | Confidence Interval | t-stat | Degrees of Freedom | Standard Deviation |
|---|---|---|---|---|---|---|
| Mass 47 and Mass 62 | 0 | 0.9894 | $-1.6957e^{-12}$; $1.6730e^{-12}$ | -0.0133 | 248 | $6.7609e^{-12}$ |
| Mass 47 Section 1 and 2 | 1 | $1.5951e^{-04}$ | $-7.1794e^{-13}$; $-23956e^{-13}$ | -3.9919 | 70 | $4.7972e^{-13}$ |
| Mass 47 section 2 and 3 | 1 | $2.1347e^{-06}$ | $7.8444e^{-14}$; $1.7780e^{-13}$ | 5.1378 | 75 | $1.0136e^{-13}$ |
| Mass 47 section 1 and 3 | 1 | $4.2348e^{-05}$ | $-5.1297e^{-13}$; $-1.8828e^{-13}$ | -4.2855 | 99 | $4.1063e^{-13}$ |
| Mass 62 Section 1 and 2 | 0 | 0.4974 | $-4.1477e^{-12}$; $8.4593e^{-12}$ | 0.6821 | 70 | $1.2642e^{-11}$ |
| Mass 62 Sections 2 and 3 | 1 | $7.7786e^{-10}$ | $-1.7002e^{-13}$; $-95029e^{-14}$ | -7.0410 | 75 | $7.6499e^{-14}$ |
| Mass 62 Sections 1 and 3 | 0 | 0.3418 | $-2.1796e^{-12}$; $6.2262e^{-12}$ | 0.9552 | 99 | $1.0631e^{-11}$ |

*Table 29 T- test of Day 1. Section 1 was defined as the data collected from the start of the run to the introduction of the first stressor. This was considered as the baseline reading. Section 2 was defined as the data collected from the addition of O18*

There was not a significant difference between the data points collected between Mass 47 and Mass 62 (Table 29). This was to be expected as there were no real stressors added. The comparison between section 1 and 2 of Mass 47 did not give significant results. This indicated that the addition of the $H_2{}^{18}O$ water did not yield any significant changes in DMS concentrations which was to be expected. The comparison between Section 2 and section 3 of Mass 47 resulted in a significant change in DMS concentrations. This was an unexpected result as the addition of the blue light to the water column should not have a stress response. The comparison between section 1 and section 3 of Mass 47 did not result in any significant changes in DMS. As both the baseline (section 1) comparisons with sections 2 and 3 of Mass 62 were not significant, there were no significant changes in DMS from the addition of the $H_2{}^{18}O$ water and blue light.

Day 5

Batch 3 Sample A was run for 2 hours and 56 minutes. The culture was 6 days old at the time of the MIMS run. Added 200 µL diluted/10 $H_2{}^{18}O_2$ to the sample. 140 µL non-dilute/2 $H_2{}^{18}O_2$ was added at 3 hours and 10 minutes

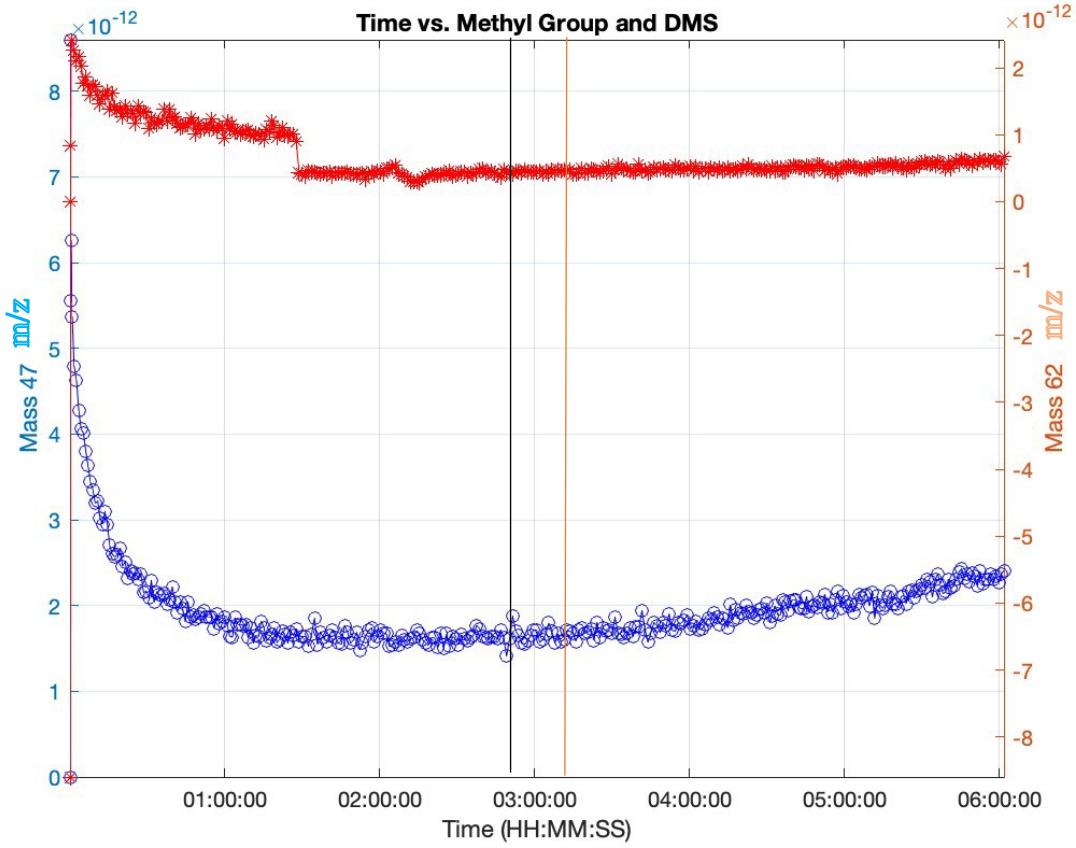


*Figure 46 Time vs. Mass 47 m/z and Mass 62 m/z over the course of 6 hours (29-05-23). The black line represents the addition of 200 µL of diluted/10 $H_2{}^{18}O_2$ and the orange line represents the addition of 140 µL of non-dilute/2 $H_2{}^{18}O_2$. Note that the Mass 47 axis started on $0e^{-12}$ and the Mass 62 axis started at $-8e^{-12}$.*

| | Standard deviation | max value | min value | average value | Max time value |
|---|---|---|---|---|---|
| Mass 47 | $6.895e^{-13}$ | $8.60e^{-12}$ | 0 | $2.00e^{-12}$ | 06:01:48 |
| Mass 62 | $6.433e^{-13}$ | $2.42e^{-12}$ | $-8.60e^{-12}$ | $6.70e^{-13}$ | 06:01:48 |

*Table 30 Average, min, and max values of Mass 47 and Mass 62 on 29-05-23*

After the addition of the 140 µL non-dilute/2 $H_2{}^{18}O_2$, the level of mass 47 methyl concentration started to gradually increase throughout the run time. There was not a notable change in the 30 minutes after the addition of the 200 µL diluted/10 $H_2{}^{18}O_2$ which was why the stronger concentrated peroxide was added (Fig. 46). Throughout the run time, there was not a strong increase or decrease in mass 62 before or after the addition of the dilute and non-dilute

$H_2{}^{18}O_2$. DMS production was slightly increased after the addition of the non-dilute/2 $H_2{}^{18}O_2$. There was a slight difference in the average concentrations of Mass 47 and Mass 62 (Table 30).

| | H value | p-value | Confidence interval | t-stat | Degrees of Freedom | Standard Deviation |
|---|---|---|---|---|---|---|
| Mass 47 and 62 | 1 | $2.0283e^{-104}$ | $1.2312e^{-12}$; $1.4317e^{-12}$ | 26.0729 | 680 | $6.6681e^{-13}$ |
| Mass 47 Sections 1 and 2 | 0 | 0.1022 | $-8.4860e^{-14}$; $9.2841e^{-13}$ | 1.6428 | 178 | $9.2250e^{-13}$ |
| Mass 47 Sections 2 and 3 | 1 | $4.7457e^{-08}$ | -4.5236; $-2.2006e^{-13}$ | -5.7134 | 173 | $2.1119e^{-13}$ |
| Mass 47 Sections 1 and 3 | 0 | 0.2697 | $-6.6665e^{-14}$; $2.3779e^{-13}$ | 1.1057 | 325 | $6.9954e^{-13}$ |
| Mass 62 Sections 1 and 2 | 0 | 0.1100 | -8.7754e-14; 8,5544$e^{-13}$ | 1.6062 | 178 | $8.5870e^{-13}$ |
| Mass 62 Sections 2 and 3 | 1 | $8.1004e^{-06}$ | $-9.2383e^{-14}$, $-3.6916e^{-14}$ | -4.6010 | 173 | $5.0427e^{-14}$ |
| Mass 62 Sections 1 and 3 | 1 | $8.1673e^{-06}$ | $1.8068e^{-13}$; $4.5771e^{-13}$ | 4.5335 | 325 | $6.3652e^{-13}$ |

*Table 31 Day 5 t-test. Section 1 was defined as the start of the runtime to the first added stressor. Section 2 was defined as the period when the 200µL of diluted/10 O18 peroxide was added to the time the next stressor was added. Section 3 was defined as the time of addition of the 140 µL of the non-dilute/2 $O^{18}$ peroxide to when the run ended.*

There was a significant change in the mean between the Mass 47 and the Mass 62 data. The high levels of degrees of freedom aid in the confidence that the end results were significant. In comparisons of Mass 47 Section 1 and 2, and Section1 and 3 there were no significant results, and the null hypothesis was not rejected in those scenarios (Table 31). The comparison between sections 2 and 3 yielded significant results confirmed with both the p-value and the tstat. There were no significant results between Section 1 and Section 2. This was to be expected as there was not a visual in situ observation. The lack of visual response was the instigator to adding

the 140 µL of non-dilute/2 $H_2{}^{18}O_2$. There was a significant difference between Section 2 and Section 3. In the comparison between Section 1 and Section 3, there was a significant difference between the two. The significance of the indicated that a substantial amount of DMS was emitted after the addition of the 140 µL of non-dilute/2 $H_2{}^{18}O_2$ when compared to the base reading in Section 1.

Day 6

Same sample as the previous day. The culture was 7 days at the time of the run. The sample was kept in the spinner overnight with the cover off. The cover remained off throughout the run time. At 4 hours and 22 minutes 200 µL diluted/10 $H_2{}^{18}O_2$. At 4 hours and 52 minutes 140 µL non-diluted/2 $H_2{}^{18}O_2$.

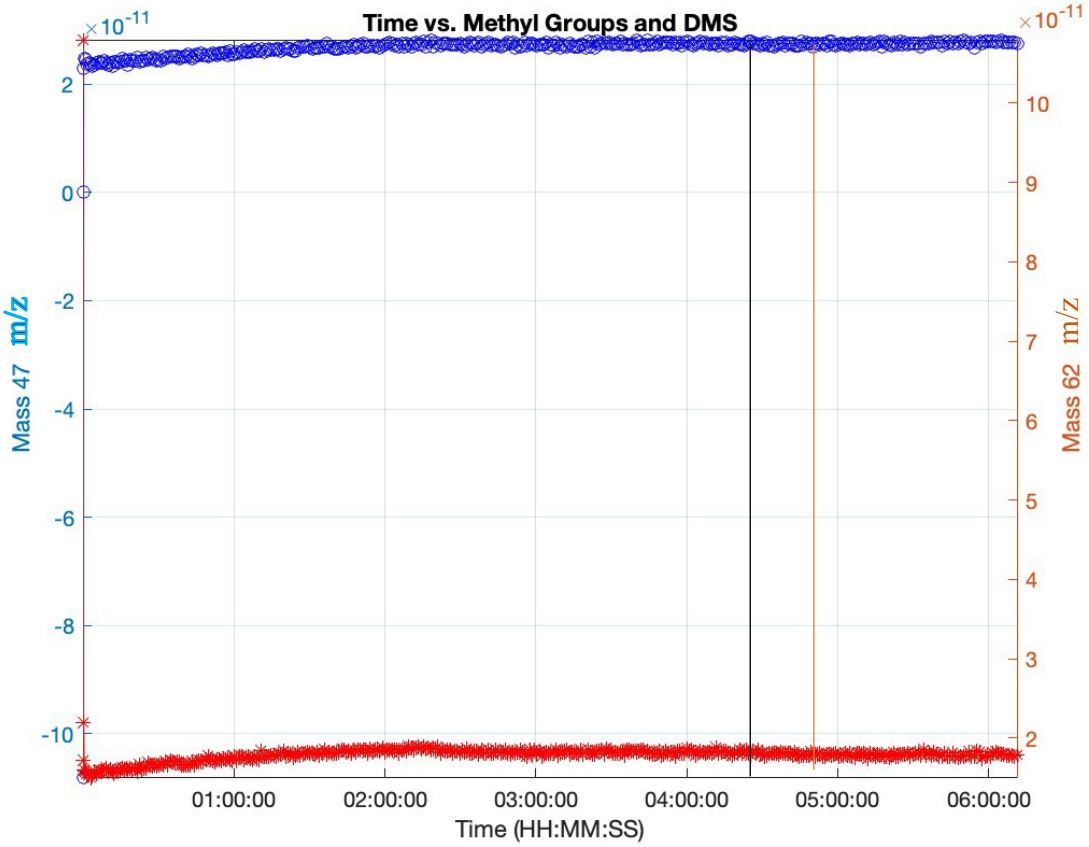


*Figure 47 Time vs. Mass 47 and Mass 62 concentrations over the course of 6 hours (30-05-23). The black line represents the addition of 200 µL diluted/10 $H_2{}^{18}O_2$ and the black line represents the addition of 140 µL non-dilute/2 $H_2{}^{18}O_2$. Note that the Mass 47 axis started at -10e$^{-11}$ and Mass 62 axis started at -2e$^{-11}$.*

| | Standard deviation | max value | min value | average value | Max time value |
|---|---|---|---|---|---|
| Mass 47 | 6.915e$^{-12}$ | 2.82e$^{-11}$ | -1.08e$^{-10}$ | 2.64e$^{-11}$ | 06:11:18 |
| Mass 62 | 4.528e$^{-12}$ | 1.08e$^{-10}$ | 1.51e$^{-11}$ | 1.81e$^{-11}$ | 06:11:18 |

*Table 32 Average, min and max concentrations of Mass 47 and Mass 62 on 30-05-23*

Throughout the night, mass 47 methyl increased so the starting concentrations were higher the second day (Table 39). The addition of the peroxide, both dilute and non-dilute, did not make a notable change to the methyl concentration in hours 4 and 5 (Fig. 47). The difference in average value between day 1 and day 2 was 2.44e$^{-11}$. The base level of DMS increased throughout the night. The addition of the dilute and non-dilute $H_2{}^{18}O_2$ did not impact the DMS

production. The difference in average value between the previous day and this run time was $1.743e^{-11}$.

| | H value | p-value | Confidence Interval | t-stat | Degrees of Freedom | Standard Deviation |
|---|---|---|---|---|---|---|
| Mass 47 and 62 | 1 | $1.4117e^{-73}$ | $7.5309e^{-12}$; $9.1540e^{-12}$ | 20.1784 | 804 | $5.8687e^{-12}$ |
| Mass 47 Section 1 and 2 | 0 | 0.2631 | $-5.0949e^{-12}$; $1.3980e^{-12}$ | -1.1217 | 237 | $8.7888e^{-12}$ |
| Mass 47 Sections 2 and 3 | 0 | 0.2631 | $-5.0949e^{-12}$; $1.3980e^{-12}$ | -1.1217 | 237 | $8.7888e^{-12}$ |
| Mass 47 Sections 1 and 3 | 1 | 0.006 | $-3.4927e^{-12}$; $-5.8912e^{-13}$ | -2.7644 | 368 | $7.0547e^{-12}$ |
| Mass 62 Sections 1 and 2 | 0 | 0.8951 | $-2.3355e^{-12}$; $2.0421e^{-12}$ | -0.1320 | 237 | $5.9255e^{-12}$ |
| Mass 62 Sections 2 and 3 | 1 | $3.1865e^{-04}$ | $7.9560e^{-14}$; $2.6493e^{-13}$ | 3.6651 | 195 | $2.4633e^{-13}$ |
| Mass 62 Sections 1 and 3 | 0 | 0.9590 | $-9.5352e^{-13}$; $1.0047e^{-12}$ | 0.0514 | 368 | $4.7578e^{-12}$ |
| Mass 47 Section 3 (Day 5) and Section 1 (Day 6) | 1 | $4.8072e^{-121}$ | $-2.516e^{-11}$; $-2.2469e^{-11}$ | -34.3706 | 397 | $6.8018e^{-12}$ |

| | | | | | | |
|---|---|---|---|---|---|---|
| Mass 62 Section 3 (Day 5) and Section 1 (Day 6) | 1 | $2.3932e^{-133}$ | $-1.8526e^{-11}$; $-1.6691e^{-11}$ | -37.7261 | 397 | $4.5786e^{-12}$ |

*Table 33 Day 6 t-test. Section 1 was defined as the beginning of the runtime to the addition of the first stressor. Section 2 was defined as the area between the addition of the 200 µL diluted/10 O18 peroxide and the addition of the second stressor. Section 3 was defined as the addition of 140 µL of non-dilute/2 $O^{18}$ peroxide.*

There was a significant difference between Mass 47 and Mass 62 over the entire run time. The high-level degrees of freedom strongly supported this. In the comparison of section 1 and 2, there was no significant result (Table 33). The comparison between sections 2 and 3 ended in no significant results. The comparison between section 1 and 3 yielded significant results. The comparison between sections 1 and 2, there were no significant results. The comparison between section 2 and 3 yielded significant results. The comparison between sections 1 and 3 resulted in non-significant results. The overnight results between Day 5 and Day 6 yielded significant results indicating that the addition of the $O^{18}$ peroxide and lack of light combination increased DMS concentrations. This indicated that there was DMS produced throughout the night, increased though the cover was taken off during the night.

Day 55

Sample CHC108 230523 B (Batch 3) was used, and samples were started at 9:30 and the cover was kept over the sample. The culture was 56 days old at the time of the MIMS run. 2 hours and 20 minutes later 100 µL Cu was added to the sample and ran for an additional 4 hours and 13 minutes.

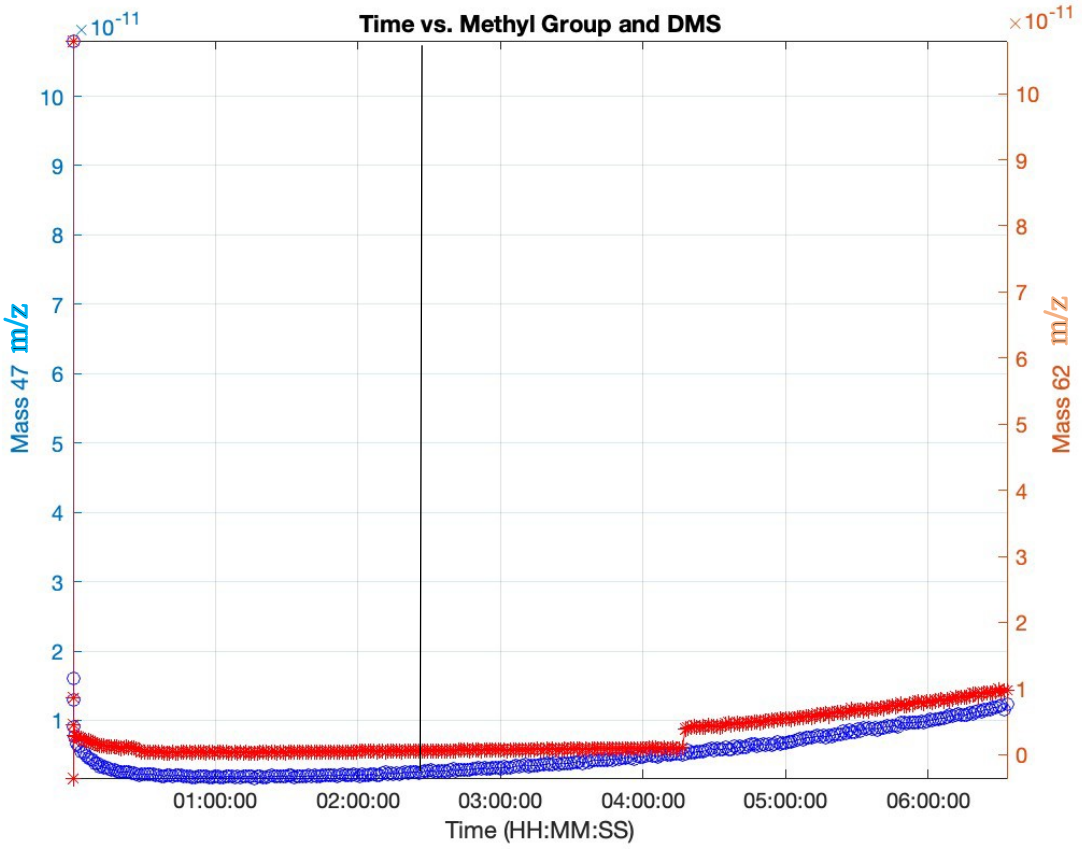


*Figure 48 Time vs. Mass 47 and Mass 62 over the course of 6 hours and 33 minutes (18-07-23). The black line is a representation of the addition of 100 µL Cu. Note that Mass 47 axis started at $0e^{-11}$ and Mass 62 axis started at $0e^{-11}$.*

| | Standard Deviation | Max Value | Min Value | Average Value | Max Time Value |
|---|---|---|---|---|---|
| Mass 47 | $6.394e^{-12}$ | $1.08e^{-10}$ | $1.69e^{-12}$ | $5.19e^{-12}$ | 06:33:12 |
| Mass 62 | $6.478e^{-12}$ | 1.08-10 | $-3.53e^{-12}$ | $3.09e^{-12}$ | 06:33:12 |

*Table 34 Average, min, max concentrations of Mass 47 and Mass 62 on 18-07-23*

Mass 47 and DMS concentrations were stable throughout the first 2 hours, which established a decent baseline of existing concentrations within Batch 3 B. After the addition of the 100 µL of copper, the concentrations of mass 47 (methyl groups) stayed constant until the increase at timestamp 4 hours 14 minutes with a large increase followed by an increase through

to 6 hours and 33 minutes (Fig. 55). Mass 62 (DMS), after the addition of the copper, increased gradually throughout the remaining run time, though the concentration on DMS never reached the level of mass 47. There was not a significant difference in the average concentrations of Mass 47 and Mass 62 (Table 40).

| | H value | p-value | Confidence Interval | t-stat | Degrees of Freedom | Standard Deviation |
|---|---|---|---|---|---|---|
| Mass 47 and Mass 62 | 1 | $3.1362e^{-05}$ | $1.1158e^{-12}$; $3.0820e^{-12}$ | 4.1923 | 664 | $6.4603e^{-12}$ |
| Mass 47 Sections 1 and 2 | 1 | $1.147e^{-4}$ | $-4.1629e^{-12}$; $-1.3732e^{-12}$ | -3.9038 | 331 | $6.2849e^{-12}$ |
| Mass 62 Sections 1 and 2 | 1 | $9.9404e^{-04}$ | $-3.8225e^{-12}$; $-9.7910e^{-13}$ | -3.3219 | 331 | $6.4060e^{-12}$ |

*Table 35 Day 55 t-test. Section 1 was defined as the data collected prior to the first added stressor. Section 2 was defined as the data collected after the addition of 100 µL of copper to the end of the run time.*

Mass 47 difference between section 1 and 2 yielded significant results and rejects the null hypothesis. Mass 62 comparisons between sections 1 and 2 yielded significant results and rejected the null hypothesis (Table 35). The addition of the copper to the water column simulated real-world events on a significantly smaller scale. The findings within the aforementioned study was in agreement with the results in this study, with stating that the coastal strains of *E. huxleyi* were more sensitive to the addition of copper when compared to the offshore strains (*Echeveste et al. 2018*) with the added note that *E. huxleyi* has been observed to be a highly adaptive species and could tolerate various changes to the copper loading in the water column.

Day 63

This batch of data was collected after CHC108 Batch 3 Culture B spent 8 days in the dark after the addition of the copper on Day 55. The culture was 64 days old at the time of the MIMS run. The total darkness was achieved through the use of a cover that completely encloses the spinner while attached to the MIMS. The spinner was left running over those 8 days.

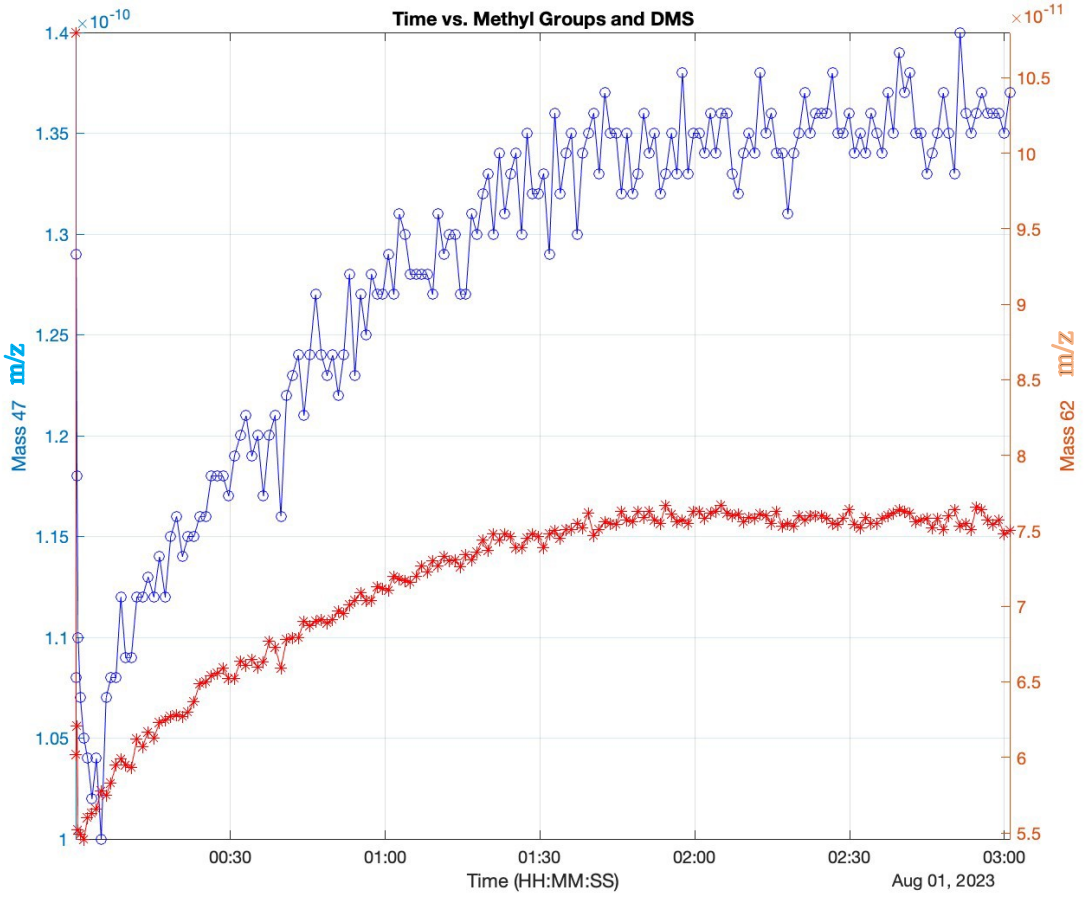


*Figure 49 Time vs. Mass 47 m/z and Mass 62 m/z. This run was performed after the sample was left in the stirrer over the course of 8 days in the dark. Note that the Mass 47 axis started at $1e^{-10}$ and Mass 62 axis started at 5.5 $e^{-11}$.*

| | Standard Deviation | Max Value | Min Value | Average Value | Max Time Value |
|---|---|---|---|---|---|
| Mass 47 | 9.37337e-12 | 1.40e-10 | 1.00e-10 | 1.28e-10 | 03:01:02 |
| Mass 62 | 6.52417e-12 | 1.08e-10 | 5.46e-11 | 7.16e-11 | 03:01:02 |

*Table 36 Average, min and max concentrations of Mass 47 and Mass 62 on 26-07-23*

There was a large spike in Mass 47 throughout the run time. Mass 62 experienced similar profiles but at a lower concentration as seen by the lower average values (Table 36). As Mass 47 approached 1 hour 30 minutes, more variation in the data points were observed (Fig. 49). Mass 62 also varied, but not to the same degree as Mass 47. Mass 62 did not increase at

the same rate as Mass 47 but started to level off around 1 hour and 30 minutes into the 3-hour mark with a slight spike near the end of the run.

| | H value | p-value | Confidence Interval | t-stat | Degrees of Freedom | Standard Deviation |
|---|---|---|---|---|---|---|
| Mass 47 and Mass 62 | 1 | $2.4400e^{-194}$ | $5.4545e^{-11}$; $5.7973e^{-11}$ | 64.5599 | 344 | $8.1047e^{-12}$ |
| Mass 47 Section 2 (Day 55) and Day 63 | 1 | 0 | $-1.2297e^{-10}$; $-1.2026e^{-10}$ | -176.4511 | 377 | $6.6836e^{-12}$ |
| Mass 62 Section 2 (Day 55) and Day 63 | 1 | $8.9295e^{-317}$ | $-6.8611e^{-11}$; $-6.6586e^{-11}$ | -131.2598 | 377 | $4.9939e^{-12}$ |

*Table 37 Comparisons of the last section of the previous run on Day 55 and the run done on Day 63 to determine if there was a significant increase in Mass 47 and Mass 62.*

There was a significant difference between the means of Mass 47 and Mass 62. This was to be expected. There was a significant difference in the results for both Mass 47 and Mass 62 between the end of run time of day and the runtime on Day 63 eight days later (Table 37). The significant difference indicated that the added stress increased both the DMS concentration and the Mass 47 concentrations.

# Discussion

## Growth Rates

One unexpected observation was that the CHC108 culture grown in the Erlenmeyer flasks did not quickly uptake the DNA stain sybr green. Cultures grown in smaller 40 mL transfer flasks easily took up the stain. One of the possible reasons was that the coccolith prevented the individual cells from being partially or completely unstained. Small side experiments were preformed to look at amount of stain vs. time spent in the orbital shakers at varying temperatures would improve the staining but there were varying degrees of success. None were consistent or successful enough to completely change the method. Other coccolithophores cultured in the usual transfer containers were able to be stained with the sybr green along with batch 1. It was not clear what the issue in staining was for batches 2, 3, and 4 as the only difference was the scale of the culture and the conical Erlenmeyer flask the cultures were grown in.

## DMS Concentrations

The average DMS production for the overnight experiments did increase as the cultures aged. The average mass 62 production of Day 5 was $3.67e^{-13}$ m/z, the average of section 3 on this day was $5.17e^{-13}$ m/z, and the average mass 62 production of Day 6 was $1.81e^{-11}$ m/z, the average of Section 1 on this day was $1.81e^{-11}$m/z. The average mass 62 production of Day 55 was $3.309e^{12}$m/z, the average of section 2 was $4.01e^{-11}$m/z, and the average mass 62 production on Day 63 was $7.16e^{-11}$ m/z. The first overnight experiment was done with Culture A and the second was done using Culture B. Culture B was stored in ideal conditions and would have no reason to have an increase in DMS production, except for limited nutrients as there were no nutrients added throughout the life span of the cultures.

The addition of the copper was done to provide a stressor to the *E. huxleyi* culture. The longer exposure to the copper along with the added stressor of lack of light resulted in a jump of DMS and a jump in methyl group. The 100 µL of copper added in this study was larger to that added in *Echeveste et al., 2018* which had ranges in 50-750nM. Copper has been involved in several cellular functions including enzymatic activity and cells would not be able to function without this heavy metal (*Echeveste et al., 2018*). Overloading Cu would be detrimental to phytoplankton populations, not just *E. huxleyi*. Deposition of atmospheric Cu loaded aerosols into the water column was a potential source, along with anthropogenic influenced deposits into rivers and other water sources along the watershed (*Echeveste et al., 2018*).

The DMS source was up for debate. In past coccolithophore cultures, it could take 3 to 4 months for the cells to degrade and the production of DMS to begin in the culture. In the ocean, as the cell begins to break down, DMSP leaks into the water column. It could then be taken up by other organisms e.g. bacteria to convert to DMS. This time period did not elapse, so the more likely candidate for the DMS production would be the accompanying bacterial populations in the cultures. There were 3 or 4 distinctive bacterial populations within the culture which take up DMSP at different rates and emitted DMS. The first population rapidly took up the DMSP, while the other had a slow start. The last group that was denoted as popn1 did not have a strong thiol signal so it would be unlikely that this population produced the DMS. The bacteria populations used the organic carbon from the coccolithophores in the DSMP conversion process further establishing the symbiotic relationship when nutrient concentrations became scarce. The low nutrient concentration was established because of the distinctive drop in chlorophyll concentrations along with the still expanding cell size, entering a phase called senescence. The expansion of the cells were further backed up in the increasing size of thiol within the cells as seen with the CMFDA staining. Another thing to consider is that as the coccolithophores start to breakdown, the bacterial numbers will increase from a rise in organic nutrients. Age may have been another factor in combination with limited nutrients as to why in the last experiment run, with an age of 3 months, the average initial DMS concentrations were higher than that of the beginning experiments.

*Note: The repeatability of these experiments was plausible, there were scheduling conflicts which was why there were no exact replicates of the DMS experiments.

# Conclusion

The production of DMS by phytoplankton is a key component of the global sulphur cycle in nearly all parts of the ocean. The flux of DMS from seawater is dependent on stressors within the marine environment, so testing different cultures at different time points in the culture lifecycle with different forms of stress. The first oxidant stress test with the addition of the $H_2{}^{18}O$ water and blue light did not result in a significant change in DMS production which was in line with the hypothesis and what other studies have found.

The CHC108 culture was subjected to lack of light over two days, in addition adding 200 µL of dilute/2 $H_2{}^{18}O_2$and 140 µL of non-dilute/2 $H_2{}^{18}O_2$. The addition of the 140 µL on both days yielded a bigger jump in both the methyl group (Mass 47) and DMS (Mass 62). There was also a significant change between the end of day 1 and the baseline reading on Day 2, which indicated that DMS and Mass 47 increased throughout the night while the cover was lifted off the sample. Any light recovery that occurred would have been during the early

morning hours prior to accessing the lab. It was not expected that the DMS concentrations would have increased with the availability of light, as the light inhibition had been lifted. The time scale that a notable concentration in DMS could be determined was up to 20 hours, even under more ideal conditions. The last parameters that were tested were the addition of 100 μL and complete darkness over 8 days. The heavy loading of Cu negatively impacted CHC108 strain which was evident with the concentrations of DMS and Mass 47. These findings indicated that DMS production can occur under various conditions, but the most effective was the addition of the copper and the lack of light in combination with the extended time period applied to this run. While loss of light for 8 days could not be applied to most areas in the ocean, it can be applied nearer to the poles. This is a new potential habitat for *E. huxleyi* as sea surface temperatures warm near the poles. The overloading of copper in marine habitats near anthropogenic areas is another threat to the wellbeing of the *E. huxleyi* communities but do provide high concentrations of DMS with other implications for the immediate surrounding environment; potential cooling.

There were many ways that this study could be improved and new directions it could go. From an experimental design side, improvements in the repeatability of each step, especially with DMS measurements. Another constraint was the time and space needed to grow and store all of the cultures to ensure the growing conditions were as identical as possible. Other avenues to be explored included using different levels of copper with varying degrees of time spent in the dark and how age alone will affect DMS production. When culturing the strain, adding an acid to ensure that the DNA stain fully penetrated all of the cells. An interesting comparison would be to look at the production rate of DMS in the adjoining bacteria both with and without the CHC108 strain. Another would be to look at the level of sulphur within the culture initially and compare it to the levels after DMS was produced. Temperature was not considered a factor in this study but is likely an important component to consider in conjunction with the stressors outlined, especially when looking at potential increasing global ocean temperatures and the implications of global warming.

# References


1. Altieri, K.E., Fawcett, S.E., and Hastings, M.G. (2021) 'Reactive nitrogen cycling in the atmosphere and Ocean', *Annual Review of Earth and Planetary Sciences*, 49(1), pp. 523–550. doi:10.1146/annurev-earth-083120-052147.
2. Ayers, G.P. and Cainey, J.M. (2007) 'The claw hypothesis: A review of the major developments', *Environmental Chemistry*, 4(6), p. 366. doi:10.1071/en07080.
3. Behringer, G. *et al.* (2018) 'Bacterial communities of diatoms display strong conservation across strains and time', *Frontiers in Microbiology*, 9. doi:10.3389/fmicb.2018.00659.
4. Bratbak, G. and Thingstad, T. (1985) 'Phytoplankton-bacteria interactions: An apparant paradox? analysis of a model system with both competition and commensalism', *Marine Ecology Progress Series*, 25, pp. 23–30. doi:10.3354/meps025023.
5. Brévière, E. and the SOLAS Scientific Steering Committee (eds.) (2016): SOLAS 2015- 2025: Science Plan and Organisation. SOLAS International Project Office, GEOMAR Helmholtz Centre for Ocean Research Kiel, Kiel, 76 pp.
6. Burlacot, A. *et al.* (2020) 'Membrane inlet mass spectrometry: A powerful tool for algal research', *Frontiers in Plant Science*, 11. doi:10.3389/fpls.2020.01302.
7. Chiu, Y.-L. and Shinzato, C. (2022) 'Evolutionary history of DMSP lyase-like genes in animals and their possible involvement in evolution of the Scleractinian coral genus, Acropora', *Frontiers in Marine Science*, 9. doi:10.3389/fmars.2022.889866.
8. Dedman, C.J. *et al.* (2023) 'The cellular response to ocean warming in Emiliania huxleyi', *Frontiers in Microbiology*, 14. doi:10.3389/fmicb.2023.1177349.
9. Echeveste, P., Croot, P. and von Dassow, P. (2018) 'Differences in the sensitivity to Cu and ligand production of coastal vs offshore strains of Emiliania huxleyi', *Science of The Total Environment*, 625, pp. 1673–1680. doi:10.1016/j.scitotenv.2017.10.050.
10. Evans, C. *et al.* (2007) 'The relative significance of viral lysis and microzooplankton grazing as pathways of dimethylsulfoniopropionate (DMSP) cleavage: An *emiliania huxleyi* culture study', *Limnology and Oceanography*, 52(3), pp. 1036–1045. doi:10.4319/lo.2007.52.3.1036.
11. Falkowski, P.G. (1994) 'The role of phytoplankton photosynthesis in global biogeochemical cycles', *Photosynthesis Research*, 39(3), pp. 235–258. doi:10.1007/bf00014586.
12. Feng, Y. *et al.* (2009) 'Effects of increased PCO2 and temperature on the North Atlantic Spring bloom. i. the phytoplankton community and biogeochemical response', *Marine Ecology Progress Series*, 388, pp. 13–25. doi:10.3354/meps08133.

13. Fernandes, M. (2012) *The influence of stress conditions on intracellular dimethylsulphoniopropionate (DMSP) and dimethylsulphide (DMS) release in Emiliania Huxleyi*. dissertation.
14. Fung, K. M., Heald, C. L., Kroll, J. H., Wang, S., Jo, D. S., Gettelman, A., Lu, Z., Liu, X., Zaveri, R. A., Apel, E. C., Blake, D. R., Jimenez, J.-L., Campuzano-Jost, P., Veres, P. R., Bates, T. S., Shilling, J. E., and Zawadowicz, M.: Exploring dimethyl sulfide (DMS) oxidation and implications for global aerosol radiative forcing, Atmos. Chem. Phys., 22, 1549–1573, https://doi.org/10.5194/acp-22-15492022, 2022.
15. Häder, D.P. and Gao, K. (2015) 'Interactions of anthropogenic stress factors on marine phytoplankton', *Frontiers in environmental science* [Preprint]. doi:10.3389/fenvs.2015.00014.
16. Herr, A.E. *et al.* (2019) 'Patterns and drivers of dimethylsulfide concentration in the Northeast Subarctic Pacific across multiple spatial and temporal scales', *Biogeosciences*, 16(8), pp. 1729–1754. doi:10.5194/bg-16-1729-2019.
17. Jarníková, T. *et al.* (2018) 'The distribution of methylated sulfur compounds, DMS and DMSP, in Canadian Subarctic and Arctic Marine Waters during summer 2015', *Biogeosciences*, 15(8), pp. 2449–2465. doi:10.5194/bg-15-2449-2018.
18. Kloster, S. *et al.* (2007) 'Response of dimethylsulfide (DMS) in the ocean and atmosphere to global warming', *Journal of Geophysical Research: Biogeosciences*, 112(G3). doi:10.1029/2006jg000224.
19. MacIntyre, H.L. and Cullen, J.J. (2016) 'Classification of phytoplankton cells as live or dead using the vital stains fluorescein diacetate and 5-Chloromethylfluorescein diacetate', *Journal of Phycology*, 52(4), pp. 572–589. doi:10.1111/jpy.12415.
20. Marie, D., Rigaut-Jalabert, F., Vaulot, D., 2014. An improved protocol for flow cytometry analysis of phytoplankton cultures and natural samples. Cytometry Part A 85, 962-968.
21. McParland, E.L. *et al.* (2020) 'Evidence for contrasting roles of dimethylsulfoniopropionate production in *emiliania huxleyi* and *thalassiosira oceanica*', *New Phytologist*, 226(2), pp. 396–409. doi:10.1111/nph.16374.
22. Menschel, E., González, H.E. and Giesecke, R. (2016) 'Coastal-oceanic distribution gradient of coccolithophores and their role in the carbonate flux of the upwelling system off Concepción, Chile (36°S)', *Journal of Plankton Research*, 38(4), pp. 798–817. doi:10.1093/plankt/fbw037.
23. Mondal, S. and Singh, S. (2022) 'Flow cytometry-based measurement of reactive oxygen species in cyanobacteria', *BIO-PROTOCOL*, 12(10). doi:10.21769/bioprotoc.4417.
24. Mordecai, G. *et al.* (2017) 'Schrödinger's Cheshire Cat: Are haploid Emiliania huxleyi cells resistant to viral infection or not?', *Viruses*, 9(3), p. 51. doi:10.3390/v9030051.
25. O'Neill, K. *et al.* (2013) 'Flow cytometry bioinformatics', *PLoS Computational Biology*, 9(12). doi:10.1371/journal.pcbi.1003365.
26. *Strain map* (no date) *Strain map | Roscoff Culture Collection*. Available at: https://roscoff-culture-collection.org/strains/strain-map?field_strain_name_value=CHC108&field_distributed_value=All&field_lost_value=All&field_class_tid_selective=All&field_genus_tid_selective=490&field

_sampling_ocean_tid_selective=843&field_sampling_regional_sea_tid_selective=All&field_sampling_country_tid_selective=1366&field_sampling_cruise_tid_selective=All&field_rcc_temperature_value%5Bmin%5D=&field_rcc_temperature_value%5Bmax%5D= (Accessed: May 5, 2023).

27. Teng, Z.-J. *et al.* (2021) 'Biogeographic traits of dimethyl sulfide and dimethylsulfoniopropionate cycling in polar oceans', *Microbiome*, 9(1). doi:10.1186/s40168-021-01153-3.

28. Thierstein, H.R. *et al.* (2004) 'Coccolithophore-derived production of dimethyl sulphide ', in *Coccolithophores: From molecular processes to global impact*. Berlin, Germany: Springer, pp. 127–164.

29. Tsuji, Y., Suzuki, I. and Shiraiwa, Y. (2008) 'Photosynthetic Carbon Assimilation in the coccolithophorid emiliania huxleyi (Haptophyta): Evidence for the predominant operation of the C3 cycle and the contribution of β-carboxylases to the active anaplerotic reaction', *Plant and Cell Physiology*, 50(2), pp. 318–329. doi:10.1093/pcp/pcn200.

30. Tyrrell, T. and Merico, A. (2004) 'Emiliania huxleyi: Bloom Observations and the conditions that induce them', *Coccolithophores*, pp. 75–97. doi:10.1007/978-3662-06278-4_4.
31. Vogt, Meike & Liss, P.. (2013). Dimethylsulfide and Climate. 10.1029/2008GM000790.
32. Yu, J. *et al.* (20221) 'Growth, DMS and DMSP production in Emiliania huxleyi under elevated CO2 and UV radiation', *Environmental Pollution*, 294, p. 118643. doi:10.1016/j.envpol.2021.118643.

# Appendix

## i. Matlab Coding Used

Coding used for the MIMS data for the resulting graphs:

```
Data = readtable ('filename.csv');

X= data.X;

Y =data.Y;

Z= data.Z;

Figure;

Yyaxis left;

Plot(X, Y, 'b-o');

Ylabel('y1 axis title');

Yyaxis right;

Plot(X, Z, 'r-*');

Ylabel('y2 axis title');

Xlabel ('x axis title');

Title('multivariable title');

Grid on;

Axis tight;
```

Coding used for T-Test on MIMS data in matlab:

```
Readtable('filename.csv');

Y=filename.Y;

Z=filename.Z;

[h, p, ci, stats] = ttest2(Y,Z);

Fprintf('Two-Sample t-Test Results:\n');

Fprintf('Mean of Group 1: %.2f\n', mean(Y));

Fprintf('Mean of Group 2: %.2f\n', mean(Z));

Fprintf('Hypothesis Test:\n');

Fprintf('HO: The means of the two groups are equal.\n');

Fprintf('Ha: The means of the two groups are different.\n');

Fprintf('t-stastistic: %.2f\n', stats.tstat);

Fprintf('Degrees of Freedom: %d\n', stats.df);

Fprintf('p-value: %.4f\n', p);
```

```
Fprintf('Confidence Interval for the Difference of Means: [%.2f, %.2f]\n', ci(1), ci(2));
If h
Fprintf('Result: Reject the null hypothesis (HO).\n');
Fprintf('Conclusion: There is a significant difference between the means of the two groups.\n'); Else
Fprintf('Result: Fail to reject the null hypothesis (HO).\n');
Fprintf('Conclusion: There is no significant difference between the means of the two groups.\n');
End
```

### ii. Batch Cell Counts

| | *Day 1* | *Day 2* | *Day 3* | *Day 4* | *Day 5* | *Day 9* | *Day 10* | *Day 11* | *Day 12* | *Day 15* | *Day 16* |
|---|---|---|---|---|---|---|---|---|---|---|---|
| *Gated count A* | *50* | *2466* | *8833* | *20864* | *35322* | *49252* | *43704* | *49495* | *47303* | *46345* | *47216* |
| *Gated count B* | *91* | *2744* | *11387* | *24346* | *39801* | *49595* | *46556* | *48682* | *49161* | *44788* | *47669* |

*Table 38 Batch 1 Gated Raw Count A and B over 16 days*

| | *Day 1* | *Day 2* | *Day 3* | *Day 4* | *Day 5* | *Day 9* | *Day 10* | *Day 11* | *Day 12* | *Day 15* | *Day 16* |
|---|---|---|---|---|---|---|---|---|---|---|---|
| *Gated count A* | *385* | *2899* | *8391* | *20719* | *36,568* | *50795* | *49229* | *49746* | *50510* | *46950* | *45273* |
| *Gated count B* | *291* | *3831* | *11754* | *26053* | *42704* | *50797* | *49064* | *50233* | *47563* | *47291* | *47791* |

Table 39 Batch 1 Gated DNA Stain Cell Counts for A and B over 16 days

| | *Day 2* | *Day 3* | *Day 4* | *Day 7* | *Day 8* | *Day 9* | *Day 10* | *Day 11* |
|---|---|---|---|---|---|---|---|---|
| *A* | *455* | *944* | *2938* | *28096* | *39500* | *42577* | *42185* | *56274* |
| *B* | *572* | *1368* | *3857* | *31038* | *43098* | *41732* | *44867* | *19328* |

Table 40 Batch 2 Gated Raw Cell Count A and B

| | Day 2 | Day 3 | Day 4 | Day 7 | Day 8 | Day 9 | Day 10 | Day 11 |
|---|---|---|---|---|---|---|---|---|
| A | 513 | 1294 | 2887 | 28220 | 42335 | 50467 | 55116 | 58192 |
| B | 755 | 1947 | 4472 | 37212 | 42674 | 49714 | 52320 | 52216 |

Table 41 Batch 2 Gated DNA Stain Cell Count of A and B over 11 days

| | *Day 1* | *Day 2* | *Day 3* | *Day 4* | *Day 7* | *Day 8* | *Day 9* |
|---|---|---|---|---|---|---|---|
| *A* | *503* | *559* | *1601* | *4360* | *30699* | *39635* | *49836* |
| *B* | *532* | *578* | *1777* | *4346* | *29729* | *29830* | *43606* |

Table 42 Batch 3 Gated Raw Cell Count of A and B over 9 days

| | *Day 1* | *Day 2* | *Day 3* | *Day 4* | *Day 7* | *Day 8* | *Day 9* |
|---|---|---|---|---|---|---|---|
| *A* | *558* | *694* | *1896* | *5016* | *35474* | *44066* | *51237* |
| *B* | *541* | *712* | *1984* | *5253* | *35870* | *45308* | *50944* |

Table 43 Batch 3 Gated DNA Stain Cell Count of A and B over 9 days.

| | *Day 1* | *Day 2* | *Day 5* | *Day 6* | *Day 7* | *Day 8* | *Day 9* | *Day 12* | *Day 14* |
|---|---|---|---|---|---|---|---|---|---|
| *A* | *249* | *253* | *4098* | *10028* | *16558* | *25345* | *42624* | *47533* | *50431* |
| *B* | *201* | *191* | *2798* | *8242* | *15696* | *29080* | *41784* | *49923* | *45764* |

Table 44 Batch 4 Gated Raw Cell Count of A and B over 14 days

| | *Day 1* | *Day 2* | *Day 5* | *Day 6* | *Day 7* | *Day 8* | *Day 9* | *Day 12* | *Day 14* |
|---|---|---|---|---|---|---|---|---|---|
| *A* | *305* | *355* | *4079* | *11332* | *19154* | *27109* | *39934* | *48077* | *50154* |
| *B* | *228* | *317* | *3782* | *8441* | *16153* | *24344* | *39385* | *48706* | *52006* |

Table 45 Batch 4 Gated DNA Stain Cell Count of A and B over 14 days

iii. Cell and Chlorophyll Size changes

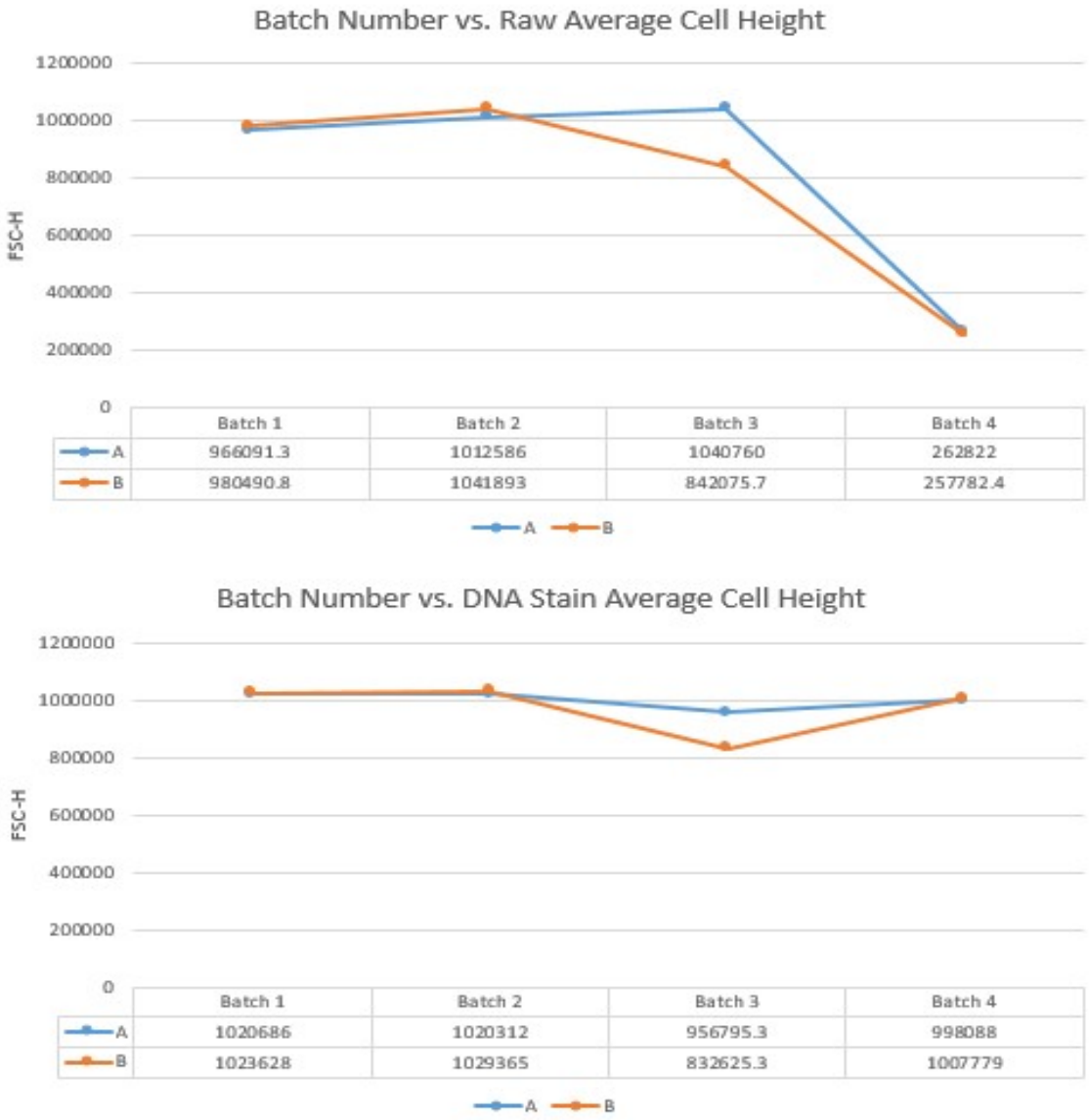


*Figure 50 Average Cell Size per Batch both Raw and Through the DNA Stain for both A and B cultures.*

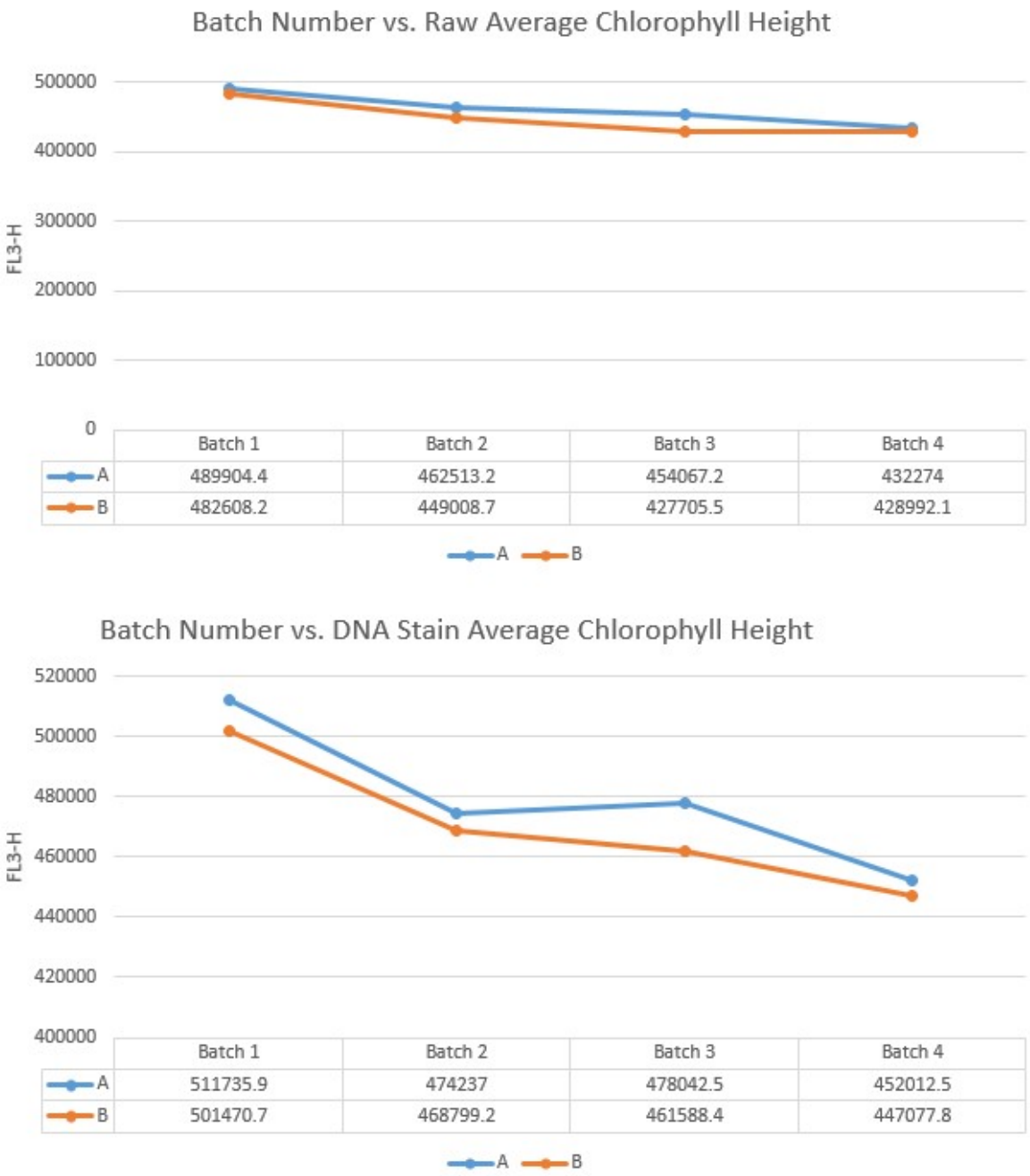


*Figure 51 Average chlorophyll size per batch for raw and DNA stain*

| | Average Raw FSC-H | Average DNA Stain FSC-H | Average CMFDA FSC-H |
|---|---|---|---|
| A | 997591.475 | 998970.325 | 1022131.65 |
| B | 961083.125 | 973349.325 | 1035639.5 |

*Table 46 Average cell size across raw, DNA, and CMFDA parameters*

| | Average Raw FL3-H | Average DNA Stain FL3-H | Average CMFDA FL3-H |
|---|---|---|---|
| A | 459690.95 | 479011.975 | 443674.6 |
| B | 447078.625 | 469734.025 | 438806.6 |

*Table 47 Average chlorophyll size across raw, DNA and CMFDA parameters*

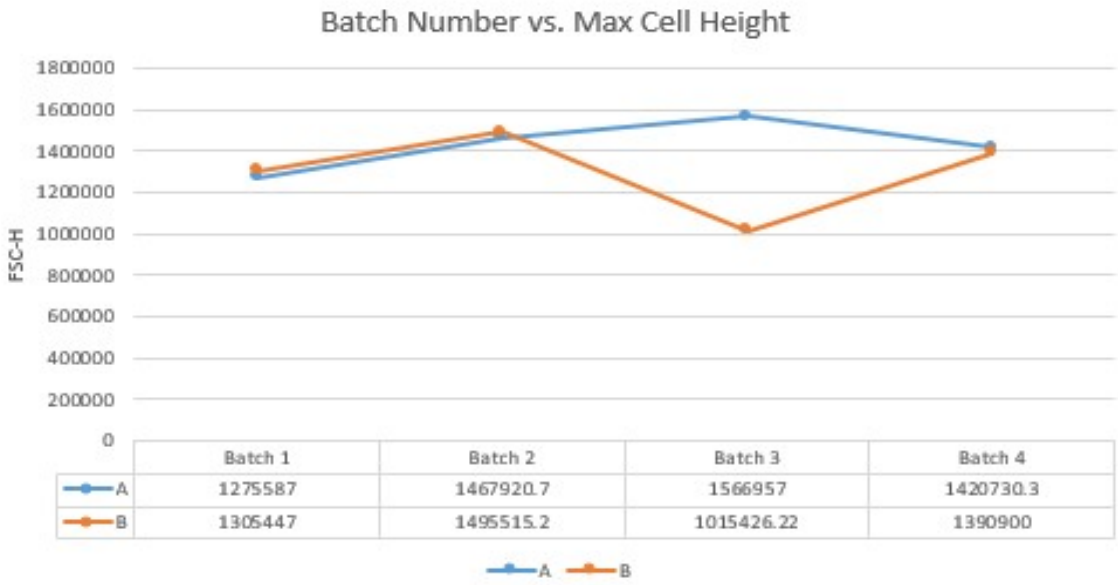


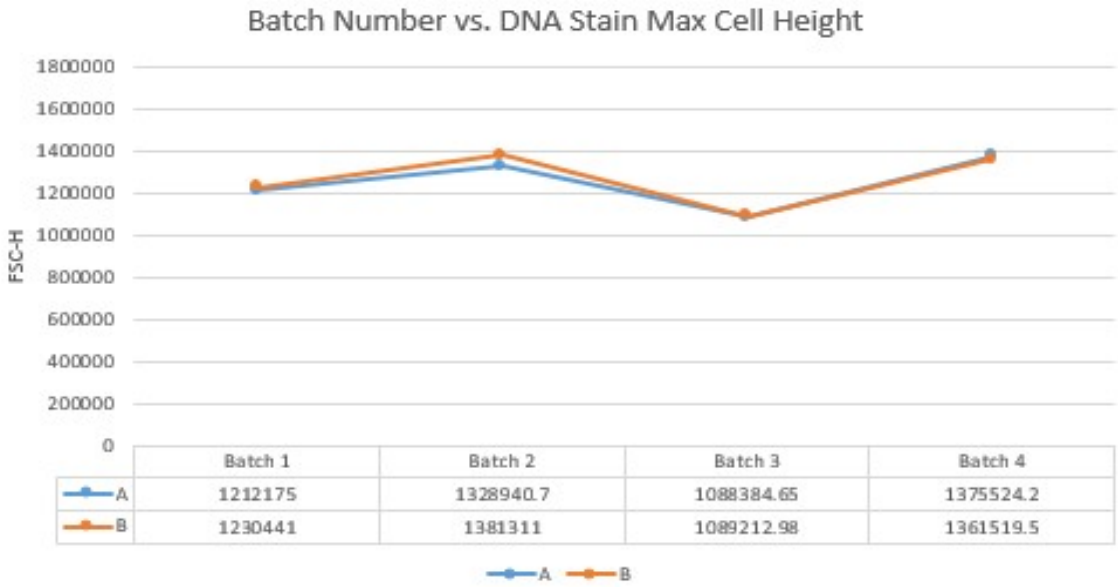


*Figure 52 Gated Max cell size per batch (raw, DNA stain)*

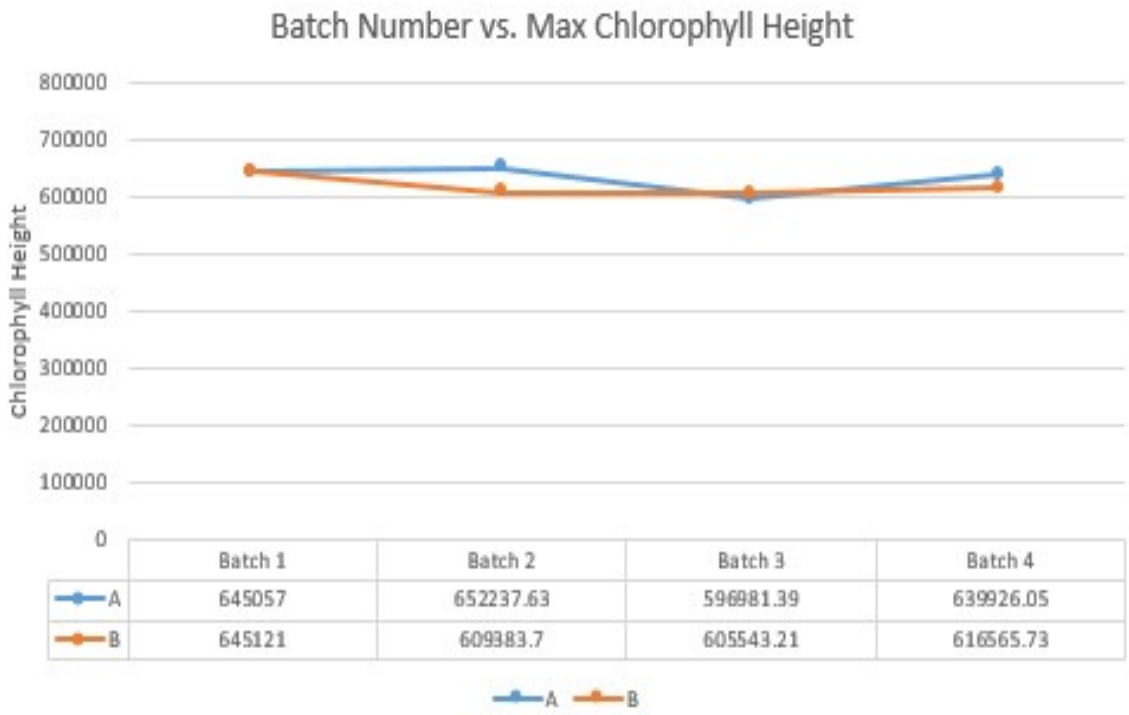


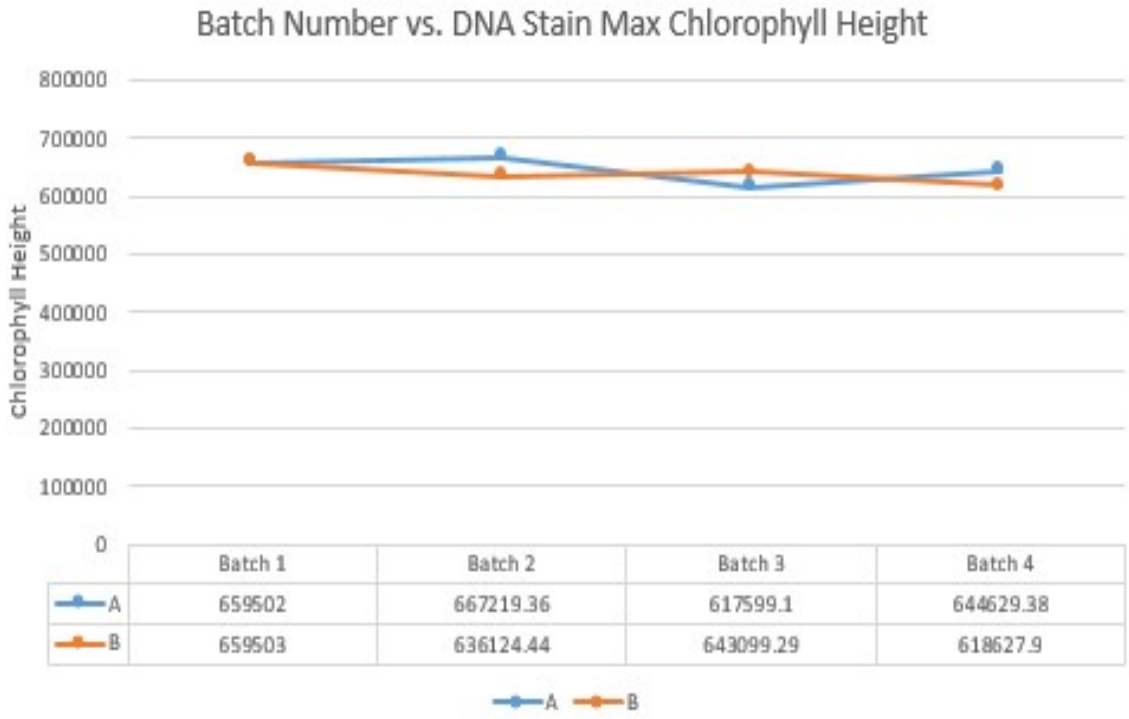


*Figure 53 Gated max chlorophyll size per batch (raw, DNA)*

iv. MIMS readings

Oxygen and Carbon Dioxide

Day 1

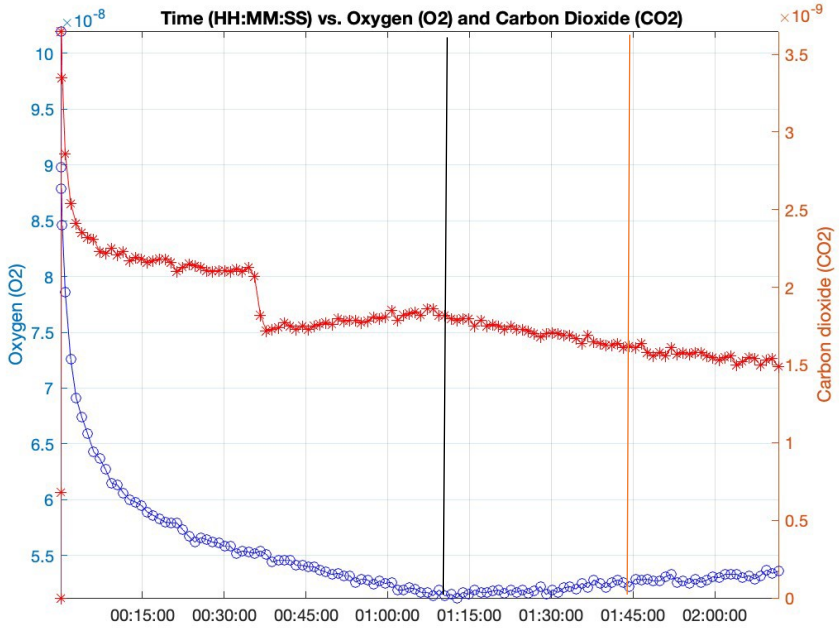


*Figure 51 Time vs. O2 and CO2. Max time is 2 hours and 11 minutes. (Day 1). The black line represents the $H_2{}^{18}O$ water being added to the water column and the orange line represents the addition of the direct blue light. Note that the left axis starts at 5.5 10e-8 m/z and the right axis started at $0e^{-9}$m/z.*

Day 5

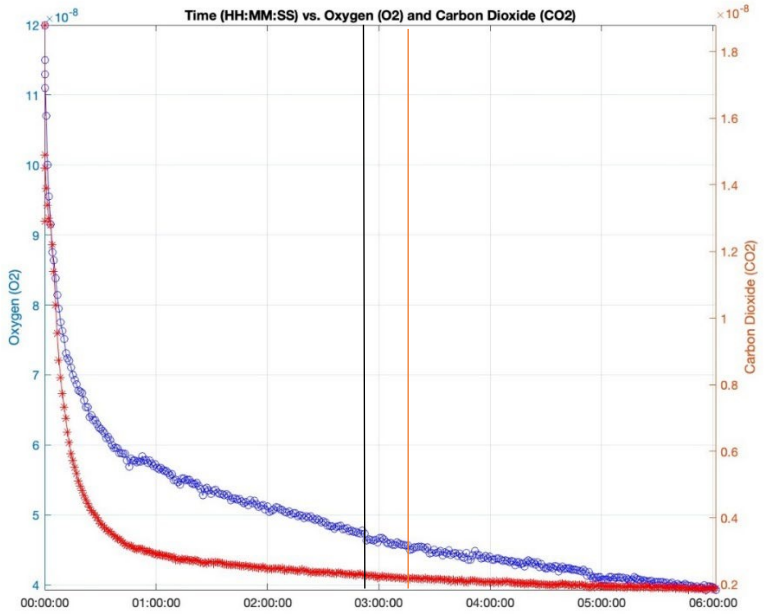


*Figure 52. Time vs. $O_2$ (Mass 32) and $CO_2$ (Mass 46) over the course of 6 hours (Day 5). The black line represents the addition of 200 µL of diluted/10 $H_2{}^{18}O_2$ and the orange line represents the addition of 140 µL of non-dilute/2 $H_2{}^{18}O_2$. Note that Mass 32 axis started at $4e^{-8}$ and Mass 46 axis started at $0.2e^{-8}$m/z.*

Day 6

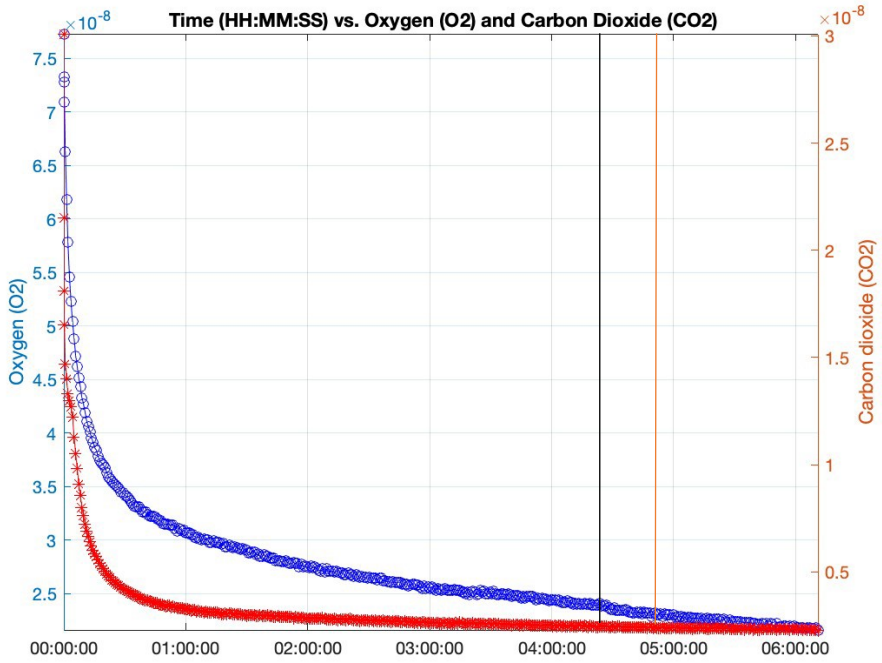


*Figure 53 Time vs. $O_2$ (Mass 32) and $CO_2$ (Mass 46) over the course of* 6 hours (Day 6). *The black line represents the addition of 200 µL diluted/10 $H_2{}^{18}O_2$ and the black line represents the addition of 140 µL non-dilute/2 $H_2{}^{18}O_2$. Note that the Mass 32 axis started at $2e^{-8}$ m/z and Mass 46 axis started at $0.25e^{-8}$ m/z.*

Day 55

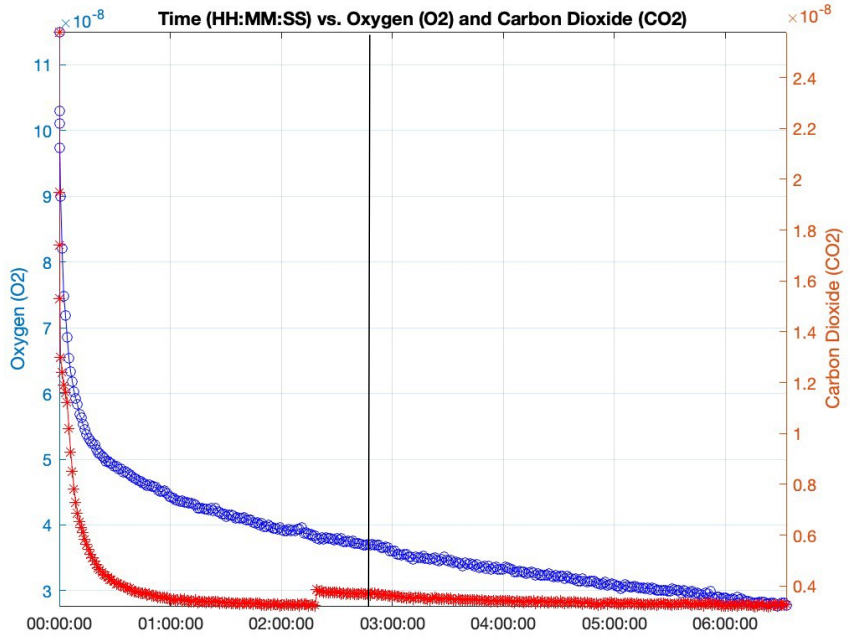


*Figure 54 Time vs. O2 (Mass 32) and CO2 (Mass 46) over the course of 6 hours and 33 minutes (Day 55). The black line is a representation of the addition of 100 µL Cu. Note that Mass 32 axis started at $3e^{-8}$ m/z and Mass 46 axis started at $0.4e^{-8}$ m/z. Note that Mass 32 axis started at $3e^{-8}$ m/z and Mass 46 axis started at $0.4e^{-8}$ m/z.*

Day 63

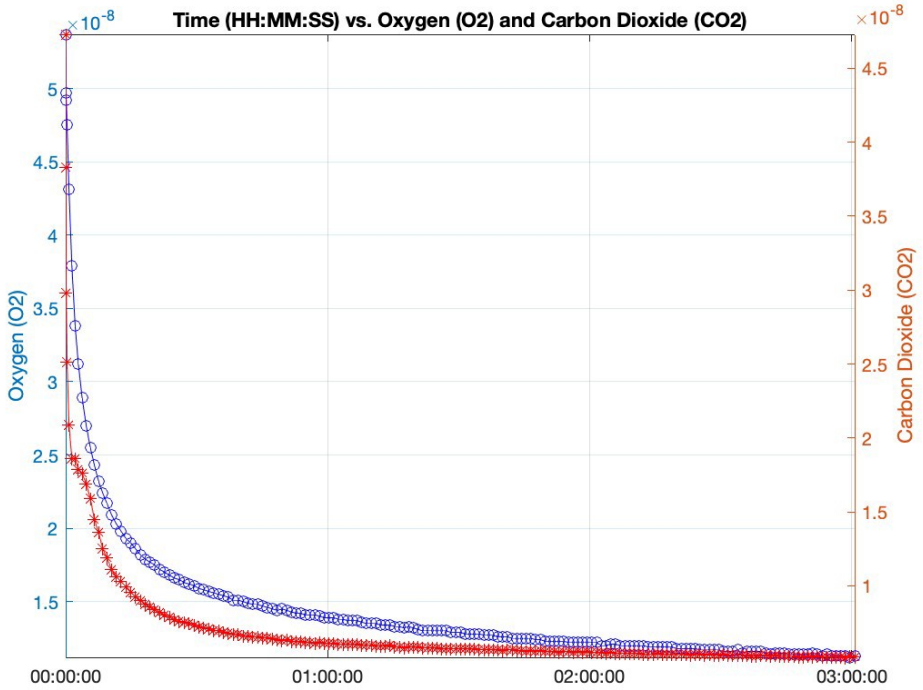


*Figure 55 Time vs. $O_2$ (Mass 32) and $CO_2$ (Mass 46). This run was performed after the sample was left in the stirrer over the course of 8 days in the dark. Note that Mass 32 axis started at$1e^{-8}$ m/z and Mass 46 axis started at $0.5e^{-8}$ m/z.*

Nitrogen (N2) and Methyl Radical

Day 1

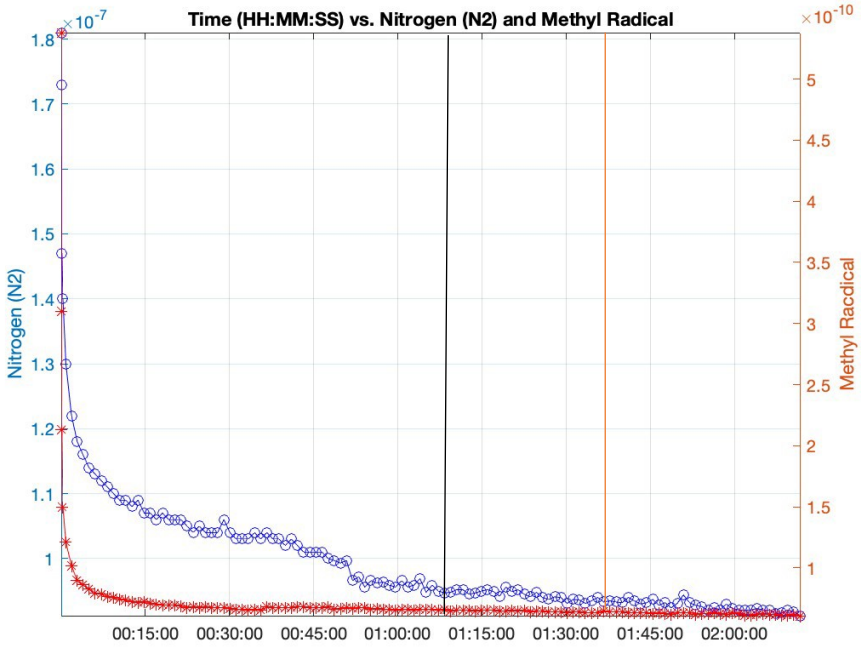


*Figure 59 Time vs. Nitrogen (Mass 28) and Methyl Radical Group (Mass 15) over the course of 2 hours and 11 minutes. (Day 1). The black line represents the $H_2{}^{18}O$ water being added to the water column and the orange line represents the addition of the direct blue light. Note that Mass 28 axis started at $0.9e^{-7}$ m/z and Mass 15 axis started at $0.9e^{-10}$m/z.*

Day 5

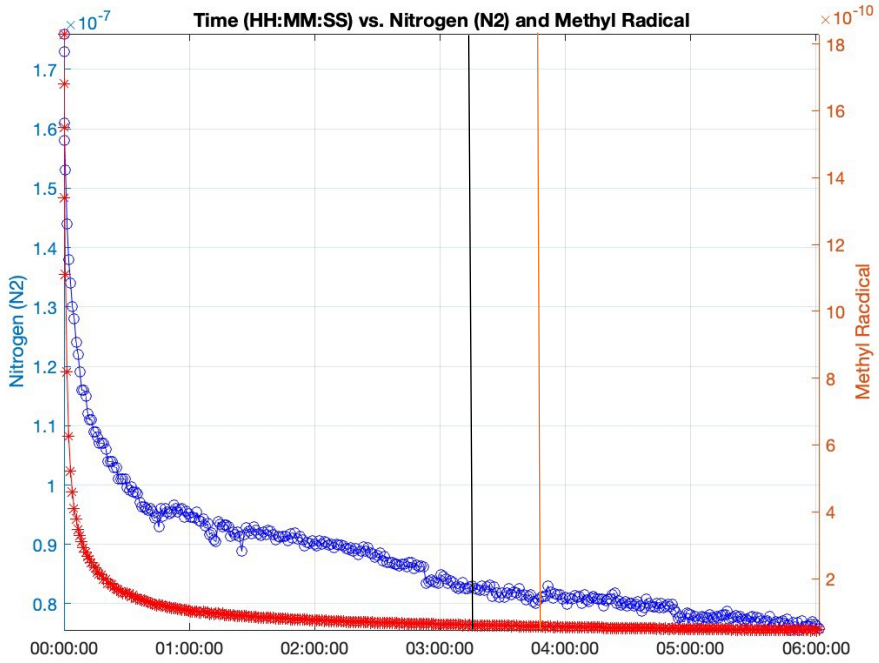


*Figure 60 Time and $N_2$ (Mass 28) and Methyl Radical ($CH_3$) (Mass 15) over the course of 6 hours (Day 5). The black line represents the addition of 200 µL of diluted/10 $H_2{}^{18}O_2$ and the orange line represents the addition of 140 µL of non-dilute/2 $H_2{}^{18}O_2$. Note that the mass 28 axis started at 0.75$e^{-7}$ m/z and mass 15 axis started at 1$e^{-10}$ m/z.*

Day 6

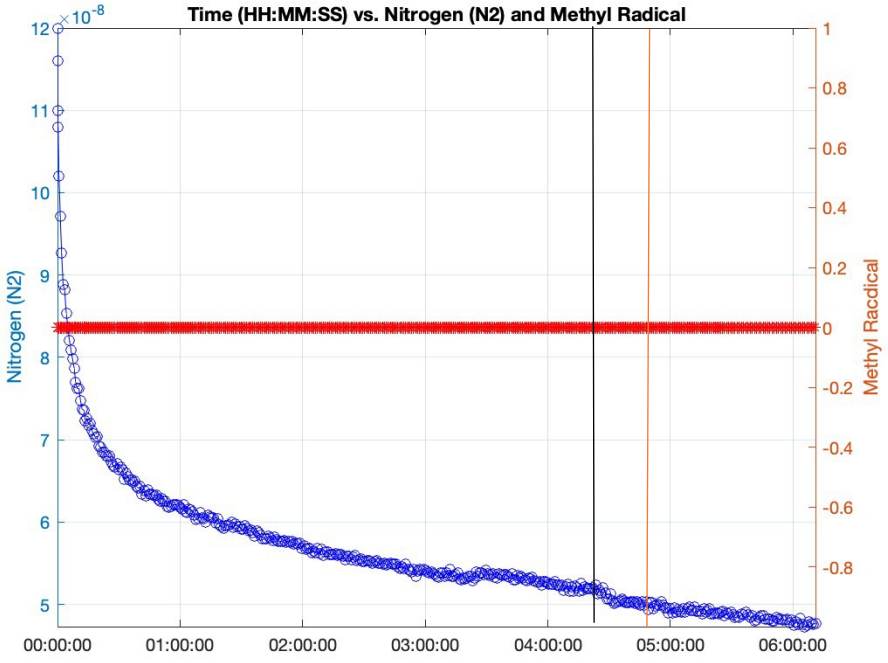


*Figure 58 Time vs. $N_2$ (Mass 28) and Methyl Radical Group (Mass 15) over the course of 6 hours (Day 6). The black line represents the addition of 200 µL diluted/10 $H_2{}^{18}O_2$ and the black line represents the addition of 140 µL non-dilute/2 $H_2{}^{18}O_2$. Note that Mass 28 axis started at 5$e^{-8}$ m/z and Mass 15 axis started at -0.7 m/z.*

Day 55

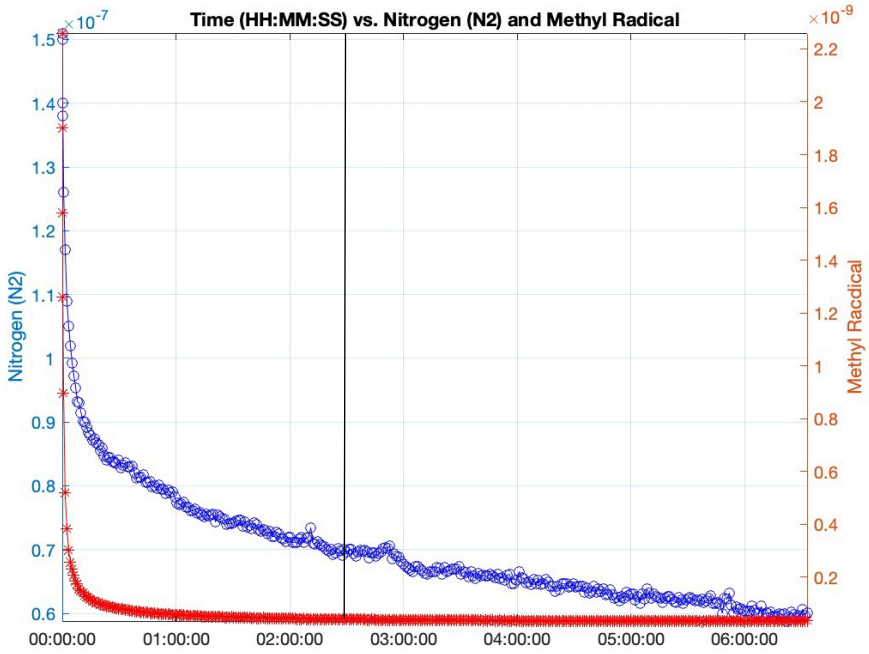


*Figure 59 Time vs. $N_2$ (Mass 28) and Methyl Radical Group ($CH_3$) (Mass 15) over the course of 6 hours and 33 minutes (Day 55). The black line is a representation of the addition of 100 µL Cu. Mass 28 axis started at $0.6e^{-7}$ m/z and Mass 15 axis started at $0.2e^{-9}$ m/z.*

Day 63

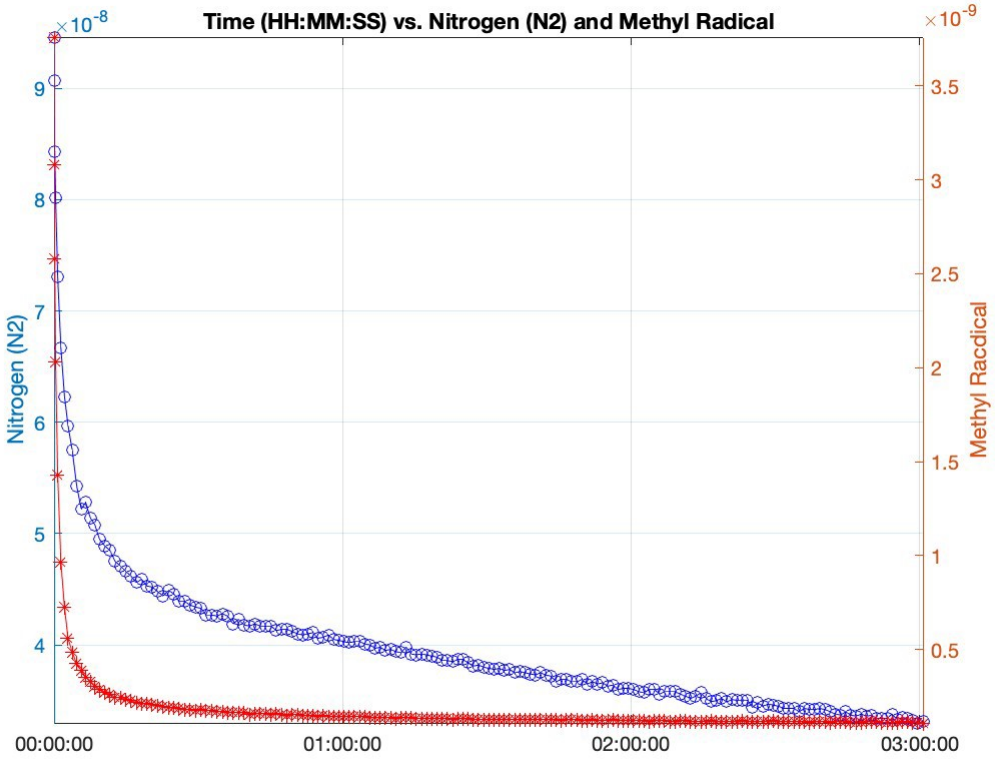


*Figure 60 Time vs. $N_2$ (Mass 28) and Methyl Radical Group ($CH_3$) (mass 15). This run was performed after the sample was left in the stirrer over the course of 8 days in the dark. Note that the Mass 28 axis started at $3e^{-8}$ m/z and Mass 15 axis started at $0e^{-9}$ m/z.*